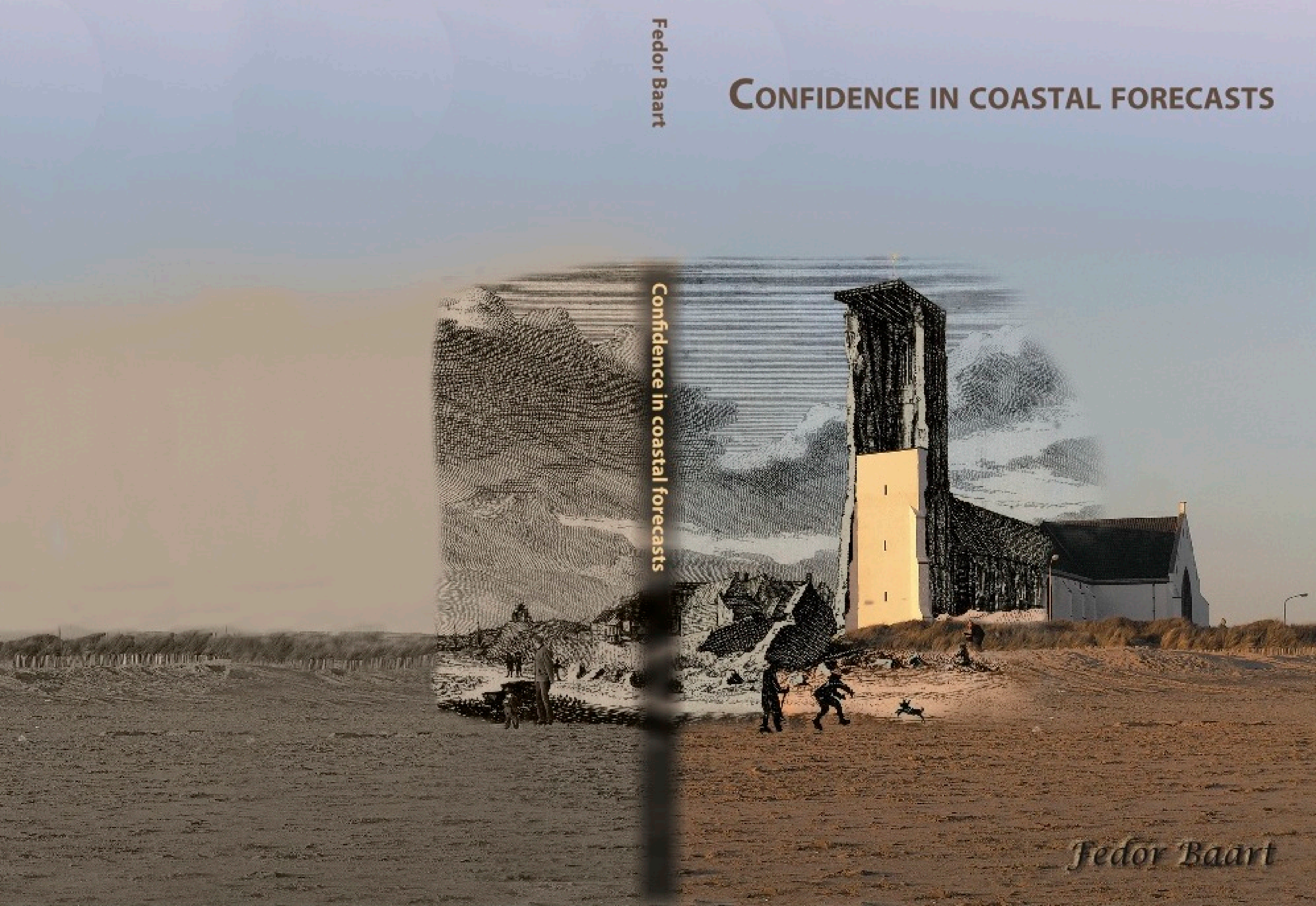
Fedor Baart
Confidence in coastal forecasts
CONFIDENCE IN COASTAL FORECASTS
Fedor Baart

CONFIDENCE IN COASTAL FORECASTS

Fedor Baart

June 5 2013

CONFIDENCE IN COASTAL FORECASTS

PROEFSCHRIFT

ter verkrijging van de graad van doctor
aan de Technische Universiteit Delft;
op gezag van de Rector Magnificus Prof. ir. K.Ch.A.M. Luyben
voorzitter van het College voor Promoties
in het openbaar te verdedigen op woensdag 5 juni 2013 om
10.00 uur.

door

Fedor BAART
Doctorandus in de psychologie
geboren te Portsmouth, United Kingdom

DIT PROEFSCHRIFT IS GOEDGEKEURD DOOR DE PROMOTOR:
Prof. dr. dr.h.c. ir. M.J.F. Stive

SAMENSTELLING PROMOTIE COMMISSIE:

Rector Magnificus	voorzitter
Prof. dr. dr.h.c. ir. M.J.F. Stive	Technische Universiteit Delft, Promotor
Prof. dr. ir. P. Ciavola	University of Ferrara (Italy)
Prof. dr. ir. J.A. Roelvink	UNESCO IHE
Prof. dr. ir. W.S.J. Uijttewaal	Technische Universiteit Delft
Prof. dr.-Ing. habil. R. Klees	Technische Universiteit Delft
Dr. ir. P.H.A.J.M van Gelder	Technische Universiteit Delft
Dr. ir. M. van Koningsveld	Technische Universiteit Delft

Dr. ir. M. van Koningsveld heeft als begeleider in belangrijke mate aan de totstandkoming van het proefschrift bijgedragen.

This research has received funding from the [European Community's] Seventh Framework Programme ([FP7/2007-2013]) under grant agreement number [202798]. Additionally, this research received funding from the Dr Cornelis Lely Foundation.

ISBN: 978-94-6191-764-5

Het lied als smeltende zang...

U hebt in de courant gelezen — van 't onheil, dat wij àllen vrezen. — De catastrofe, ja de ramp — als een Zuid-Pool-Geleerden-Kamp — het Pool-ijs ginder plots laat smelten. — Dan loopt van Groningen tot Elten — van Middelburg tot in Den Helder — het water niet slechts in de kelder. — doch vèr boven de huizen uit. — Geen sterveling geeft meer geluid. —

U hebt het allemaal gelezen: — de ZEESPIEGEL, opééns gerezen! — 't Is een gedachte. die mij kwèlt — het Zuid-pool-ijs, dat plots'ling smelt......

DE ZEESPIEGEL stijgt veertig meter. — Ik ben volstrekt geen béter-weter — doch praat slechts ná, wat ik zo lees. — Dit smeltend „lied" is vol van vrees.....

O, hooggeleerde, wijze heren! — Laat de Zuidpool toch in haar sferen. — Want Nederland is dan géén boffer. — Dat wordt het allereerste offer. — Ons hele lieve land loopt ónder — hier helpt geen voetstuk en geen vlonder. —

VOORAL 't „Ballet der Lage Landen" — zal cultureel volkomen stranden — omdat het géén Waterballet is — doch op een podium gezet is. — En vèrder, in de Lage Landen — zal àlles zinken en verzanden. — De huiskamer èn Tweede Kamer — zal machteloos zijn (onbekwamer) — want lest een mr. Kortenhorst — aan het gesmolten ijs zijn dorst? — Ook HIJ verdrinkt, hij, dierbaar pan.. — de praesesshamer in de hand. —

GELEERDEN! Staakt Uw vlijtig pogen — en houdt het onheil scherp voor ogen. — Al aast Gij ook op Eerbewijzen — laat toch de ZEESPIEGEL niet rijzen!

Laat Scheerspiegels stijgen in prijzen — Toiletspiegels omhoog gaan rijzen — laat Lachspiegels hun kunst bewijzen. — geen sterveling zal U misprijzen. — Laat in confectie-magazijnen — de Pas-spiegel héél hoog verschijnen — laat Keelspiegel (van specialist) — omhoog gaan, dat brengt leed noch twist — verhoog desnoods in heel het land — het „Spiegeltje, spiegeltje aan de wand" — van ons geliefde kind Sneeuwwitje. — Maak 't sprookje duur, jawel ik bid je. —

LAAT de manoeuvres der soldaten — om reden van het geld niet laten. — Die zullen ons niet fnuiken, knéchten — want dát zijn maar SPIEGEL-gevechten. — Laat SPIEGEL-eieren maar bakken — geen NACHTSPIEGEL zal ons verzwakken. —

Het SPIEGEL stijgen van de ZEE..... o heren, doet daar niet aan mee.

WOUTERTJE.

Figure 0.1: Letter to the editor, Nieuwsblad van het Noorden, August 9 1958

CONFIDENCE IN COASTAL FORECASTS

This thesis answers the question "How can we show and improve our confidence in coastal forecasts?". The question is answered by providing four examples of common coastal forecasts. For each forecast it is shown how confidence intervals can be created and improved.

The coastal forecasts discussed in this thesis all have some relation to safety. The forecasts are separated into two parts: forecasts related to mitigation and forecasts related to preparation. Preparation and mitigation are two links in the safety chain, commonly used in emergency management. It is argued that in both phases coastal forecasts are important. It is shown that although the time and spatial scales are different, the methods used to generate confidence bands are the same for both preparation and mitigation.

For the mitigation approach to coastal safety, which includes measures that prevent a disaster from taking place or reducing the effect, the one in ten thousand year storm-surge level estimate is used as the first of three examples.

For the design of cost-effective coastal defence a precise estimate is needed of the $1/10000 \text{yr}^{-1}$ storm surge level. A more precise estimate requires more observations. Therefore, the three greatest storm surges that hit the northern part of the Holland Coast in the 18^{th} century are reconstructed. The reconstructions are based on paintings, drawings, written records and shell deposits that have recently appeared. The storm-surge levels of these storms have been estimated using numerical modeling of the coastal processes. The analysis of these storms shows how these reconstructions can be used in combination with extreme value statistics to give a more confident estimate of low probability events.

The second example of a coastal forecast is the erosion trend. It is shown that the confidence interval can be used to determine how much the erosion trend is affected by the recent policy change. It is also shown that the confidence bands, in this case, can be improved by taking into account the autocorrelated errors.

The third example of a coastal forecast is the sea-level trend. Sea-level rise rates have become important drivers for policy makers dealing with the long-term protection of coastal populations. Scenario studies suggest that an acceleration in sea-level rise is imminent. The anticipated acceleration is hard to detect because of spatial and temporal variability, which consequently, have become important research topics. A known decadal-scale variation is the 18.6-year nodal cycle. The study of sea-level rise forecasts shows how failing to account for the nodal cycle resulted in an overestimation of Dutch sea-level rise.

Accounting for the nodal cycle increases the probability of detecting acceleration in the rate of sea-level rise. In an analysis of the Dutch coast, however, still no significant acceleration was found. The nodal cycle causes sea level to drop or to rise at an increased rate; therefore, accounting for it is crucial to accurately estimate regional sea-level rise. This is an example of how including a confounder can increase the explained variance and thereby the probability to detect acceleration. A global map of the nodal tide is presented in this thesis.

The second part of this thesis addresses the preparation approach to coastal safety. The preparation phase involves influencing behaviour to limit the impact of a disaster. In the last decades a lot of effort has been put into systems that forecast hydrodynamic conditions at the coast, a few days ahead. The preparation part describes the expansion of the operational forecast systems with information on coastal morphology.

For practical applications of the operational morphological forecasting system the question is "how confident can we be in morphological predictions of several days ahead?". This question is answered by assessing the prediction skill as a function of forecast lead time. It is shown that the intertidal beach volume change at the Egmond study site can be predicted up to three days ahead with a reasonable skill. It is argued that this is not enough. Reasonable is not good enough when taking into account the effect of false alarms.

The operational forecasts are also extended with confidence intervals. What error source should be used for our confidence band around morphological forecasts? Two methods to compute confidence bands are compared. 1. The morphological error method is based on the assumption that old forecast errors are representative for future forecast errors. 2. The ensemble method is based on propagating the ensemble errors through a chain of nested numerical models. The method based on morphological errors gives a more accurate confidence interval.

This thesis concludes with a discussion where the different methods to include confidence intervals are compared. It is argued that including confidence intervals around forecasts is part of a broader movement to work towards an evidence based practice.

The new and improved confidence intervals can be used to make more realistic and more cost effective decisions.

VERTROUWEN IN KUSTVOORSPELLINGEN

Dit proefschrift beantwoordt de vraag: "Hoe kunnen we vertrouwen in kustvoorspellingen laten zien en verbeteren?". Deze vraag wordt beantwoord aan de hand van vier voorbeelden van typische kustvoorspellingen. Voor elke voorspelling worden betrouwbaarheidsintervallen bepaald en verbeterd.

De kustvoorspellingen hebben alle vier een relatie met kustveiligheid. De voorspellingen zijn onderverdeeld in twee delen: voorspellingen gerelateerd aan mitigatie en voorspellingen voor preparatie. Preparatie en mitigatie zijn twee schakels uit de veiligheidsketen. In beide schakels zijn kustvoorspellingen belangrijk. De methoden om betrouwbaarheidsintervallen te bepalen voor deze twee schakels zijn gelijk, ook al variëren de tijd- en ruimteschaal.

De mitigatie aanpak omvat de maatregelen om te voorkomen dat een ramp plaats zal vinden of om de gevolgen te beperken. De eerste van de vier voorspellingen is het stormvloed peil met een terugkeerkans van een tienduizendste per jaar. Voor het ontwerpen van een kosteneffectieve kustverdediging is een precieze schatting van het $1/10000 yr^{-1}$ stormvloed peil nodig. Een meer precieze schatting vereist meer observaties. De drie grootste stormen die de kust teisterden in de 18e eeuw werden gereconstrueerd op basis van historische gegevens (tekeningen, schilderijen, geschriften en schelpenlagen) en een numeriek model om de kustprocessen beschrijven. De analyse van deze stormen laat zien hoe een combinatie gemaakt kan worden van reconstructies en extreme waarde statistiek met als doel het verbeteren van de betrouwbaarheid.

De tweede voorspelling is de erosietrend. Met behulp van een statistisch model wordt bepaald hoe de erosie trend is veranderd door de recente beleidsverandering. Dit voorbeeld laat zien dat betrouwbaarheidsintervallen kunnen worden verbeterd door rekening te houden met de autogecorreleerde fouten.

De derde kustvoorspelling is de zeespiegeltrend. De snelheid van de zeespiegelstijging is een belangrijk kengetal geworden voor kustbeheerders. Studies die uitgaan van scenario's suggereren een aanstaande versnelling van de zeespiegel. Deze versnelling is moeilijk te detecteren vanwege de ruimtelijke en temporele variaties. Een bekende variatie is het 18.6-jarig getij. Het onderzoek naar het 18.6-jarig getij laat zien dat, door het langjarig getij niet mee te nemen, de Nederlandse zeespiegelstijging is overschat. Door deze cyclus wel mee te nemen, is de kans om versnellingen te detecteren vergroot. Desondanks is er nog geen aanwijzing in de metingen voor een recente versnelling. Het 18.6-jarig getij is belangrijk om mee te nemen in regionale trendschattingen, omdat de trend anders over- of onderschat wordt. Dit is een voorbeeld van het verbeteren van betrouwbaarheidsintervallen door het meenemen van een confounder. Van het 18.6-jarig getij is een wereldwijde kaart gemaakt.

Het tweede deel van dit proefschrift behandeld een voorbeeld van een preparatie aanpak voor kustveiligheid. De preparatiefase omvat het beïnvloeden van gedrag met als doel het voorkomen dat een gevaar een ramp wordt.

In de laatste jaren is er veel moeite gestopt in het ontwikkelen van operationele systemen om de hydrodynamische condities langs de kust een paar dagen vooruit te kunnen voorspellen. Dit deel van het proefschrift beschrijft de uitbreiding van het operationale systeem met informatie over kustmorfologie.

Voor de praktische bruikbaarheid van het operationele morfologische voorspellingssysteem wordt de vraag gesteld: "Hoe goed kunnen we de morfologische voorspellingen, een paar dagen vooruit vertrouwen?". Deze vraag wordt beantwoord door de voorspelvaardigheid te bekijken als functie van de voorspelhorizon. Voor de studielocatie Egmond vinden we dat we de morfologieveranderingen in de komende drie dagen met een redelijke vaardigheid kunnen voorspellen. Redelijk is echter niet goed genoeg als we de negatieve gevolgen van het verstrekken van valse waarschuwingen in overweging nemen.

De operationele voorspellingen zijn uitgebreid met betrouwbaarheidintervallen. Hiertoe zijn twee methoden vergeleken, elk met een andere bron van fouten. 1. De morfologische fouten aanpak. Deze gaat ervan uit dat fouten uit het verleden een goede voorspeller zijn voor fouten in de toekomst. 2. De ensemble aanpak. Deze is gebaseerd op de aanpak van error propagatie door de modelketen. De morfologische fouten aanpak geeft meer valide betrouwbaarheidsintervallen.

Dit proefschrift eindigt met een discussie van de verschillende methode om betrouwbaarheidsintervallen toe te voegen. Het toevoegen van betrouwbaarheidsintervallen om voorspellingen kan als onderdeel worden gezien van de bredere beweging om naar een "evidence based practice" toe te werken.

De nieuwe en verbeterde betrouwbaarheidsintervallen kunnen worden gebruikt om meer realistische en meer kosteneffectieve beslissingen te nemen.

CONTENTS

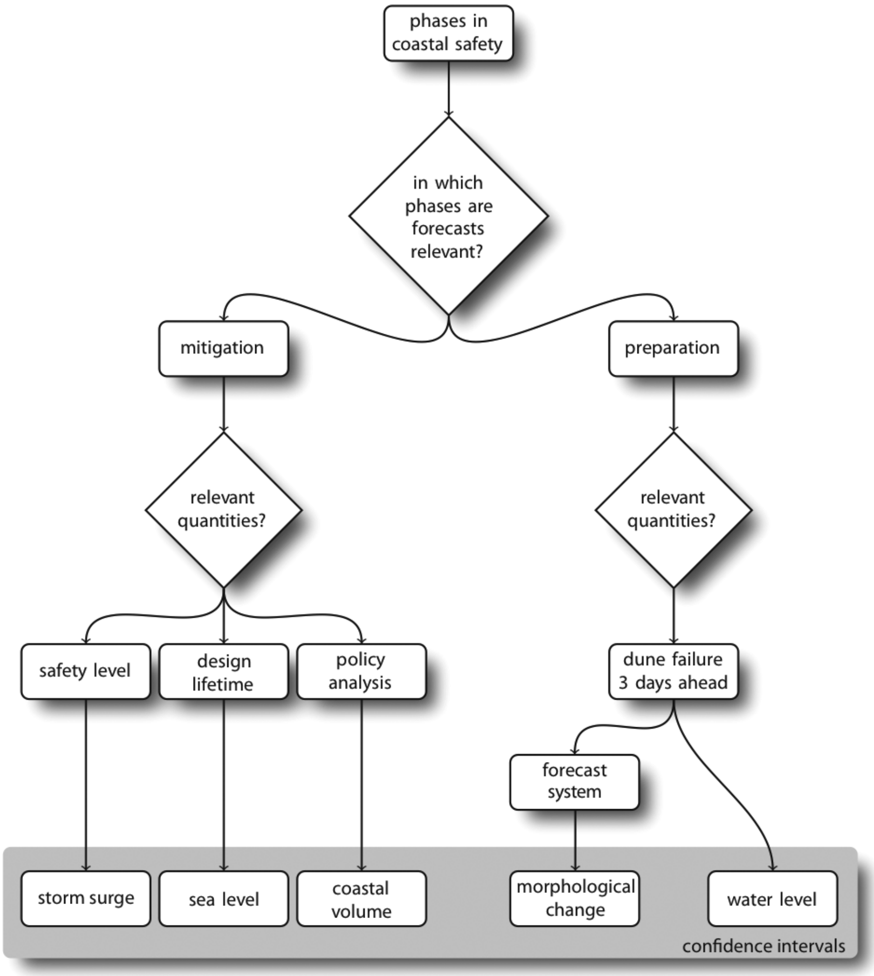

Figure 0.2: Visual table of contents

LIST OF FIGURES

LIST OF TABLES

LIST OF RESEARCH QUESTIONS

The following questions are answered in this thesis. Some of these questions are answered by using existing literature. A complete overview is presented to indicate the relations between the questions.

1

REPAIR OR PREPARE?

Contents

> It was the night of February 28th 2010, when the coastal town of La Faute-sur-Mer flooded. The people knew that the Xynthia storm was coming, but they did not know that the 200-year-old sea wall would breach. They were not informed of the expected water levels and closed their electric shutters to protect their windows from the wind gusts of over 25 m s^{-1}. People woke up with their beds floating in 1.5 m water, only to realize that without the electricity to open the shutters, there was no escape. In France 47 people died, most of them from drowning [Kolen et al., 2010].

The above illustrates how the coastal safety chain can fail. The safety chain, commonly used in emergency management [for example Settle, 1985], consists of four links: *i*) mitigation *ii*) preparation *iii*) response *iv*) recovery . Each of these links represents a phase.

This answers Question 2.1 .

The mitigation link covers the design and maintenance of a coastal defence that withstands the effects of a storm. The level of protection of the coastal defence is always limited. Or at least it should be, for the extra costs needed for a higher safety level should be weighed against other possible investments.

For coastal towns like La Faute-sur-Mer such a cost-benefit evaluation results in a relatively low economically optimal safety level. The coastal defence only protects a small town and not the entire hinterland. The low safety level was indeed in effect. Even though the levees were past their design lifetime, the strengthening was delayed. It was thought that money was best spent elsewhere. Unfortunately this risk culture was not shared between government and the inhabitants [Chauveau et al., 2011]. The risk awareness of the inhabitants would have been greater, if they were informed of their updated (increased) flooding probability due to the lack of maintenance [Anziani, 2010].

The preparation link should have provided the people with relevant and timely information. People were informed of an approaching storm, but not of a probability of a breach in the sea defence, nor of the probability of water levels rising so fast. Mayor Marratier was informed of a possible flooding four hours before it occurred [Parisien, 2011]. This was not timely enough for him to retract the advice that inhabitants should stay in their homes.

The other two phases of the safety chain are response and recovery. The response phase entails the activities when a disaster is occurring. The recovery phase covers the activities that take place after the disaster has occurred.

This example illustrates that a coastal defence should consist of both a mitigation and a preparation link. Unfortunately, for the 29 inhabitants of La Faute-sur-Mer that lost their lives that night, both links failed.

This answers Question 2.2 .

In both the mitigation and preparation phase coastal forecasts are important. The forecasts for these two phases are covered in the two main parts of this thesis (Part i: Mitigation, Part ii: Preparation). Splitting up the coastal forecasts by safety link makes it easier to discuss different forecasts. The time and spatial scale for mitigation and preparation are different, in the order of decades and greater for mitigation and in the order of days for preparation.

For the response and recovery phases there are also interesting forecasts to be made, but these are not specifically coastal.

The response phase occurs when a disaster is happening. The main question is "Where did it go wrong?", rather than "Where could it go wrong?", based on observations rather than forecasts. The relevant forecasts in this phase are often nowcasts and less specific for coastal disasters. An example is "What is the number of casualties?" [see for example Jonkman and Vrijling, 2008]. The number of casualties from a flood is similar to estimating the casualties caused by other natural disasters, epidemics or an act of war.

The recovery phase occurs after the disaster. Examples of recovery are the rebuilding of property and the accompanying spatial planning problems. Here also, the forecasts that are relevant are not specifically coastal. For example the question "How long are the repairs going to take" is relevant for people to know when they are able to return, but it is not a coastal specific forecast.

This answers Question 2 .

1.2 CONFIDENCE INTERVALS

Coastal forecasts predict hydrodynamic and morphodynamic processes that vary in time and space. This variation can be predicted partially. To represent this variation a "confidence interval" can be used. This section starts with a description of the wider concept of an interval estimate, followed by examples of different interval estimates, with the goal to explain what distinguishes confidence intervals from other interval estimates.

1.2.1 *Definition*

Let us start with a definition of an interval estimate, following [Neyman, 1937].

Definition 1.1 (Interval estimate)**.** The estimate T of population parameter θ by giving the limits $(\underline{\theta}, \overline{\theta})$, between which the true value of θ presumably falls. ■

An interval estimate, as opposed to a point estimate, represents the idea that it is very unlikely that an estimated parameter T is exactly equal to the true, population parameter θ. In coastal forecasts the parameter of interest is often a physical quantity, a variable with a unit of measurement.

The estimate of the size of the interval is often deferred from the precision, the reciprocal of variance [pp 245 Gauss, 1809]. The source of the variance depends on the parameter of interest. Figure 1.1 shows examples of interval estimates, each based on a different source of variance.

(a) Inter-model

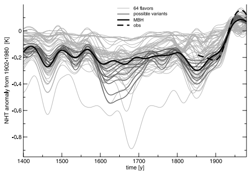

(b) Inter-method [Bürger and Cubasch, 2005]

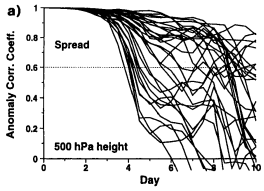

(c) Ensembles [Molteni et al., 1996]

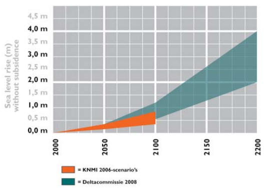

(d) Scenarios [Deltacommissie, 2008]

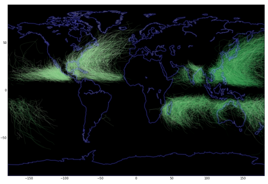

(e) Observations

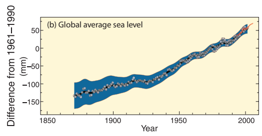

(f) Mixed [Pachauri and Reisinger, 2007]

Figure 1.1: Different sources of variation used to plot interval forecasts.

The inter-model variance (1.1a) is used to indicate the possible landfall locations. Here one could wonder if the interval represents the parameter of interest. One would expect the interval to represent the most likely interval where the storm would make landfall, given a probability.

The inter-method variance (1.1b) in the spaghetti plot represents how sensitive the temperature curve is to arbitrary choices made in the analysis, another source of variation that does not necessarily represent the parameter of interest. It is also not quite an interval estimate, although when the individual spaghetti are plotted with opacity, it is visually the same.

The inter-ensemble variance (1.1c) represents how sensitive the model is to the initial conditions. Ensembles are commonly used to introduce variance into a chaotic (sensitive to initial conditions) model. New observed values will not always lie within the predicted range [Whitaker and Loughe, 1998].

The interval based on scenarios (1.1d) is based on different possible human induced changes in climate. These scenarios do not have a probability assigned to them. As the scenarios only include medium to high end scenarios, the interval does not represent the most likely range.

The inter-observation variance (1.1e) represents the spread of observations, not of a parameter.

A final example is the "mixed uncertainty" interval (1.1f). This interval represents the ambiguous "uncertainty interval estimated from a comprehensive analysis of known uncertainties" [Pachauri and Reisinger, 2007].

The forecasts in Figure 1.1 represent different interval forecasts with a different source of variance. All these intervals represent some form of "confidence" in the forecast, but they are formally not confidence intervals. This is clear when we compare the definition of an interval estimate with the definition of the confidence interval.

Definition 1.2 (95% Confidence interval)**.** A confidence interval for a population parameter θ, is a random interval, calculated from the sample that contains θ with a 95% prabability [Rice, 2007] ∎

This definition introduces the concept of a population (sometimes referred to as "true") parameter. This assumes an unbiased parameter estimate and indicates that the variance is a measure of error. It further defines the confidence interval as a frequentist interval, as opposed to the Bayesian alternative: the credible interval. The credible interval represents the interval that has a 95% probability of containing the true value of the parameter given the data. Finally it makes it clear that the interval represents the interval of a parameter and not of observations. The interval that contains 95% of the observations, if more samples were drawn from the same population, is called the prediction interval.

1.2.2 *Relevance of confidence in coastal forecasts*

Adding a confidence interval to a forecast has many different applications, as will be shown in this thesis. The relevance of adding a confidence interval has been argued many times in literature. Arguments include, for example, the improved perception of information and the reduced cost in decision-making.

When forecasts are presented, people tend to focus only on the most likely estimate. This was seen, for example, in the 2004 hurricane season in the US [Broad et al., 2007]. Because the confidence interval was presented with a most likely estimate as a solid black line, many people refused to evacuate. In the 2011 hurricane season, the solid black line was replaced by the inter-model variability in combination with a confidence cone (see Figure 1.1a). Sometimes it is better to present only the confidence interval [Spiegelhalter et al., 2011], because even the confidence range itself is an underestimate in 2.5% of the cases.

The reduced cost of decision-making can be shown using the estimate of damage if the dunes fail to protect the hinterland. Let us assume that the damage is a function of the storm surge level, where each extra meter of water leads to double the cost (2). Let's assume that a water level (h) of 5 m gives a damage of 1 G€ (V). This gives us the cost function in Equation 1.1, following Kind [2011].

The factor of 2 is arbitrary. Damage factors are not defined for the Dutch coast (see Section 4.3).

$$V(h) = 1000000000 * 2^{h-5} € \quad (1.1)$$

Now let's assume that the most likely estimate of the $1/10000\text{yr}^{-1}$ storm surge is 5 m. Under the assumption of a standard deviation of 0 m, this would result in a most likely estimate of the damage caused by the $1/10000\text{yr}^{-1}$ storm surge to be 1 GEUR.

If the estimate of the $1/10000\text{yr}^{-1}$ storm surge has a standard deviation of 1 m, the cost function from Equation 1.1 can be multiplied with the normal distribution with $\mu = 5$ and $\sigma = 1$. This gives a mean estimate of the damage caused by the storm surge of 1.27 GEUR. Thus, given the exponential cost function and a low-confident estimate, the expected damage increases.

This is also the case if the distribution of the estimate is skewed. Let's not assume normal distribution for the $1/10000\text{yr}^{-1}$ storm surge, but a Gumbel distribution with a mean $\mu = 5$ and a standard deviation $\sigma = 1$. This corresponds to a scale (β) of $\frac{\sqrt{6}*\sigma}{\pi}$ and a location of $\mu - \gamma * \beta$, where γ denotes the Euler-Mascheroni constant. Because this distribution is skewed to the right (skewness=1.1, a thicker tail on the right), the expected damage increases even more to 1.34 GEUR.

As a final example let's assume we have a normal distribution with a standard deviation of 1.5 m, the expected damage increases to 1.7 GEUR. An overview of the distributions of the expected damage is given in Figure 1.2.

Thus, for the example of this cost function, the expected damage without taking into account the confidence interval is highly underestimated. This is even worse when the skewness is not taken into account. Another example of how including a confidence interval can result in a more valid estimate is given by Roscoe and Diermanse [2011], who showed that taking into account the confidence interval of the surge increased the best estimate of the critical retreat distance, by 34% to 93% for five locations along the Dutch coast.

Note that if the cost function is linear, then the standard deviation does not affect the expected cost estimate. The expected value of a random variable that is multiplied with a constant is the same as the constant multiplied with the expected value of the random variable ($E(CX) = CE(X)$), the same goes for adding a constant ($E(X + C) = E(X) + C$), independent of the variance.

This answers Question 1.1 and 1.2.

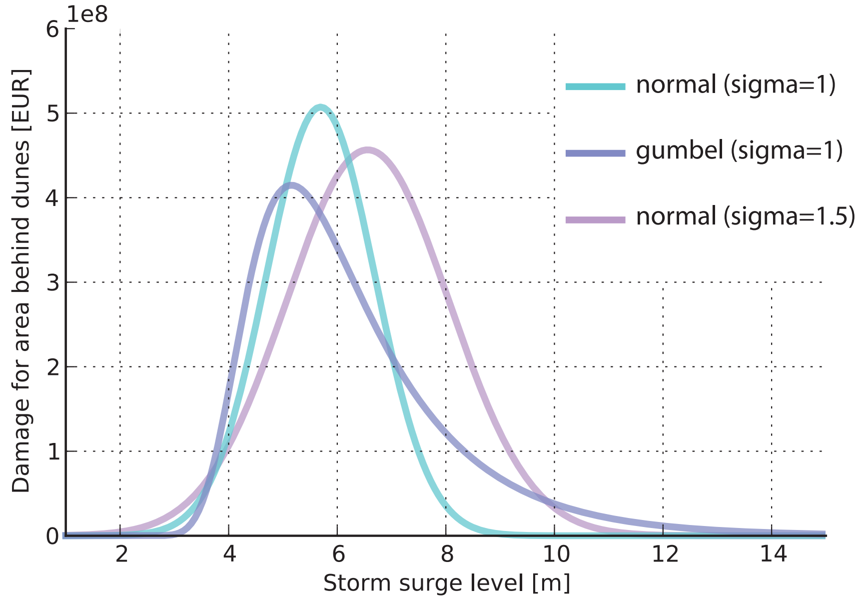

Figure 1.2: Distribution of the expected damage of the $1/10000 yr^{-1}$ storm surge under different distribution functions. Expected damages: N(5,0)=1 (not plotted), N(5,1)=1.27, G(5,1)=1.34, N(5,1.5)=1.7 (all in billion EUR).

1.3 OBJECTIVE

Concluding that coastal forecasts are important for the mitigation and preparation link in the safety chain and that confidence intervals are important for coastal forecasts, triggers the main question of this thesis: "How can we show and improve the confidence in coastal forecasts?". This methodological question is answered by providing examples of different types of coastal forecasts, each with a different type and application of a confidence interval. The confidence interval is used as a measure to represent the confidence in the forecast. The forecasts are applicable to dune coasts and most forecasts are also applicable to other coasts. The Dutch town "Egmond aan Zee" and the Dutch coast are used as example locations for the forecasts.

1.4 MAJOR CONTRIBUTIONS

This thesis makes important contributions to existing research in four ways: *i*) by extending knowledge on coastal processes *ii*) by improving working methods of coastal science *iii*) by giving examples of creating confidence intervals around coastal forecasts *iv*) by introducing methods from different fields into the coastal research field .

The extension of existing knowledge of coastal processes consists of showing the global effect of the nodal cycle (Section 4.1). Another example is the extension of coastal forecasting systems with morphological forecasts, to which this thesis contributes (Chapter 5). This extension provides more relevant forecasts for coastal inhabitants.

Although only briefly mentioned, the work done for this thesis contributes to the working methods for coastal scientists. The efforts of making model results and data available and improving the way numerical models are integrated are discussed in separate papers [Baart et al., 2012b; van Koningsveld et al., 2010; Baart and Donchyts, 2010].

Examples of creating confidence intervals are given for periodic (Section 4.1) and autocorrelated trends (Section 4.3), extreme values (Section 3.1) and forecasts from numerical models (Chapter 6). For each of these examples the current research is presented with extensions that show and increase the confidence.

Methods from different fields introduced in this thesis are the evidence based practice (Chapter 7), meta-analysis (Section 4.2) and the use of paintings to reconstruct coastal erosion (Section 3.2).

1.5 READING GUIDE

This thesis combines methods from different research fields. If time is limited, the list below can be used to skip to the parts and chapters of most interest to a particular research field.

STATISTICIANS will find the most interesting parts in Chapter 2 and Chapter 6.

COASTAL POLICY MAKERS will find the most interesting parts in Chapter 1, 7 and 8

COASTAL RESEARCHERS (DECADAL SCALE) will find the most interesting parts in Part i

COASTAL RESEARCHERS (DIURNAL SCALE) will find the most interesting parts in Part ii

CLIMATE RESEARCHERS will find the most interesting parts in Chapter 4

HISTORIANS will find the most interesting parts in Chapter 3

MODELLERS will find the most interesting parts in Chapter 5 and Chapter 6.

Part I

MITIGATION

In this Part we show and improve confidence intervals for coastal forecasts in the mitigation phase. Chapter 2 determines and selects relevant quantities for dune safety level, design lifetime and policy analysis. Chapter 3 describes the $1/10000 \mathrm{yr}^{-1}$ storm surge level, a quantity relevant for a safety level. Chapter 4 describes storminess, sea-level rise and erosion trends, quantities relevant for design lifetime and policy analysis.

2

QUANTITIES FOR DUNE SAFETY LEVEL, LIFETIME AND POLICY ANALYSIS

Contents

This chapter describes the relevant processes and corresponding quantities for evaluating the safety of a dune, designing interventions and evaluating policy. For each quantity the related developments in coastal policy for the Netherlands are briefly mentioned and a few psychological themes are noted. In the following two chapters we will show how to estimate and improve the quantities.

Different physical and other natural processes interact with coastal dunes. The time window and spatial scale determine which processes are relevant. Time windows that are relevant for dune changes range from seconds (a single wave) to tens of thousands of years (for example tectonic movements). De Vriend [1991] showed that each timescale has a corresponding spatial scale, with which it interacts: the primary-scale relationship. An overview of spatial versus time scales for fluid motion and bed response [based on Stive et al., 1995], extended with external forces, is shown in Figure 2.1. Human induced changes of the same quantities can occur on much shorter time and spatial scales, for example subsidence as the result of groundwater extraction [Phien-wej et al., 2006].

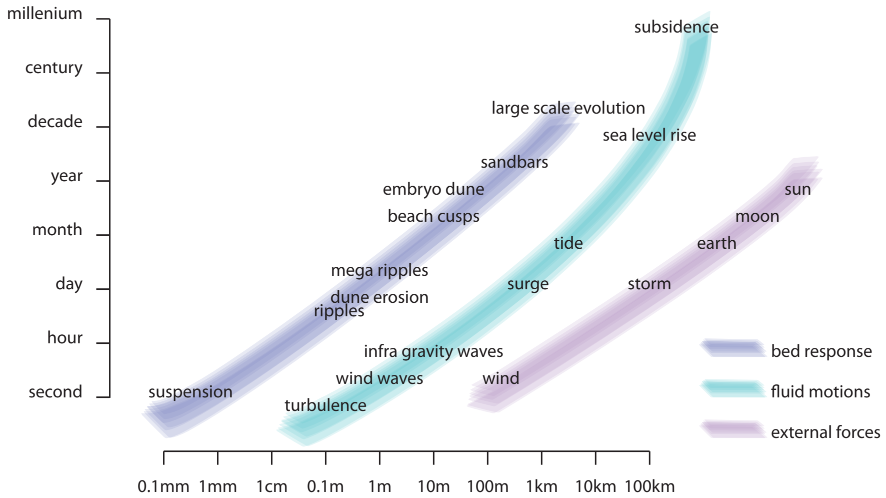

Figure 2.1: Time and spacial scales of bed responses in the coastal zone, fluid motions and external natural forces. Based on Stive et al. [1995].

Some of the processes in Figure 2.1 are relevant for the safety of dune based coasts. The failure modes for dunes [Mai et al., 2007] are a subset of the failure modes for dikes [Vrijling, 2001]. The failure modes for dunes include erosion, overtopping, wave overtopping. Sallenger [2000] described these as impact regimes and showed that they can be coupled to forcings and to properties of the coast, such as the geometry. The processes and properties that are relevant for the failure modes can be described by one or more measurable quantities. Figure 2.2 gives an overview of some of the quantities relevant for coastal dunes.

In the mitigation phase there is a repeated cycle of development, implementation and evaluation [van Koningsveld and Mulder, 2004]. In this Part the quantities for the following elements of this cycle will be distinguished: *i*) optimal safety level *ii*) design lifetime *iii*) policy analysis .

This answers Question 3.1.

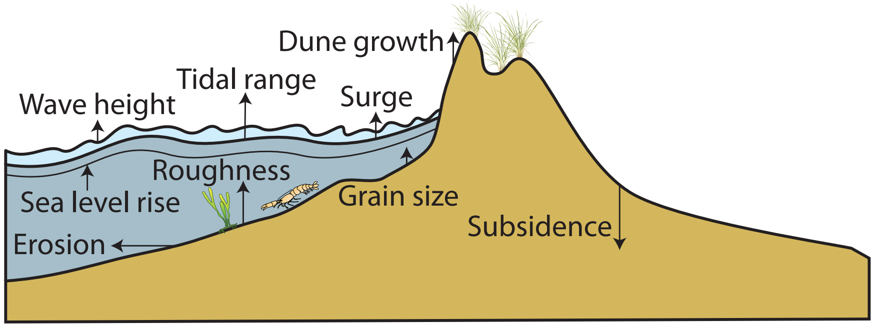

Figure 2.2: Quantities relevant for changes in the safety of a dune coast

2.2 SAFETY LEVEL

The optimal safety level is a quantity, used in the design of a coastal defence. It is optimal when the level is determined using a cost benefit analysis. Generally the higher the safety level, the higher the building and or maintenance costs. In a cost benefit analysis these costs are weighed against benefits of reducing the risk of dune failure.

There are several processes that cause failure of the dune. For the Dutch coast, failure occurs during storm events. Overviews of the processes during a storm surge are given by Kriebel and Dean [1985]; van de Graaff [1986]; Vellinga [1986]; Larson et al. [2004]; van Thiel de Vries [2009]; van de Graaff [1986]. The quantities that describe these processes include wave height, wave period, wave runup, surge height, storm duration and water level.

For the safety level these quantities are combined into a hypothetical extreme event. This extreme event is quantified using the water level that corresponds to its return period. Even though a raised water level itself does not cause failure until the water level reaches the dune top, it is a necessary precondition for other processes to be effective in destroying a dune. Furthermore it is correlated with the other processes that affect the dunes (e.g. extreme water levels come together with high waves). The properties that define the strength of the dune, for example vegetation and dune volume, are implicitly included because a dune with more strength is able to withstand a storm that corresponds with more extreme water levels. Chapter 3 describes the forecast of the $1/10000 \mathrm{yr}^{-1}$ water level.

This answers Question 3.2.

For the Northern Holland coast in the Netherlands, the area of interest in this thesis, this $1/10000 \mathrm{yr}^{-1}$ level is the design level. The probability that is used for a dyke ring depends on the economic value of the low lying area behind the dyke ring. For example, the Wadden islands have a lower economic value and thus a lower design water level. The economic evaluation dates back to the 1960's [van Dantzig, 1956; Deltacommissie, 1960]. The strategy for the Dutch coastal defence was defined by the first Delta Committee, after the storm of

February 1953 that caused 2165 casualties [Gerritsen, 2005; van Koningsveld et al., 2008]. This strategy resulted in the Deltaworks, a series of structures that were built with the goal to increase the strength of the coast to withstand the design storm surge level.

The calculation of the safety levels based on economic value was recently repeated [Kind, 2011], but the main part of the coast, the dunes, were left out of the calculation of the probability of failure, under the assumption that a breach is almost negligible. The second opinion on this study criticized this decision [Eijgenraam and Zwaneveld, 2011]. It is, however, an understandable decision because future events with negative consequences are notorious hard to grasp by humans [Izuma and Adolphs, 2011].

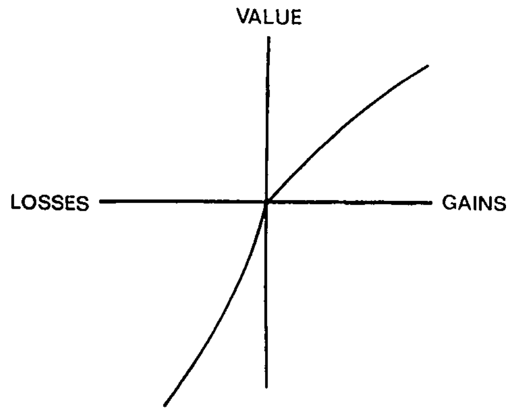

Figure 2.3: Hypothetical value function showing the concave for gains and convex for losses [from Kahneman and Tversky, 1979].

It is still open for discussion if this also holds for the low probability events that are relevant in coastal forecasts. Kahneman and Tversky [1979] argued that for high probability events with negative consequences people tend to be risk seeking and that for low probability events with negative consequences people tend to be risk averse, as can be seen in the convex value function in Figure 2.3.

2.3 DESIGN LIFETIME

The second quantity is used for evaluating the design lifetime. Once a safety level is defined and it is found that the coastal defence does not meet the safety level or will not meet the safety level in the future, one would like to make an optimal, cost effective, decision. Intervene or not? What is the best type of intervention? Intervene now or later? For the cost effective decision the variable design lifetime is a variable in the equation [van Dantzig, 1956].

Relevant processes for the design lifetime are those that change during the lifetime of a coastal defence. Most coastal interventions are planned with an expected lifetime of several years through several decades. The processes that determine the expected lifetime are the same processes as discussed for the safety level, but described with a different statistic. For the optimal safety level the expected extreme event is interesting, for the design lifetime it is the decadal trend that is relevant. The probability distribution of the processes over several years is referred to as climate. Change in climate can affect the expected lifetime of an intervention.

The sea-level trend and storminess trend are two quantities that relate to the processes that could change during the design lifetime.

From these two quantities the sea-level trend is used most often to estimate the lifetime. Chapter 4 discusses the sea-level trends in detail and the change in storminess briefly.

This answers Question 3.4.

The forecasts of these two quantities, in the climate reports of the Royal Netherlands Meteorological Institute (KNMI) [van den Hurk et al., 2006], initiated the formation of a new Delta Committee [Netwerk, 2007].

This second Delta Committee broadened the scope of the coastal protection policy in two ways. Following the direction of "Integrated Coastal Zone Management" [based on the UN action plan "Agenda 21" Nations, 1993], the scope was broadened by introducing an integrated approach. The safety aspects of the coast were combined with other water related questions, including fresh water supplies, the preservation of nature and recreation, sustainable energy, water quality and ecology [Kabat et al., 2009]. Second, it broadened the temporal scope. The focus used to be on a few years up to a few decades ahead. With the second Delta Committee it changed to a century ahead. This also changed the methodological approach, from observation-based to scenario-based forecasts [Deltacommissie, 2008; Ministerie van Verkeer en Waterstaat, 2009].

From a psychological perspective, an interesting topic in this context is the negativity bias [Rozin and Royzman, 2001] that results in natural tendency to over-report results with a negative consequence [as discussed in for example Economist, 2010].

2.4 POLICY ANALYSIS

This partially answers Question 3.4.

For policy analysis, in a coastal context, one is not so much interested in processes that affect the coast, but more in the state of the coast. Policy can not influence the quantities discussed earlier, but can, using interventions, affect the state of the coast. Commonly used quantities that describe this state include shoreline position, beach width and beach volume.

In the analysis of policy the question of interest is often if the policy was effective. We will discuss how to use confidence intervals to show the effect of a change in policy using a quantity related to beach volume in Section 4.3 .

This answers Question 3.6.

The Dutch coastline is maintained at a fixed line that is a proxy for the coastal volume [van Koningsveld and Mulder, 2004]. This policy was introduced when Dutch coastal management switched from a repair to a dynamic maintenance mode. The goal of maintaining this fixed line is that the coast can persist in functioning as a safety buffer, for recreation and as an ecological environment.

The main quantity that is used for Dutch coastal maintenance is the Momentary Coast Line (MKL). This is a compound quantity that depends on several others quantities, for example the mean low water level, the dune topography between low and high water level and an arbitrary reference line (see Figure 2.4).

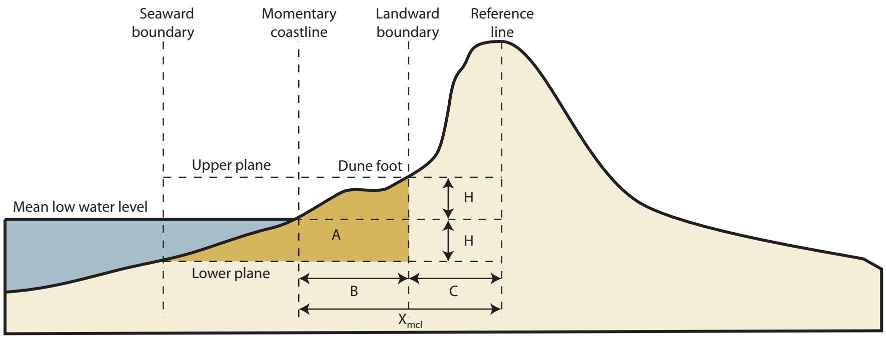

Figure 2.4: Calculation of the momentary coastline, based on [van Koningsveld and Mulder, 2004]

The change from a mere safety approach towards increasing the support for recreational and ecological value can be seen in the context of human motivation theory. The needs over the last decades have stepped up the steps of the Maslow [Maslow, 1943] pyramid (see Figure 2.5). After the 1953 flood the Netherlands found itself at the lowest level, having physiological needs of warmth, shelter and not drowning. After that, stepping up through higher levels of the feeling of safety and property protection. The Netherlands has now reached the level were it can concern itself with the need for improving our self-esteem in the form of prestigious constructions and with the need to self-actualization through creative processes and moral concerns such as taking into account the "experiential value" of the coast [Ministerie van Verkeer en Waterstaat, 2000].

Figure 2.5: The relation between human motivation and the development in coastal protection policy.

3

OPTIMAL SAFETY LEVEL

Contents

A safety level is an important estimate for coastal policy. The safety level for dune coasts is usually based on a design storm surge level. This Chapter presents a method to increase the confidence in the estimate of the effects of this extreme storm. The preparation forecast system that will be presented in Chapter 5 will also use this estimate as a design criterion.

The extreme safety standards reflect the vulnerability of the economically most valuable part of the Netherlands, which is mostly below sea level [van Dantzig, 1956; Deltacommissie, 1960]. Working with such extremely low exceedance probabilities presents a number of statistical challenges, as tide-gauge records are at most three centuries long. The most extreme storm-surge events are likely not represented in these. This makes the estimate of the $1/10000\,\mathrm{yr}^{-1}$ storm-surge level an interesting quantity to estimate and to improve the confidence level of.

The official estimates for the Dutch coast are based on the report by Philippart et al. [1995]. The estimate of the $1/10000\,\mathrm{yr}^{-1}$ storm-surge level was 5.1 m for IJmuiden.

3.1.1 *Datasets of tidal records*

The estimate of the $1/10000\,\mathrm{yr}^{-1}$ storm-surge level requires a dataset of water levels. Here we use the dataset of the station IJmuiden Buitenhaven as an example.

The station is located at 52.46° north, 4.55° east. There is a long record of sea-level data in IJmuiden but the measurements at the Buitenhaven station only started in January 1st 1981. Here we examine the records up to December 19th 2010.

One aspect to look at for records from tide gauges such as the one from IJmuiden Buitenhaven is the measurement frequency. For the estimate of the maximum over a period, a dataset with a uniform frequency is preferred. A series with a higher frequency has a higher maximum level. In this station the recorded water level frequency increased on January 1st 1988, when the frequency was raised from $1\,\mathrm{h}^{-1}$ to $6\,\mathrm{h}^{-1}$. In order to get a homogeneous frequency we leave out 5 out of 6 records after 1988.

Another option is to interpolate data within the hour, for example using a piecewise polynomial fit (see Chapter 2 for an example). The hourly records for station IJmuiden Buitenhaven are shown in Figure 3.1.

3.1.2 *Extreme value analysis*

To quantify the extreme storm surges, the distribution of observed surges as distilled from tide-gauge records is extrapolated by applying extreme value statistics [de Haan, 1990; Coles, 2001]. This is based on the assumption that somehow the more extreme observations are more representative for the population of interest than the more frequent occurring values. Using this technique an estimate can be given of various properties of the $1/10000\,\mathrm{yr}^{-1}$ storm-surge level.

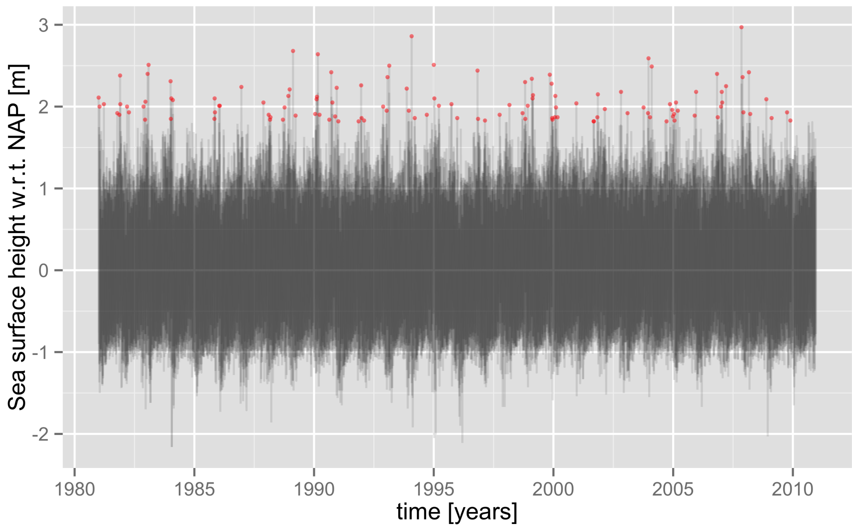

Figure 3.1: Sea-surface heights as measured at the IJmuiden Buitenhaven station.

Continuing on the example of IJmuiden Buitenhaven, we can see the dual modes (the bumps at y-axis equal to −0.57 m and 0.54 m) of Figure 3.2 of sea-surface heights in the records. These modi are caused by the semi-diurnal tide in IJmuiden and correspond to the "Mean low water neaps" and "Mean high water neaps" [see for example Pugh, 1987]. The distribution is right skewed (skewness 0.27) resulting in a fatter right tail. This means that higher water levels occur more often than under a normal distribution. The distribution is also more peaked than a normal distribution (kurtosis 2.27).

There are two commonly used methods to infer a distribution of the extreme values. The two methods differ in the a priori distribution that is used and the requirements of the datasets. The "peak over threshold" approach uses all values over a threshold (for example all water levels over 2 m). A Generalized Pareto Distribution (GPD) is then fit to these water levels (Equation 3.1, see for example Coles [2001]). In Equation 3.1 x is the water level, μ is the location parameter, σ the scale parameter and ξ the shape parameter. The second approach is to use the "block maxima" approach (for example maximum water level per year. This distribution is the Generalized Extreme Value (GEV), formulated as Equation 3.2, with the same parameters as Equation 3.1). If the shape parameter is assumed to be 0, then the GEV distribution simplifies to a *Gumbel distribution* (Equation 3.3, Gumbel and Lieblein [1954]). Van den Brink et al. [2005] showed that the first two methods give comparable results for estimating the

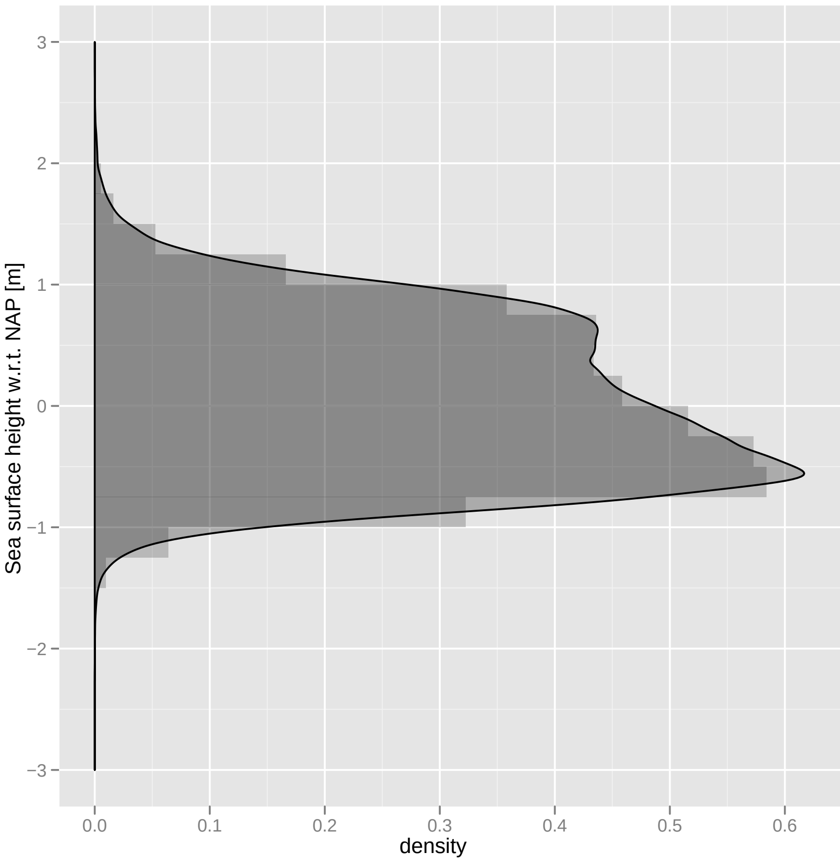

Figure 3.2: Histogram (grey bins) and kernel density (black line) of sea-surface heights as measured at the IJmuiden Buitenhaven station.

$1/10000 \text{yr}^{-1}$ water level along the Dutch coast using a threshold of 3 m and annual maxima.

$$F_{(\xi,\mu,\sigma)}(x) = \begin{cases} 1 - \left(1 + \frac{\xi(x-\mu)}{\sigma}\right)^{-1/\xi} & \text{for } \xi \neq 0, \\ 1 - \exp\left(-\frac{x-\mu}{\sigma}\right) & \text{for } \xi = 0. \end{cases} \tag{3.1}$$

$$F_{(\xi,\mu,\sigma)}(x) = \exp\left(-\left[1 + \xi\left(\frac{x-\mu}{\sigma}\right)\right]^{-1/\xi}\right) \tag{3.2}$$

$$F_{(\mu,\sigma)}(x) = e^{-e^{-(x-\mu)/\sigma}}. \tag{3.3}$$

Besides the method there are a number of other choices to be made. One can choose to estimate the extreme sea-surface height (tide + surge) or only the surge component. The quantity of interest for the coastal protection is the combination of tide and surge. Here we refer to the peak sea-surface height during a storm surge as *storm-surge level* [like Jelgersma et al., 1995, who defined the storm-surge level as relative to Normaal Amsterdams Peil (Amsterdam Ordnance Datum) (NAP)]. The term *storm tide* is also used as the extreme water level during a storm surge [NOAA, 2013] in combination with the quantity *storm surge* as the difference in sea-surface height and astronomical tide [NOAA, 2013]. The *storm-surge level* has also been used as the water level in excess of predicted tide [Ranasinghe et al., 2005].

The storm-surge level is also better for use with both the "peak over threshold" and "block maxima" approach. One can compute the surge part of the sea-surface height by subtracting the astronomical tide (under the assumption that tide is independent from storm surge height) but for historic records or for records in the form of yearly maxima this is not always possible.

Based on these two methods there are many variations and extensions described in literature. The main variations include:

MULTIVARIATE describing the extreme value of multiple quantitities at the same time, mostly surge height, wave height. As most quantities are highly correlated, given the occurence of a storm, this is essential when describing multiple quantities.

NON STATIONARITY under the assumption of changing storminess or changing sea-level it make sense to take this variation over time into account. Examples include:

SPATIAL VARIATION extreme events are often recorded over multiple tide gauges. By combining the records of these stations, taking into account the spatial correlations, one can make more accurate estimates [see for example Bruun and Tawn, 1998; de Haan, 1990; de Haan and Ferreira, 2006].

As an example we will apply the "peak over threshold" approach here. For this we need a relatively short series (a few decades) of high frequent (hourly) measurements. Before we fit the GPD distribution we need a series of independent events over the threshold. Having independent events is important because that is one of the assumptions of the distribution fitting method (a poisson point process) [de Haan and Ferreira, 2006]. The threshold is important because we are assuming that the observations of higher water levels are more representative than the more average water levels. This makes sense here because the higher water levels occur during a storm and the more average water levels occur every day.

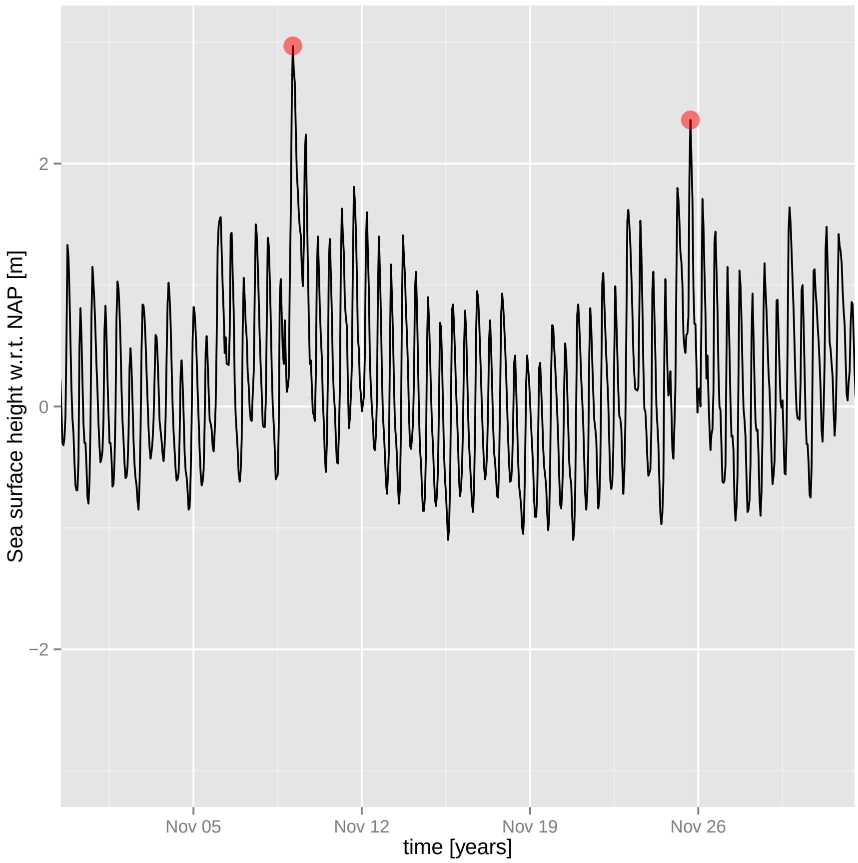

Figure 3.3: Detection of unique storm events (red dots) in sea-surface heights using a window of 3 days and a threshold of 2 meters.

Choosing a threshold is a bit arbitrary but there are some pointers. From a physical point of view it makes sense to choose a threshold over the high tide level (at IJmuiden 1.5 m). One can look at the sensitivity of the shape parameters of the distribution on the threshold. In this case the parameters become very sensitive at a threshold greater than 2.2 m. Philippart et al. [1995] used a criterion of a threshold that should yield at least 2 observations per year. That gives us a threshold of 1.82 m. This threshold is used, because it meets the other criteria as well and makes the results easier to compare. In total 121 peaks over the threshold are selected in the time window 1981 – 2010. We cluster the observations by looking at the highest water level in a window of 3 days. Clustering is done by starting a cluster once the water level goes over the threshold and stopping the cluster the last time the water level goes below the threshold within the 3 days from the maximum in the cluster. The highest value within a cluster is defined as the peak. The result of this clustering for the month November 2007 can be seen in Figure 3.3.

Equation 3.1 can be fitted through the observations, taking into account the number of events of $2\,\mathrm{yr}^{-1}$. Based on the fitted shape ($\xi = -0.06 \pm 0.10\,\mathrm{m}$) and scale ($\sigma = 0.26 \pm 0.04$) parameters a confidence interval can be computed. In this example we do this by a bootstrap method, based on 200 randomly generated values per return level. A smooth curve (loess) is drawn through the simulated return levels. There are a few things to note about the results, as shown in Figure 3.4. First the estimated return level based on the last 29 years is about 1 m lower than based on the 101 yr before that. This can be attributed, at least partially due to fact that the largest storms have occurred before 1981, for example 1916, 1953 and 1976. The confidence interval does not include the older estimate of the period 1884–1984. This implies that the storm-surge levels in the last 30 years were significantly lower than in the earlier period. Which could indicate a reduced storminess, see the discussion in Section 4.2.

The observed return period can be computed in different ways. A common way is to compute the return period of the largest event that occurred in n yr as $1/(1-(n-1)/n)$ but in Figure 3.4b the observed probability is computed as $1/1-(n-0.35)/n$. The different options are discussed by Benard and Bos-Levenbach [1953].

Computations were done using the R software [R Development Core Team, 2009] with the ismev [Coles and Stephenson, 2010] package and a modified version (custom log-likelihood method for confidence bounds) of the fExtreme [Wuertz, 2009] package.

This answers Question 3.3.1

3.2 Improving the $1/10000\,\mathrm{yr}^{-1}$ storm-surge level estimate using 18th century storm-surge data

This section is based on the article "Using 18th century storm-surge data from the Dutch Coast to improve the confidence in flood-risk estimates" [Baart et al., 2011a].

Although the original calculations on the safety level by van Dantzig [1956] resulted in a safety level determined in meters, the safety level by law is defined as a probability. This makes sense because it is a measure that is robust against changes of the coast and climate and can be uniformly applied to the coast. It is also a measure that is indifferent to the causes of an extreme sea level.

One problem with the safety level defined as a probability is that it is hard to give a solid estimate of the corresponding storm conditions that the coast should withstand.

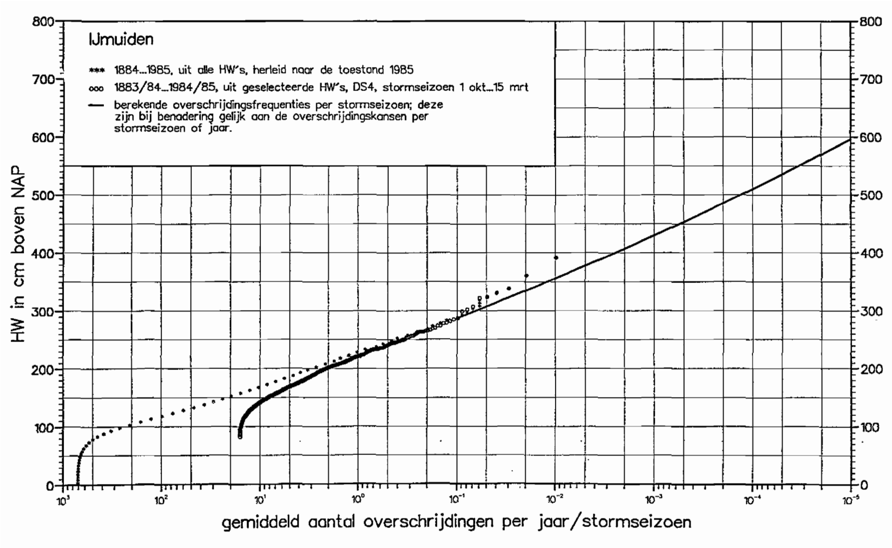

(a) Based on the period 1884–1985 [Philippart et al., 1995]

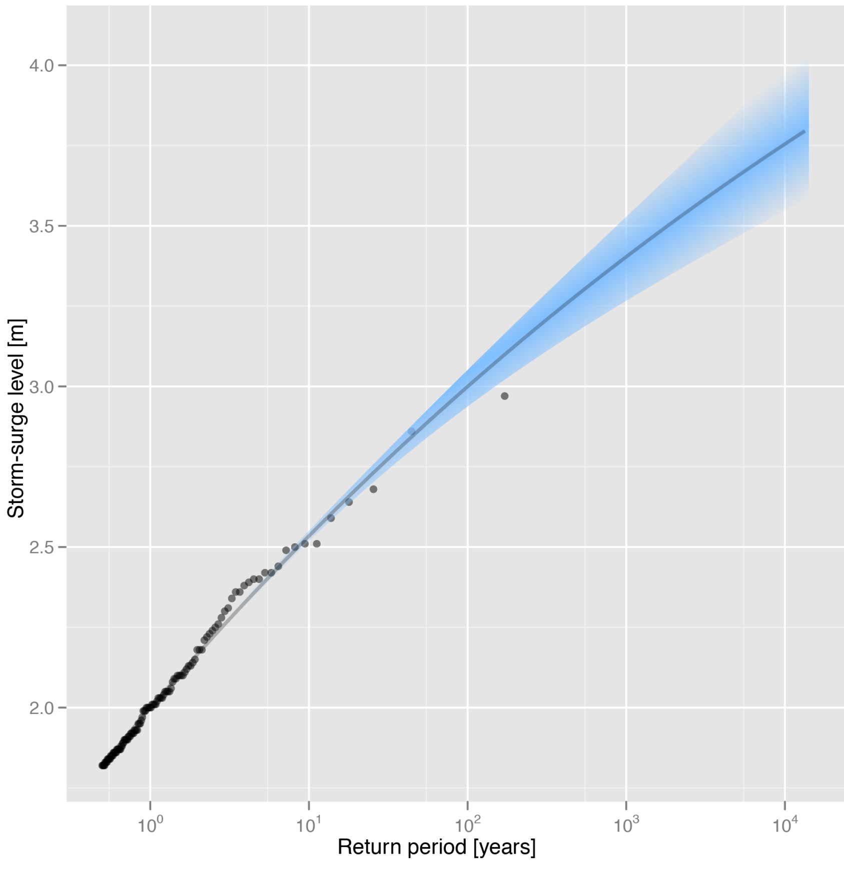

(b) Based on the period 1981–2010

Figure 3.4: Two analyses of the $1/10000\,\mathrm{yr}^{-1}$ storm-surge level for IJmuiden

When compared to the safety level that are used in other countries the low return period might appear unreasonable. The reasonability lies in that it is the result of a cost benefit analysis, wheighing the costs of maintaining a safety level versus the economic value of the interland. One could argue that it is inadvisable to concentrate most of the economic activity in an area prone to flooding. This however also has many benefits, such as direct access to the major ports and rivers for transportation. The dunes that protect the greater part of the Dutch coast provide a self-organizing, self-repairing protection system, keeping the maintenance cost low.

The effective design of the coastal defence depends on how high a $1/10000 \mathrm{yr}^{-1}$ storm surge will be. Using extreme value statistics, van den Brink et al. [2004] showed that the confidence interval of the $1/10000 \mathrm{yr}^{-1}$ surge is between 2.9 and 6.5 m for the Hoek van Holland station (Figure 3.5). Using the upper limit of this rather large confidence interval would likely lead to an unnecessarily expensive design of the coastal defence system. One could neglect the large confidence interval and just use the most likely estimate. This would still give a valid cost estimate if the cost is a linear function of water height, but this is not likely the case.

Figure 3.5: Map of the locations mentioned in this section. The Christmas flood of 1717 is analysed at the location of Egmond aan Zee. The 1775 storm is analysed at the Heemskerk location.

A better alternative would be to reduce the size of the confidence interval. This can be done by increasing the number of observations (the size of the confidence interval depends on $n^{-\frac{1}{2}}$, where n is the number of observations) or by introducing other variables that reduce the error in the surge estimates. In this study we focus on increasing the number of observations by adding data from discrete events described and analysed in historical records. This is possible with a relatively limited number of observations because the extreme value distribution is sensitive to the most extreme events.

Previous studies on creating a more reliable estimate of the $1/10000 \text{yr}^{-1}$ storm surges have combined data from various sources. Storm surges for which data are available can be subdivided into four groups, on the bases of surge data availability.

PRE-HISTORIC No measurements or written records are available. The effect of individual storms are traced back using geological records. Sedimentological analyses provide estimates of surge or run-up, but commonly the date of the storm cannot be constrained well. An example of a geological study on surge heights was published by Jelgersma et al. [1995], who concluded that storm surges of up to 5 m occurred in the past.

HISTORIC Written records and artworks are available and can be used to trace back the magnitude and impact of a storm. The date of the storm is usually known and the associated magnitude can be constrained from descriptions or from incidental measurements. No monitoring series of regular consistent measurements are available. Although the earliest records date from 838 AD [Buisman and Engelen, 1995], they become increasingly abundant (with multiple accounts for single events) from the 16th century onwards [Buisman and Engelen, 1996; Gottschalk, 1971]. One disadvantage of using these older records is that the exact time of the peak water level is commonly missing. Therefore, the difference between the peak water level and the astronomical tide can not always be determined. Examples of late historic records are ship logs, used for example by Wheeler et al. [2010].

MEASURED Series of measurements are available, collected by automated monitoring systems or by dedicated and trained officials. For the Dutch coast the earliest tidal station in Amsterdam was installed in 1700. Most of the main stations along the North Sea coast that are still in use were installed during the late 19th century.

MODELLED Based on variable input data, series of models are run to create a wide variety of possible storms and associated surges. Van den Brink et al. [2004] used a dataset of seasonal forecast ensemble runs that were used as samples in an extreme value analysis. Because the confidence interval is dependent on sample size, they were able to reduce the interval from 3.6 m to 0.9 m.

In this section we focus on historic storms, more specifically the greatest storm surges along the Northern Holland coast of the 18th century. We combine the results with an analysis of measured data from the 20th century. Pooling historical records with measurement series has proved useful for estimating flood frequencies for return periods > 100 yr in fluvial research [Macdonald et al., 2006]. We do not include the 19th century because including this period requires a different approach. The romanticism movement and later the impressionism movement didn't result paintings that are very useful for coastal reconstructions. Measurements from the 19th century are more prevalent but these need to be checked with special attention to possible errors and changes in for example vertical reference levels. This extra effort makes the 19th century records an interesting topic for future research.

From a statistical view, combining information on storm surges from the 18th and 20th century implies that the storms from the 18th century are from the same "population" as the storms from the 20th century. The trend in storminess is sensitive to the area and period. For example, De Kraker [2005] found that was no significant change in storm climate over the period 1400-1625 for Southern Holland. Others [Smits et al., 2005; Vautard et al., 2010] found that if there has been a change in storminess, it is more likely a decrease than an increase, based on the periods 1962-2002 and 1979-2008. The decrease can be partly attributed to increased surface roughness (for example due to urbanisation, growth of forests). Another view is that there might exist a second population of extratropical "superstorms" besides the regular population of European wind storms [van den Brink et al., 2005].

Another important aspect is the relative sea-level rise. The sea-level rise along the Dutch coast has been constant since at least 1890 (Section 4.1) and possibly longer [Jevrejeva et al., 2008]. For this study we assume a constant storminess and constant relative sea-level rise over the last century.

This answers Question 3.3.3 .

Several inventories of 18th century extreme events provide a good collection of information. Extreme water levels and related flood marks (stones with inscriptions) were listed and discussed by Van Malde [2003] and the numerous written records were assembled by Buisman and Engelen [2006]. These inventories can be supplemented by information from historical paintings. An example of such an approach is given by Camuffo and Sturaro [2003] who used paintings of Venice (Italy) to determine a constant sea-level rise between 1700 and 2000. McInnes [2008] uses art to show coastal changes along the coast of the Isle of Wight (United Kingdom).

In this study we analyse historical paintings and drawings. In addition, we combine the analytical results with information obtained from geological records, field measurements and numerical models, to constrain the estimate of the $1/10000\,\mathrm{yr}^{-1}$ water level and the associated morphological effect.

3.2.1 *The storm surges of the 18th century*

To be able to reduce the large confidence interval of the predicted $1/10000\,\mathrm{yr}^{-1}$ storm surge it is insufficient to have observations or estimates of high surges, as it is unknown for which period and ordinal an individual surge is a representative value. Is it the biggest surge in a century or is it the second biggest surge in a decade? A fixed time window and an ordering of the storms are required to improve the estimate of the $1/10000\,\mathrm{yr}^{-1}$ water level.

To determine which storm surges are the three biggest, the ordering has to be found. Several studies of historical floods [Buisman and Engelen, 2006; van Gelder, 1996; van Malde, 2003] were used to determine the order of the storm surges. The time window used in this study is the 18th century and we try to estimate the three highest storm surges along the Northern part of the Holland Coast. The two most severe storm events occurred in 1775 and 1776. The storm surge of 1715 is also designated as a moderately severe storm [van Gelder, 1996], but for the northern part of the Netherlands it was not so severe. For the study area the 1717 storm is ranked the third biggest of the 18th century as shown in Table 3.1.

For the three biggest storm surges (1717, 1775, 1776) we reconstruct the peak water level. For the 1717 storm we use paintings as our main source. For the 1775 we use geological records. The 1776 storm is estimated on the basis of the average difference of reported water level from the 1775 and 1776 storm.

Christmas flood 1717

Lang and Homann [1963] recount the conditions during the storm of 1717. An extract:

> On the 25th of December, around 1am, the NW storm increased rapidly and abruptly in strength until it formed a hurricane of such proportions that it seemed as if the earth was shaking. The sea was whipped to such an extent that several skippers reported that it was no longer possible to distinguish air and water. The hurricane lasted all night and did not lose much of its strength during Christmas Day. The evening was marked

Table 3.1: Storm surges of the 18th century

Year	Classification [a]	Order [b,*]
1715	D	5 [c]
1717	D	3
1741	/	4 [d]
1775	D	1 [e]
1776	C	2 [f]

[*] Because several different-sized inches were used in the 18th century (varying in length between 0.024 and 0.027 m), it is not always clear what the exact metric translation is. Hence some of the notes below are given in inches. These values are only used to determine the ranking in the order column.

[a] Based on van Gelder [2000] A: very severe floods; B: heavy floods; C: less heavy floods; D: small floods.

[b] For the North Holland coast

[c] In Amsterdam "0.31 m lower than 1717"; in Harlingen "9 inches lower than 1717"

[d] In Amsterdam and Rheede the water level "has not been so high since 1717"; in Amsterdam"7 inches lower than 1717"; "3 inches less than 1717" [van Malde, 2003], no comparison with 1715 was found

[e] In Amsterdam "as high as in 1717"; in Elburg "this flood is far higher than that of 1717"; in Delfshaven: flood stone: NAP +2.675 m [van Malde, 2003]

[f] Some reports indicate that this storm resulted in a higher surge than 1775, for example in Beulake (village drowned in 1776), "1 feet higher than 1775", Delfshaven "higher than in 1775", flood stone: NAP +2.704 m [van Malde, 2003]. On average for Northern Holland coast records the water level was 0.2 m lower.

> by severe thunder-, rain- and hailstorms. The storm kept blowing from the NW direction [...] until the 26th of December. In the morning of Boxing Day the storm lost some of its strength, but around 3pm the storm regained some of its strength and brought a downburst with rain and hail. It was not until the 27th that the weather cleared and the sun reappeared.

The storm caused major floods in the northern Dutch provinces Friesland and Groningen, in northern Germany and in Denmark. Extensive damage reports were made after the storm (Extract van, 1717b). The number of victims exceeded 10,000.

Because the damage and number of casualties were so great the 1717 storm is well documented. Information about the characteristics of the storm and its effect can be found in incidental measurements, maps, one flood mark and historical records such as letters and poems. A brief overview of the historical records of the 1717 storm was given by Lang and Homann [1963]. A very detailed analysis of the storm and the effects in Germany can be found in Jakubowski-Tiessen [1992]. Associated surge levels are included in an inventory of storm surges made by Van Malde [2003]. Temperature records are available through the Royal Netherlands Meteorological Institute [cf. Buisman and Engelen, 1995]. Several documents provide narrative overviews and damage reports, including Nette aantekeningen [1717a]; Extract van [1717b]; Cramer von Baumgarten [1817]; Bógaert [1719]; Specht [1740]; Schenk [1740]; van Brussel [1776].

Focussing on our area of interest, the Northern Holland coast, and in particular on Egmond aan Zee (Figure 3.5), paintings and drawings of Egmond beach, before and after the storm, were analysed to reconstruct the coast.

Because there is such a large collection of paintings available for the 1717 storm, we were able to reconstruct pre- and post-storm profiles of Egmond beach.

The post-storm profile was measured on the 8th of February 1718, just over a month after the storm. The measurement recorded the angles and elevations of the beach and the adjacent dune relative to mean high water.

Reconstructing the pre-storm profile required a combination of different data resources. Starting point was the analysis of a collection of paintings and drawings available of the Egmond aan Zee area between 1600 and 1700. A map of 1686 was used to determine the position of the church, the most prominent structure of the town, located near the beach. Most of the painters chose a view where at least the church tower was visible without obstructions. The church was positioned in a three-dimensional model of the coastal town. The paintings were aligned using the church as a reference point (Figure 3.6).

Structural coastal erosion can be seen in the fact that the paintings from the earlier part of the 17^{th} century were painted from a vantage point farther from the coast than that of those from later times. The positioning of a series of pictures from 1620 in the 3D model gives an estimate of the contemporary coastline. From comparing the 1686 map with reconstructions based on the older paintings, we estimate that the structural retreat of the coast was about 66 m in the period 1620–1686, i.e. $1\,\mathrm{m\,yr^{-1}}$. This rate corresponds to the rate reported by de Ruig [1998]. When using this rate to extrapolate the map of 1686 to 1717 we obtain an estimate of the width of the dune top would have been approximately 17 m (48 m in 1686 minus $31 \times 1\,\mathrm{m\,yr}^{-1}$, see Figure 3.6). The beach width is assumed to be the same as that of the post-storm profile and angles of the beach and dune are assumed to have been similar to the slopes from the average of that same area between 1963–1973 [de Graaf et al., 2003, profile 7-3800 from the Dutch Annual Coastal Measurement (JARKUS) dataset].

As no paleobathymetry information is available both the pre- and post-storm profile up to mean high water are based on the bathymetry from the 1963 profile of the JARKUS dataset.

To get a rough estimate of the precision of the paintings, we analysed the intra- and inter-painter variance. As reference points we use the upper two parts of the Egmond aan Zee church tower. This church is present on 80 of the 96 paintings and drawings. The ratio between the height of the upper and second highest part of the steeple are determined for each image. The average ratio was 0.95, with a standard deviation overall of 0.22 (Figure 3.6). Images with ratios below 0.7 and above 1.2 were not included in the final analysis.

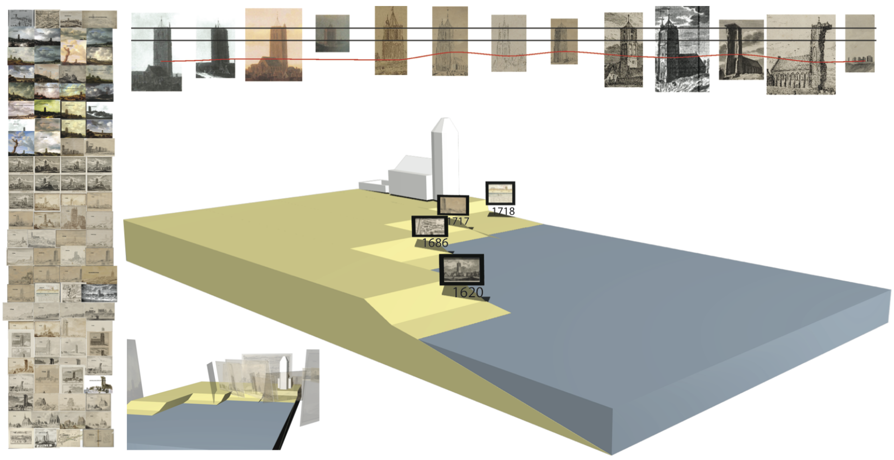

Figure 3.6: Left: overview of the paintings and sketches used in the reconstruction. Top: determining the painter reliability by comparing the ratio between the upper two parts of the Egmond aan Zee church tower. Bottom: 3D reconstruction of the coastal town of Egmond aan Zee. Center: four reconstructed profiles for the years (from front to back) 1620, 1686, December 25^{th} 1717 and February 8^{th} 1718.

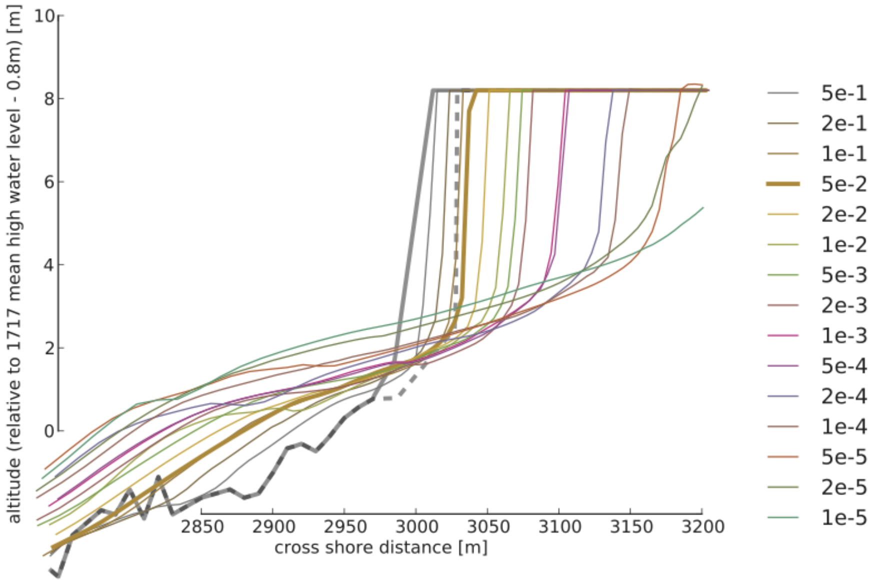

Figure 3.7: Modelled and reconstructed profiles of the 1717 storm at Egmond aan Zee. Gray solid line: pre-storm reconstructed profile. Gray dashed line: post-storm reconstructed profile. Colored lines: modelled profiles. Thick colored line: modelled profile that best matches the pre- and post-storm reconstructions within the measured area with an occurrence probability 5/100 per year (return period 20 years).

The pre-storm profile was used to set up an XBeach model [cf. Roelvink et al., 2009]. XBeach is a morphodynamic model capable of capturing the physical processes in the nearshore that cause most of the coastline change during storm surges. The XBeach model uses the following parameters as input: water level, significant wave height, peak wave period, grain diameter and bathymetry/topography. The result of interest here is an estimate of the post-storm profile. Starting with the pre-storm profile, the XBeach model was run using different storm-surge levels. The surge levels, wave height and peak periods were drawn from the same distribution that is used for the safety-assessment method [WL | Delft Hydraulics, 2007], as provided by OpenEarth [van Koningsveld et al., 2010]. The storm-surge level with the erosion closest to the "observed" erosion was selected, as judged from the erosion volume. This gave an estimated magnitude of 5/100 per year (Figure 3.7), which corresponds to a water level of 3.1 m together with a significant wave height of 6.8 m and a peak period of 10.4 s.

This answers Question 3.3.2

The storm surge of November 15, 1775

The largest storm surge of the 18th century was caused by the November 1775 storm. Buisman [1984] and Buisman and Engelen [2012] described the storm as follows:

> In the late afternoon of November, 14^{th} and the night of November, $14^{th}/15^{th}$ a severe WNW-NW storm raged accompanied by heavy rain, hail and thunder. Sea level rose higher than every flood before, especially higher than the severe storm surges of 1682 and 1717. [..] At the North Sea coasts, dune damage developed, e.g. near Terheyde and Scheveningen ("half of it covered by the sea"). Part of the Hondsbossche sea defence is destroyed. [..] Many ships were wrecked, especially on the North Sea. "Along the entire beach one saw nothing but ship wrecks, rigging, cargo and bodies being washed to the shore." 200 Ships were lost!

More records exists for the 1775 storm than for the 1717 storm. Unfortunately the church at Egmond aan Zee was no longer available as a reference point for a 3D reconstruction because the steeple fell into the sea during the storm surge of 1741. In 1746 a new church was built at the landward end of the village. Most relevant records for the 1775 event were gathered by interested individuals who made meteorological and hydrodynamic measurements. Historical records about morphology, such as the post-storm profile for 1717, are not known for this storm.

New useful evidence about the 1775 storm became available recently. After a storm surge hit the Dutch coast on November 9, 2007, old storm-surge deposits were discovered in the eroded dunes near Heemskerk (Figure 3.5). These deposits were recognized as the remnants of one or two historical storm surges. The layers consisted of sand, shells and bricks. Details of the layers and the associated reconstruction were provided by Cunningham et al. [2011]. Luminescence dating placed the storm-surge layers at the end of the 18^{th} century [Cunningham et al., 2009, 2011]. Major storm surges occurred in 1775 and 1776. The maximum observed water level in Petten (the location closest to Heemskerk with observations) was the same. So no clear distinction was possible between the two storm surges. In the modeling used to reconstruct the storm it was assumed that the deposits were from the 1775 storm surge [Pool, 2009].

Other useful information used to reconstruct the 1775 storm damage to the coast are the wind-force observations from 20 km south of Heemskerk [KNMI, 2011, maximum wind force 14 "noppen", 17.2 – 20.7 m/s], the maximum storm-surge-related water level recorded at Petten (25 km north of Heemskerk, 2.8m above the 1775 MSL) [van Malde, 2003] and the median grain diameter, as derived from a sieve analysis of sand in the deposits. The water-level observation comes from a 1793 report on the sea-defence system at Petten and is not accurate [Conrad, 1864]. Conrad emphasized that the reference level used was about 1 m too high, requiring an upward correction of the surge level, and that open-coast storm-surge measurements made before the 19th century are commonly inaccurate.

	1717	1775
Wind	general path + duration	3x per day observations
Water level	Inundation map	Water levels in Petten
Grain distribution	No data	Grain distribution from storm-surge layer

Table 3.2: Overview of available data per storm

Like for the 1717 storm, we need to constrain the values of the relevant parameters to be used as input for the XBeach model. The 1775 event has rather detailed information available on the driving conditions (wind force) but little on the post-storm profile. The approach to fill in the missing gaps therefore differs from the approach used for the 1717 storm. Forward modeling starting from the wind force was used instead of inverse modeling.

The water levels, significant wave height and peak period all depend on the magnitude of the storm. The wind speeds that were measured in Zwanenburg, a land-based station south of Egmond, were used as stochastic variable. They were translated to North Sea wind speeds using the open water transformation [van Ledden et al., 2005] based on the Charnock's relation [Charnock, 1955], an empirical expression for aerodynamic roughness. These offshore wind speeds were used to estimate the wind induced surge using the Weenink method [Weenink, 1958]. The tide was estimated on the basis of water-level observations made at Katwijk during the period 1737–1739. The wave characteristics were estimated using the Sverdrup-Munk-Brettschneider growth curves [Holthuijsen, 2007]. The median grain diameter was derived from the grain-size distribution of the storm-surge deposits [Cunningham et al., 2009]. The palaeobathymetry was based on a combination of JARKUS data and sounding data [de Graaf et al., 2003], as for the 1717 scenario, assuming that the bathymetry did not change much over the period 1775–2011. The validity of this assumption is likely, in the light of a comparison of the recent bathymetry with a reconstruction of historic contour lines by Haartsen et al. [1997]. For the construction of the palaeotopography the 2007 data were used from the Actueel Hoogtebestand Nederland (AHN). The beach and the strongly anthropogenic frontal dune were removed, assuming that the topography behind the dune resembles the topography in 1775 (before frontal dunes were under heavy anthropogenic influence). From this reconstructed bathymetry and topography a characteristic transect was selected for further analysis. The same XBeach model was used as for the 1717 storm, but with different boundary conditions and paramater settings. Unlike for 1717, the goal was not inverse modeling the erosion profile but to assess-

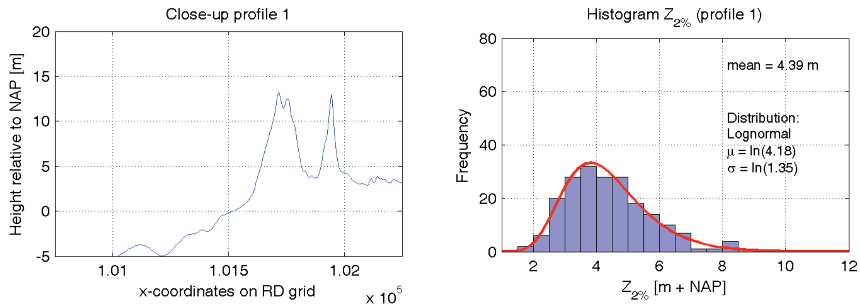

Figure 3.8: Left panel: close-up bathymetry profile 1. Right panel: histogram Z2% and best-fit distribution for profile 1

ing what type of storm could have resulted in a surge and run up capable of depositing the shell beds that were exposed in the dune scarp following the 2007 storm surge. The 2% exceedance level of the run-up is assumed to be the level where the shell would have been deposited.

We find that the storm profile of the confidence interval of the run-up level includes the height of the storm-surge layer at 6.5 m (Figure 3.8). Therefore we assume that the found shell deposits can indeed be from the 1775 storm. Using the exceedance lines for run-up levels as calculated by Philippart et al. [1995] the associated storm surge has a 3/10000 per year exceedance probability.

The storm surge of November 21, 1776

This storm surge occurred only one year after the major storm surge of 1775. This storm surge is measured on several locations along the Dutch coast. We estimate that the storm of 1776 resulted in a storm surge approximately 0.2 m lower than the 1775 storm surge. This difference is based on the average of the differences of locations where both the 1775 and 1776 stations were recorded [van Malde, 2003].

The corresponding exceedance probability would be 8/10000 per year, based on the probability distributions estimated by Philippart et al. [1995].

3.2.2 *An updated confidence interval for the 1/10000yr^{-1} storm surge*

To improve the confidence interval associated with the extrapolation of the monitoring series of water levels that started in the late 19th century we used a method comparable to the one developed by Van Gelder [1996]. From the three new data points (water levels for 1717, 1775, 1776), the a posteriori distribution for the 1/10000yr^{-1} storm surge can be created. The availability of estimates of the three highest annual water-level maxima of the 18th century implies that the other 97 years must have had lower annual maxima than the 1717 storm surge.

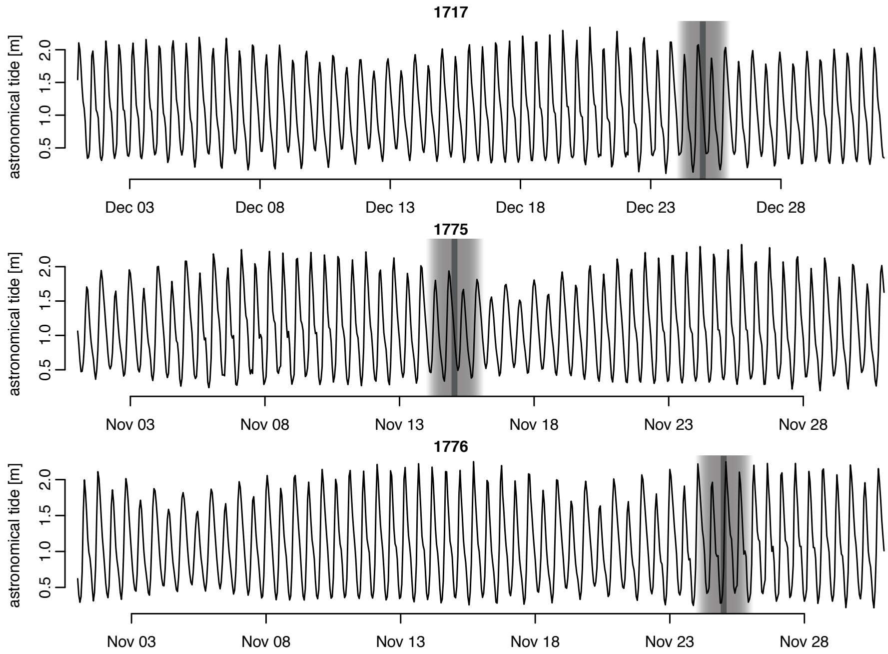

Figure 3.9: Astronomical tide for the IJmuiden station during the storms of 1717, 1775 and 1776 (marked in grey).

We used this censored information to create the new distribution for high-end storms along the northern part of the Holland coast. We used the block-maxima approach in order to integrate the historical observations with the water-level monitoring series.

The reconstruction in this study has resulted in new estimates for the magnitude of the three biggest storm surges in the 18th century. The characteristics of the storms are shown in Table 3.3. The return periods are derived from the data in Table 3.3, using the normative storm calculation method [WL | Delft Hydraulics, 2007].

By using this information we were able to constrain the confidence interval for the $1/10000\text{yr}^{-1}$ storm surge. Using the Gumbel method, the confidence interval decreased by 30% because the number of observations increased almost twofold.

For the GEV approach, with a free shape parameter, the confidence interval is much larger. The large confidence interval here is caused by the large standard error of the shape parameter. This can be seen in Figure 3.10 that shows the records for Egmond, based on a combination of a inverse-squared-distance weight of the records from the IJmuiden station Noordersluis ($\leqslant$1981), IJmuiden Buitenhaven (>1981) and Den Helder.

Because two of the three storms from the 18th century all have a lower observed return period than their estimated return period, the GEV fit results in a positive shape parameter. This positive shape also results in a higher estimate of the $1/10000\text{yr}^{-1}$ water level (6 m combined versus 4.6 m for the 20th century).

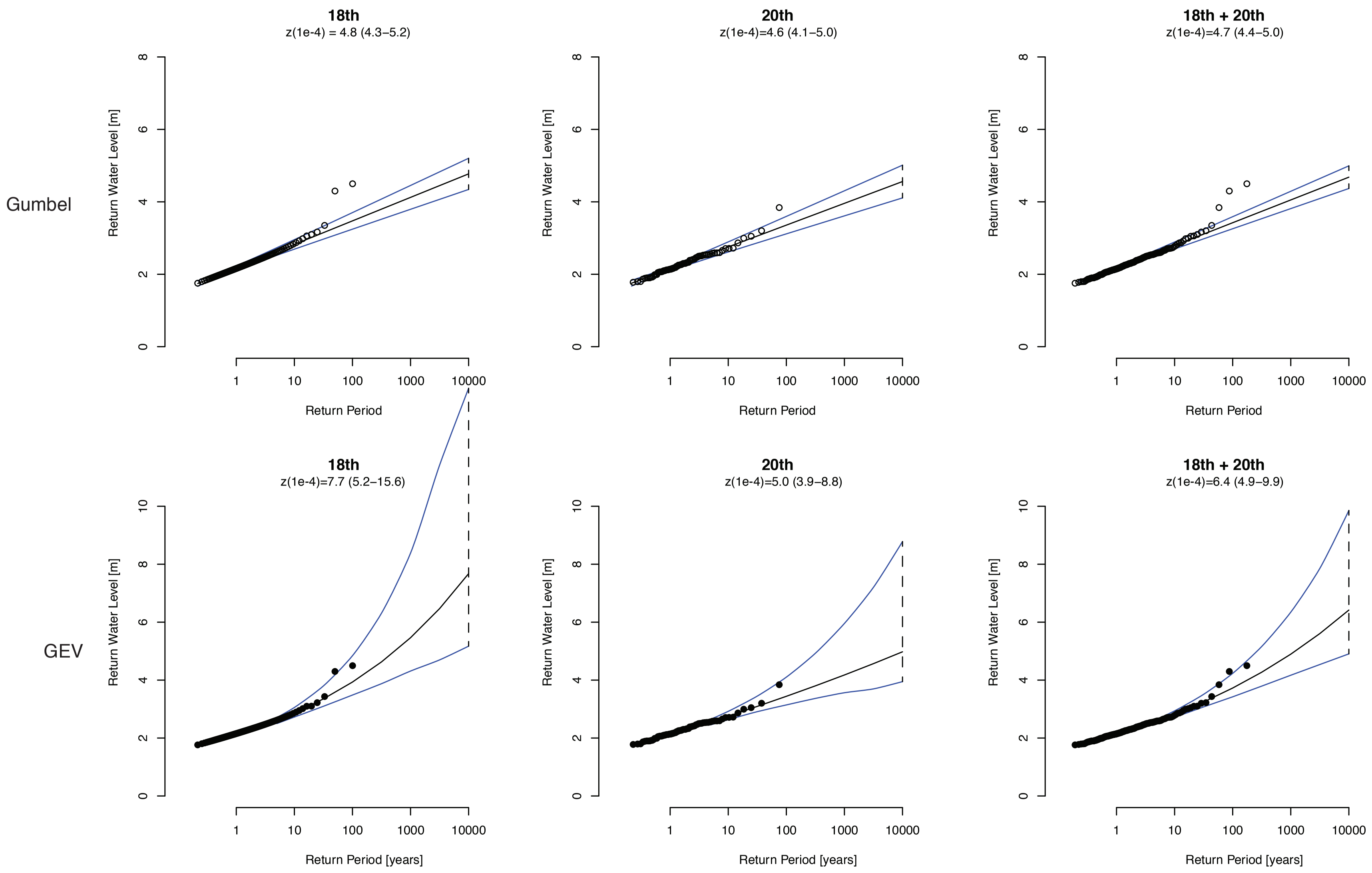

Figure 3.10: Return level plot for the location Egmond for the period 1932–2010, 1700–1800 and the combined fit. The upper row represents a fit using the Gumbel distribution (GEV distribution with $\xi = 0$). The lower row represents a fit using the GEV distribution using a free ξ parameter. The circles represent observed (1932–2010) and estimated (1700–1800) water levels plotted against the observed return period. The black solid line represents the fitted return water level as a function of the return period. The outer blue lines follow the lower and upper bound of the 95% confidence interval. The vertical dashed line marks the confidence interval for the $1/10000\,yr^{-1}$ water level.

Table 3.3: Estimated magnitude of the three largest storm surges of the 18^{th} century at the Northern Holland coast

Year	Water level	Wave height	Wave period	Return period
1717	3.1 m	6.8 m	10.4 s	20 years
1775	4.6 m	8.8 m	13.9 s	3300 years
1776	4.3 m	8.5 m	13.4 s	1300 years

3.2.3 *Discussion*

The reconstructed water levels from the three storms are very high. They correspond to return periods of 20 yr, 3300 yr and 1300 yr as derived from extrapolation of the monitoring records. Clearly, caution is required when combining these water-level return periods with the water levels measured by tide gauges. A number of possible causes of the apparent mismatch are inaccurate reconstruction and parameterization, coincidence or change in storm climate.

It is difficult to give a solid estimate of the precision of these numbers, but based on the painter reliability and on the skill of the XBeach model (used with a lot of unknown inputs), the standard error of the high-water estimates could be around 25% or 1 m. So it could well be that the storms were in fact smaller than estimated here. Lower peak levels would of course result in a lower and narrower confidence region. It is difficult to give a proper estimate of the probability that three such large storms have occurred in the 18^{th} century, since such an assessment cannot be made solely on the basis of the 20^{th} century monitoring series.

Research into changes in storminess over periods of decades has not shown any clear indications that the coastal storminess changed, see Section 4.2. Research into changes over the period of three centuries shows a decrease in storminess. This can be seen in relation to the stormy end of the Little Ice Age [e.g. Hass, 1996].

Although higher storm surges were found in an earlier century than the last one, this research should not be used to conclude that the coastal storminess decreased. The best approach to analyse changes in storminess over a multi century timescale would be to construct a meta-analysis, using different types of records, over a wider area, as discussed in Section 4.2.

3.2.4 *Conclusions and recommendations*

In this study we use historical records, a 3D reconstruction of Egmond aan Zee and storm-surge layers in the dunes to reduce the size of the confidence interval associated with the $1/10000\text{yr}^{-1}$ storm surge as determined by extrapolation of tide gauge monitoring series. This approach was successful in the procedure where the confidence interval was based on a Gumbel distribution, but not in the GEV approach. For the GEV approach the estimate of the $1/10000\text{yr}^{-1}$ water level is much higher and the confidence interval is slightly larger if the historic reconstructions are included with the GEV approach. One possible cause for the larger effect of storms can be that the storminess has reduced as discussed in Section 4.2.

This large difference between the two statistical methods is indicative for the high sensitivity to the assumptions that can be made when estimating the $1/10000\text{yr}^{-1}$ storm surge. Using the historic and measured data sources one assumes that the events observed are representative for the population of events.

A logical step for further research would be to include storms from the other centuries where historic records are available. Also, the statistical method to include historical observations can still be improved, perhaps by applying a Bayesian approach to the combination of measurements, historical records and model simulations.

Although partially successful, our approach is less effective in increasing the confidence than the method used by Van den Brink et al. [2004] as the confidence interval depends on the number of (real and modelled) observations or datapoints. The maximum number of observations that can be extracted from history is limited by the length of history itself, which is much shorter than the return period of the design storm used in safety assessments of the Dutch coast.

The method presented in this study and the alternatives have strong assumptions. Simulations are limited by the physical assumptions that are put into the simulation model. Geological records can provide additional insight into storm surges that left geological signatures, but from a statistical point of view these are hard to incorporate as the representative period is unknown. Using measurements from other coasts to create a combined distributions of multiple coasts has a questionable generalizability.

Paintings and other images are a valuable data source in determining coastal change and, indirectly, storm-surge magnitude. Although the paintings are not always reliable, series of images covering extensive time periods provide a solid basis for reconstructing structural erosion. When combined with data from monitoring and measurement surveys, they may be very useful in many coastal areas in the developed world.

This answers Question 3.3 .

4

DESIGN LIFETIME & POLICY ANALYSIS: DECADAL SCALE CHANGES

Contents

This chapter describes the analysis of two quantities that are used for the design lifetime of coastal interventions the sea-level trend and storminess. The local erosion trend is used to show how confidence intervals can be used for policy analysis.

4.1 DESIGN LIFETIME: THE EFFECT OF THE LUNAR NODAL CYCLE ON SEA-LEVEL RISE ESTIMATES

This section was published as [Baart et al., 2012c]

The current and expected sea-level rise rates are important drivers for policy makers dealing with the long-term protection of coastal areas and populations. An example of an area where sea-level rise is important is the Dutch coast. There are several interventions planned to deal with the expected accelerated sea-level rise, which will cost up to €1.6 billion /yr until 2050 [Kabat et al., 2009]. The long history of tidal records and the economic value in the area below sea level make the Dutch coast an interesting case to analyse sea-level measurements and scenarios and to compare the local with global estimates.

Local trends

Sea-level changes are usually reported in the form of trends, often determined over a period of one or more decades. For the Netherlands an important trend was given after the 1953 flooding, when a 0.15 cm to 0.20 cm yr^{-1} relative sea-level rise was estimated for the design of the Delta Works. The first Delta Committee report [Deltacommissie, 1960] referred to this change rate as "relative land subsidence". Relative sea level, the current term, is the sea-level elevation relative to the continental crust as measured by tide gauges. Absolute sea level is relative to a reference ellipsoid and measured by satellites. A recent estimate [van den Hurk et al., 2007] showed that the relative sea level rose with a rate of 0.27 cm yr^{-1} over the period 1990-2005. The land subsidence at the Dutch coast varies around 0.04 cm yr^{-1} $\pm$ 0.12 [Kooi et al., 1998].

Local forecasts

Because coastal policy is shifting from observation-based reaction to scenario based anticipation [Ministerie van Verkeer en Waterstaat, 2009] it is interesting to compare observed trends with predicted rates. Sea-level scenarios often predict not only rise but also accelerated rise. The earliest Dutch scenario, published after the 1953 storm, forecasts a rise of several meters due to Greenland ice melting over an unspecified period [Deltacommissie, 1960]. Van Dantzig [1956] used a more concrete number of 70 cm for the next century in a related publication. The latest study by the Royal Netherlands Meteorological Institute (KNMI) [van den Hurk et al., 2007; Katsman et al., 2008] resulted in a low and a high scenario. The low scenario gives an expected rise of 0.25 cm yr^{-1} in the period 1990 through 2050 and 0.32 cm yr^{-1} for the period 2050 through 2100. The high scenario predicts 0.58 cm yr^{-1} and 0.77 cm yr^{-1} for the same periods. A high-end estimate of 2.02 cm yr^{-1} was reported by the second Delta Committee in 2008, based on the Intergovernmental Panel on Climate

Change (IPCC) A1FI scenario for the period 2050 through 2100 [Deltacommissie, 2008, see Figure 4, page 24]. This extreme scenario was used to assess the sustainability of the Dutch coastal policy. The study was extended in Katsman et al. [2011], where the elasto-gravity effect was added. When ice masses on land melt, the resulting melt water is not expected to distribute evenly over the oceans.

Global trends

The global measurement of relative sea-level started in 1933 when the Permanent Service for Mean Sea Level (PSMSL) began collecting sea-level data from the global network of tide gauges [Woodworth and Player, 2003]. Trends based on these measurements vary around 0.17 cm yr^{-1}. For example, Holgate reported 0.145 cm yr^{-1} over the period 1954-2003 [Holgate, 2007] and Church et al. reported 0.18 cm yr^{-1} over the period 1961-2003 [Church et al., 2008]. With the launch of the TOPEX/Poseidon satellite in 1992, measurements of absolute sea level have become available with a near global coverage and high resolution in time and space. These measurements were used in the latest estimates, summarized in the IPCC report [Bindoff et al., 2007], giving a 0.31 cm yr^{-1} absolute sea-level rise over the period 1993-2003. Despite the apparent difference the reconstrcutions based on tidal measurements compare well with satellite data when accounting for corrections, start of time window and the geographical location [Prandi et al., 2009].

An open question, which we'll address here, is why the analysis of individual tide gauges does not show this acceleration [Houston and Dean, 2011b].

Global forecasts

Of the global scenarios for future sea-level rise, the most influential are the current model based IPCC scenarios [Bindoff et al., 2007]. The estimated rise varies from 0.17 cm yr^{-1} (lower B1) through 0.56 cm yr^{-1} (higher A1FI) over the period 1980-1999 through 2090-2099 [Meehl et al., 2007]. All scenarios result in a most likely sea-level rise that is higher than the average rate of 0.18 cm yr^{-1} over the period 1961 to 2003.

Detecting acceleration

Even though sea-level rise acceleration was expected to become apparent in the early years of this century [Woodworth, 1990], there is no overall statistical significant acceleration present, other than in the early 20th century [Church and White, 2006; Jevrejeva et al., 2008]. The probability of detecting an acceleration in sea-level rise is low, due to the effect of decadal variations [Douglas, 1992; Holgate, 2007].

Accounting for decadal variations can therefore enhance the detection power of acceleration.

The nodal cycle

One such decadal variation is the lunar nodal cycle. The tide on the Earth is driven by six different forcing components with periods varying from 1 day to 20940 years. The fifth component is the 18.6 yearly lunar nodal cycle [Doodson, 1921]. The term nodal cycle is best explained while looking up from the Earth. Consider the node as the intersection of the ecliptic plane, that follows the path of the Sun, and the orbital plane, that follows the path of the Moon. This node moves westward, making a circle every 18.6 years.

The main effect of this cycle is that it influences the tidal amplitude [Woodworth, 1999; Gratiot et al., 2008]. There are indications that the 18.6 yearly cycle also influences regional mean sea level, for example at the Dutch coast [Dillingh et al., 1993] and a collection of other tidal stations [Lisitzin, 1957; Houston and Dean, 2011a]. Global variation studies on tide gauges using spectral analysis by Trupin and Wahr [1990] and on satellite data using harmonic analysis [Cherniawsky et al., 2010] also indicate a cycle in regional mean sea levels.

Observed tide is often compared with the equilibrium tide. The equilibrium tide is the tide that would exist if the earth were completely covered by water and if there were no friction. The equilibrium tide theory builds on the work of Doodson [1921]; Cartwright and Tayler [1971]; Cartwright and Edden [1973].

Following Rossiter [1967], we have Equation 4.1 for the equilibrium elevation ζ and the resulting nodal amplitude A (mm), with M mass of moon in kg, E mass of earth in kg, e mean radius of earth (km), ρ mean distance between earth centre and moon centre (km), λ latitude in radians, N the longitude of the Moon's ascending node (from $18°18'$ to $28°36'$.). The phase ϕ is $0°$ for $|\lambda| > 35.3°$ and $180°$ for $|\lambda| <= 35.3°$.

$$
\begin{aligned}
\zeta &= \frac{9}{8}\frac{M}{E} e \left(\frac{e}{\rho}\right)^3 \left(\sin^2\lambda - \frac{1}{3}\right) \cos \qquad (4.1) \\
N' \times 0.06552A &= 26.3 \left|\sin^2\lambda - \frac{1}{3}\right| \\
M &= 5.9736e24 \\
E &= 7.3477e22 \\
e &= 6371000 \\
\rho &= 384403000
\end{aligned}
$$

Proudman [1960] showed, that the nodal tide should follow the equilibrium tide with regard to friction. The earth tide should also be taken into account. Rossiter [1967] corrected by a factor of 0.7 to allow for the effect of a yielding Earth. This is also the approach used by Pugh [1987] and [Cherniawsky et al., 2010]. The correction factor is based on the combined effect of the change in the height of the equilibrium level above the solid earth, given by the formula $1 - k - h\frac{\Omega_p}{g}$, where k and h are the love numbers [Love, 1909]. The elastic response of the earth has an amplitude of $h\Omega_p/g$, where h is a known elastic constant, Ω_p is the gravitational potential and g is the gravity constant. When the tidal periods become longer not only the elastic response but also the viscose response is important and therefore the factor of 0.7 may not be appropriate [Pugh, 1987].

For the regional sea-level rise estimates the spatial variability of the nodal cycle is relevant. This spatial variability is also relevant for the estimate of the global mean sea level estimates. The global mean sea level itself is not affected by this cycle but trend estimates can be, because both tide gauges and satellites have a limited coverage of the world. Tide gauges have a higher coverage on the Northern Hemisphere and the altimetry satellites only cover the area between –64° and 64°.

Examining the agreement with the equilibrium tide is relevant because it determines the best method to estimate local effects of the nodal cycle. Previous comparisons with the equilibrium tide have shown agreement, for example Currie [1976]; Trupin and Wahr [1990].

Accounting for the nodal cycle should increase the probability of finding sea-level rise acceleration or deceleration [Baart et al., 2010; Houston and Dean, 2011a]. In this article we determine whether accounting for the nodal cycle affects sea-level rise estimates locally and analyse how the nodal cycle varies across the globe.

4.1.1 *Methods*

The phase and amplitude of the nodal cycle are estimated by multiple linear regression using Equation 4.2. Variable t is time in Julian years (365.25 days) since 1970, β_0 is the initial mean sea level (cm), β_1 is the rise (cm yr^{-1}) and a and b can be transformed into the amplitude $A = \sqrt{a^2 + b^2}$ (cm) and phase $\phi = \arctan \frac{a}{b}$ (rad). Acceleration is tested by comparing the regression model with the quadratic term β_2 (cm/year ^{2}) with the regression model without the quadratic term.

$$\begin{aligned} h(t) &= \underbrace{\beta_0}_{\text{mean level}} + \underbrace{\beta_1 t}_{\text{trend}} \underbrace{(+\beta_2 t^2)}_{\text{acceleration}} \\ &+ \underbrace{a \sin(\frac{2\pi t}{18.6}) + b \cos(\frac{2\pi t}{18.6})}_{\text{nodal cycle}}. \end{aligned} \tag{4.2}$$

We use a spectral analysis only to determine if the nodal cycle is the most dominant signal in the spectrum for cycles with a period greater than a year. The stacking method was not used because the "detrending before fitting the cycle" approach leads to an underestimate of the amplitude when the timeseries length is not several times as long as the 18.6 yr period. Therefore we use the same harmonic analysis approach as Battjes and Gerritsen [2002] and Houston and Dean [2011a].

When fitting a trend through a periodic signal, variance that is due to the cycle is fitted by the regression line. This leaves less variance for the amplitude of the estimate of the periodic signal.

Besides the frequentist linear regression approach, a Bayesian approach is used. The analysis is comparable to Equation 4.2, with an extra parameter of the switch point t_0 (see also Equation 4.7). The switch point is the time where the trend can differ. To account for this the parameter t_0 can be varied by the Marcov Chain Monte Carlo (MCMC) algorithm. The parameter is used by the dummy (dichotomous, boolean) variable $t' > 0$. The circular Von Mises distribution [Fisher, 1993] was used for the ϕ parameter in Equation 4.3.

$$\begin{aligned} t' &= t - t_0 \\ h(t') &= b_0 + b_1 t' + b_2 t'(t' > 0) + A\cos(\frac{2\pi t'}{18.613} - \phi) \end{aligned} \tag{4.3}$$

The MCMC model [Gelman et al., 2004] is setup using the prior distributions $\mathcal{U}(min = -25, max = 25)$ for β_0, $\mathcal{N}(\mu = 0, \tau = 1)$ for β_1 and β_2, $\mathcal{U}(min = 1980, max = 2000)$ for the switch point t_0, $A = \mathcal{U}(min = 0, max = 30)$, ϕ as $\mathcal{V}(\mu = 0, \kappa = 1)$ and y as an observed node with $\mathcal{N}(\mu = h_{modelled}, \tau = 1/(\sigma^2)$ where $\sigma = \mathcal{U}(min = 0, max = 50)$. The symbols $\mathcal{N}$, $\mathcal{U}$, $\mathcal{V}$ correspond to the normal, uniform and Von Mises distribution. For the analysis of the sea-level reconstruction the terms A and ϕ are omitted.

Possible causes of the difference between the trends found when averaging tide gauges [Houston and Dean, 2011b] and tide gauge reconstructions [Church and White, 2011] are a placement bias (non-random placement) and a censoring biases (non-random removal of tide gauges). Dealing with censored data, data that is cut off (in this case in time), is common in reliability and survival analysis. To check for this we create a simple sea-level reconstruction defined by Equation 4.5. Note that this method does not take into account any spatial correlations. This method is similar to the one used in [Church and White, 2006], except here no Empirical Orthogonal Function (EOF) is applied. We do apply the same Glacio Isostatic Adjustment (GIA) correction [Peltier, 2004].

$$\begin{aligned} \Delta h_{reconstruction}(t) &= \frac{\sum_{i=0}^{n_{stations}} (h_i(t) - h_i(t-1))}{n_{stations}} \\ h_{reconstruction}(t) &= \sum_{x=0}^{t} (\Delta h_{reconstruction}(x)) \end{aligned} \tag{4.4}$$

Datasets

This study uses three different datasets for local relative sea level (Dutch coast), local absolute sea level (North Sea) and global relative sea level. For the local relative sea level at the Dutch coast the six main tide gauges are used, as provided by the "helpdesk water". These records consist of the yearly averaged observed sea surface altitude over the period 1827-2010. The mean over the six stations is used to describe the average trend for the Dutch coast. A window from 1890-2010 is selected because for this period all stations have measurements and show consistent trends. The data was corrected for atmospheric pressure variation using an inverse barometer correction, based on the records of the Metoffice service `http://hadobs.metoffice.com/hadslp2/`. The six main tide gauges include Delfzijl, Harlingen, Den Helder, Hoek Van Holland, IJmuiden and Vlissingen.

The local absolute sea level for the North Sea from the Topex, Jason1 and Jason2 satellites was provided by the Laboratory for Satellite Altimetry, generated by the National Oceanic and Atmospheric Administration (NOAA) Sea Level Rise (`http://ibis.grdl.noaa.gov/SAT/SeaLevelRise/`) and Radar Altimeter Database System (`http://www.deos.tudelft.nl/altim/rads/`) on January 22, 2010.

The global relative sea-level variation is analysed using the PSMSL tide gauge dataset as retrieved on June 29, 2011. From the PSMSL consists of a "Metric" and a "RLR" (revised local reference) datasets. Only the latter is considered suitable for research purposes.

The Dutch dataset, calculation routines and methods to read the file formats of the PSMSL are made available through the R Project for Statistical Computing (R) *sealevel* package `https://r-forge.r-project.org/projects/sealevel/`.

4.1.2 *Results*

Local relative sea level

To determine the relevance of the nodal cycle at the Dutch coast a spectral analysis is carried out on the yearly means of six main tidal gauges over the period 1890-2010. A periodogram is used to show the relative strength of cosine-sine pairs at various frequencies in the overall behavior of the series [Cryer and Chan, 2008]. The periodogram (Figure 4.1a) shows a clear peak at the 18.6 yr period. The multiple linear regression yields a sea-level rise (β_1) of 0.19 cm yr^{-1} $\pm$ 0.015 (95%), an amplitude (A) of 1.2 cm $\pm$ 0.92 and a phase (ϕ) of -1.16 rad (with 1970 as 0 rad), resulting in a peak in February 2005 (Figure 4.1). No significant acceleration (inclusion of β_2) was found. Figure 4.2 shows the nodal cycle per station.

This answers Question 3.5.1.

Acceleration detection probability

The nodal cycle explains 9% of the variance in the detrended mean sea level. Explaining more variance has the advantage that other effects become more clear. We use this to determine the change in sea-

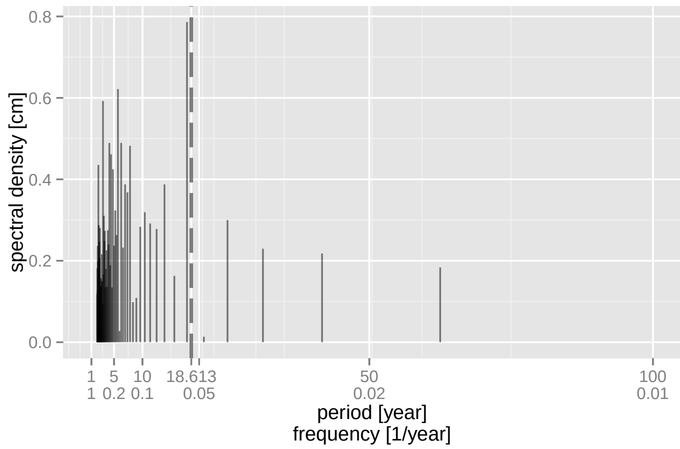

(a) Periodogram of the mean of 6 tidal stations in the period 1890–2010. The dashed line marks 18.6 year.

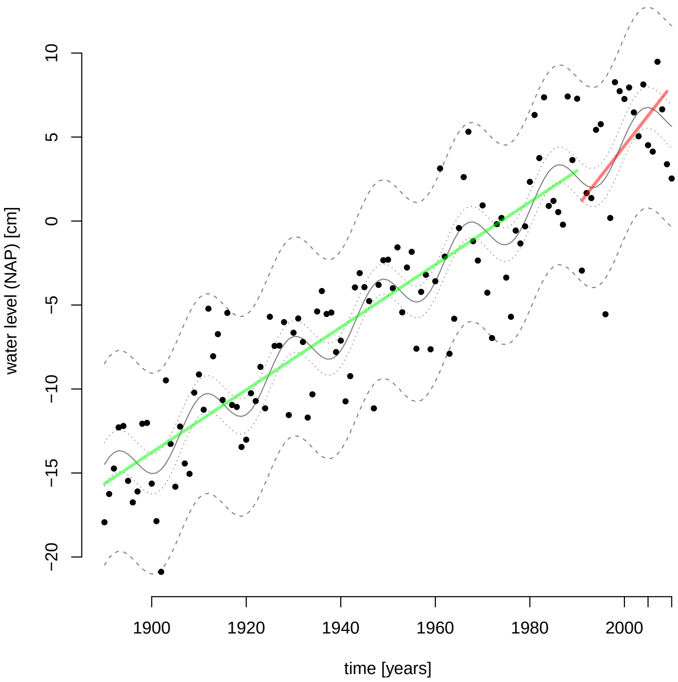

(b) Annual mean sea level averaged over 6 Dutch tidal stations (black dots). Multiple linear regression with a nodal cycle (solid curve) with confidence interval (dotted curve) and prediction interval (dashed curve). Linear regression line through the period 1890–1990 (green). Linear regression line through the period 1991-2010 (red).

Figure 4.1: Mean relative sea level at the Dutch coast

Figure 4.2: Annual mean sea level for 6 Dutch tidal stations, coloured solid line shows the trend fitted with Equation 4.2. The corresponding coloured bands show the 95% confidence band. The black solid line and corresponding grey band show the trend for the mean of the stations. The dashed line shows the loess smoothed fit, showing a corresponding trend to the nodal cycle.

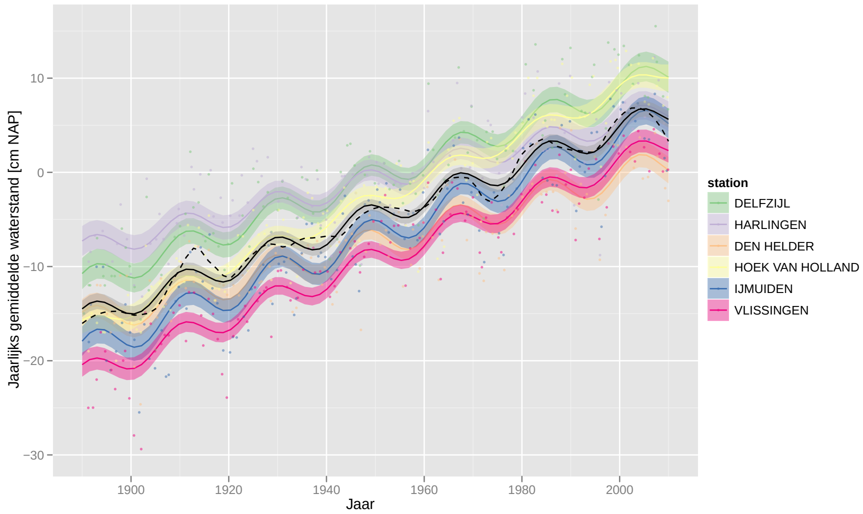

level acceleration detection probability. This probability, the statistical power, is calculated for the lower and higher KNMI scenarios [van den Hurk et al., 2007] for the Dutch coast. The power was estimated using a simulation, with a generated dataset, based on the broken linear trends from the scenarios from van den Hurk et al.. On top of this the Dutch nodal cycle was imposed but with a random uniform distributed phase, as well as random normal distributed error, based on the residuals after fitting the nodal cycle for the mean of the Dutch stations. The simulation was performed with 200 samples per condition. The detection of acceleration was done by comparing the linear regression model with a model with an acceleration term included using an analysis of variance with 1 degree of freedom. The sea-level acceleration detection probability for the lower scenario went up from 46% without to 48% with the nodal cycle. The probability to detect the high-end scenario went up from 82% without to 84% with the nodal cycle included. Generally 80% is considered an acceptable level. Thus it can be concluded that, even without accounting for the nodal cycle, it was likely that the acceleration of the higher scenario, if it were present, would have been found.

An alternative method to detect the acceleration is to use the MCMC method. This shows that there is no trend break. The switch point variable t_0 has a posteriori distribution of 1976 ± 15 yr (95% confidence interval), the A parameter is estimated as 1.5 ± 1.0 cm, the σ parameter is estimated as -1.2 ± 0.6 rad, corresponding to a peak in

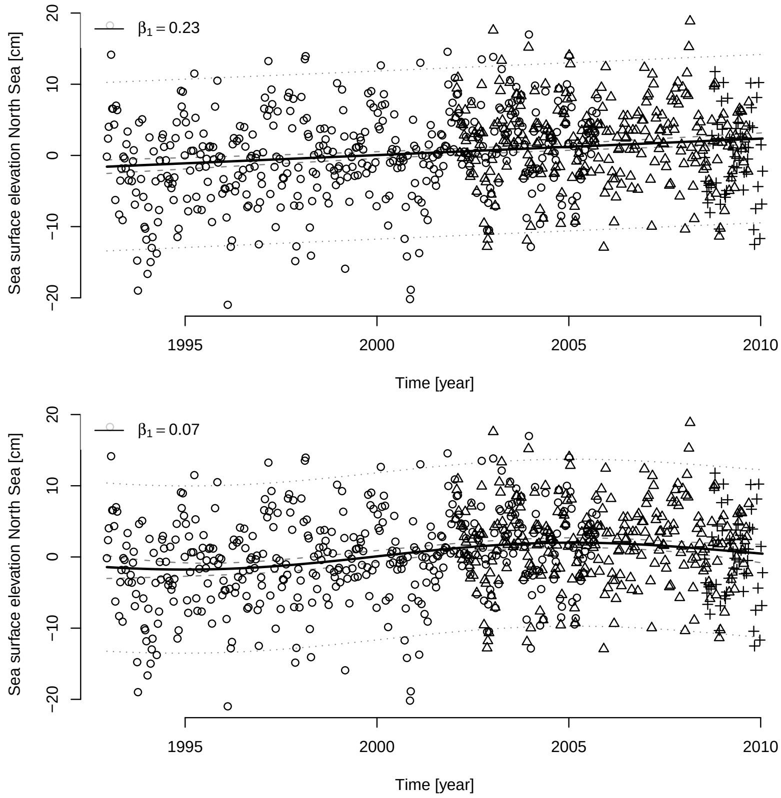

Figure 4.3: Absolute sea level in the North Sea. *Top figure*: Linear regression fitted through corrected satellite observations for the North Sea from Topex (○), Jason1(△) and Jason2 (+). Gray dashed line represents the confidence interval, dotted line represents the prediction interval. *Lower figure*: Seasonal regression (Equation 4.2) fitted through corrected satellite observations for the North Sea from Topex (○), Jason1(△) and Jason2 (+). Gray dashed line represents the confidence interval, dotted line represents the prediction interval.

the year 2005, the a posteriori estimate of the trend before the switch point is $0.18 \pm 0.03\,\mathrm{cm\,yr^{-1}}$ and the a posteriori increased sea-level rise after the break (β_2 in Equation 4.3) is $0.0 \pm 0.1\,\mathrm{cm\,yr^{-1}}$. This confirms that there is no sign of an accelerated sea level along the Dutch coast.

Local absolute sea level

Again the nodal fit using Equation 4.2 on the North Sea satellite data over the period 1993–2010 yields the same nodal cycle (Figure 4.3). By including the nodal cycle the absolute sea-level rise lowers from $0.23\,\mathrm{cm\,yr^{-1}}$ to $0.07\,\mathrm{cm\,yr^{-1}}$ because coincidently the time window starts at the bottom and ends in the peak of the nodal cycle. This clearly shows how including the nodal cycle may affect sea-level rise estimates.

Global distribution of the nodal cycle

Now that it is known that the nodal cycle is important for local sea-level rise estimates, the next question is how the nodal cycle varies across the globe. From the 1157 gauges in the PSMSL dataset, 511 were selected based on their recorded history of at least 57 (3×19) years. The analysis of spectral densities of the tidal stations is skipped because it has already been performed in detail [Trupin and Wahr, 1990], showing a peak at 18.6 years.

Equation 4.2 is applied to the selected stations, where 134 stations show an amplitude (A) that is significantly different from 0. This confirms the global presence of the effect of the lunar nodal cycle, with a median amplitude of 2.2 cm. The global phase and amplitudes variation are shown in Figure 4.6.

Global sea-level reconstruction

Here again we apply the MCMC method to detect if there is a trend break in sea-level rise. This time we use the reconstruction of Church and White [2011]. The most clear trend break occurred in the 1930's, which is found by setting the distribution of the switch point to $\mathcal{U}(min = 1900, max = 2000)$ and the distribution for the water level in the switch point accordingly. Most recent studies assume that there is a switch point in the early 1990's, therefor we assume that the switch point is somewhere between 1980 and 1990. This gives 1987 ± 2 yr as the obvious switch point, given the data. In this year the trend doubles from 1.44 ± 0.02 mm yr^{-1} to 2.59 ± 0.20 mm yr^{-1}, a significant trend break (Figure 4.4). It is smaller than the 3.2 mm yr^{-1}, because using Equation 4.3 forces a continuity in sea level. Others have created a higher recent sea-level rise by allowing for a new intercept in the trend break. Starting the new trend lower than the old trend creates a sink of $O(1 \times 10^{11}\,\text{m}^3)$ (the discontinuity insinuates that the ocean volume decreased by a total volume of sea-level difference times ocean surface).

Another possible explanation is a censoring bias. Are stations more likely to be discontinued in places where sea-level rise is not increasing? It is not difficult to imagine the economic considerations that make it more likely for a tide gauge to be continued if sea-level rise is a problem. Other causes are that if a tide gauge is placed in a place where sea level is dropping significantly, the tide gauge will eventually run dry.

To analyse this, global sea level is reconstructed as a function of starting year. For this we use the PSMSL revised local reference (rlr) dataset of 1350 tidal gauges [Woodworth and Player, 2003]. The sea-level reconstruction is defined by Equation 4.5, where $h_i(t)$ is the sea level in station i in year t. A glacial isostatic adjustment [Peltier, 2004]

Figure 4.4: Bayesian MCMC fit (100 black lines, with alpha of 1%) showing the confidence interval around the pre- and post trend break sea-level rise. The trend break has most likely occurred in the year 1987. The Church and White [2011] reconstruction is shown in the blue line

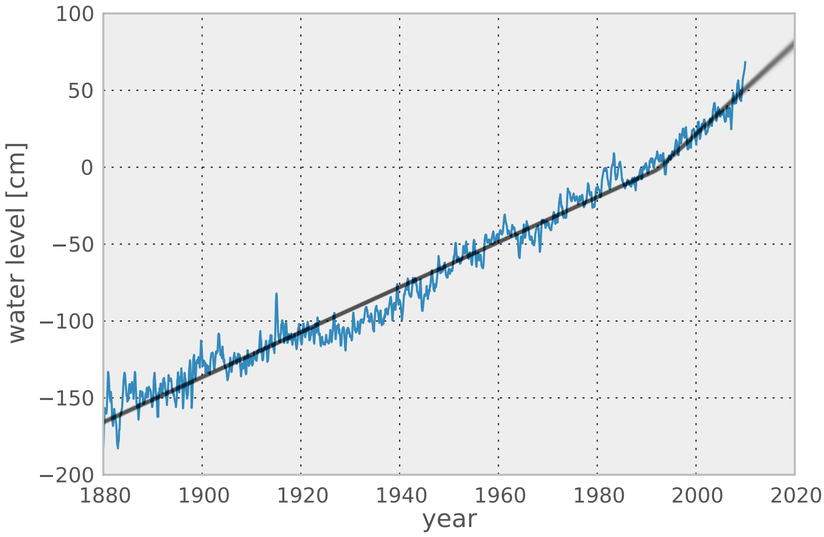

is applied to compensate for the higher portion of Scandinavian tide gauges at the switch of the 19th to the 20th century.

No other spatial weighing, corrections and EOF's are applied in order to focus on a possible positioning bias. The tide gauges are split up into four periods, based on starting year with regular intervals of 50 years and the break point of 1987. The periods are referred to as *old* (-1900), *classic* (1900-1950), *new* (1950-1987) and *newest* (1987-). Periods without at least 50 years of data are not shown.

$$\Delta h_{reconstruction}(t) = \frac{\sum_{i=0}^{n_{stations}} (h_i(t) - h_i(t-1))}{n_{stations}}$$
$$h_{reconstruction}(t) = \sum_{x=t}^{0} (\Delta h_{reconstruction}(x)) \tag{4.5}$$

Figure 4.5 shows that there is a clear difference between sea-level rise measured by *old*, *classic* tide gauges and measured by *new* and the *newest* tide gauges.

This confirms the hypothesis that new tide gauges are more likely to be placed in areas with higher sea-level rise. This can explain the lack of acceleration found in areas where there are older tide gauges.

This comparison of old versus new tide gauges shows that they are indeed different. It does not tell us which gauges are "correct" or why they differ. One thing that is known about *old* tide gauges is that they are more often located in places in the Northern Hemisphere. Thus are we looking at a censoring bias, where tide gauges that show lower sea-level rise are removed or are we looking at a positioning bias, tide gauges are placed at locations with higher sea-level rise?

A confirmation of the censoring bias is that tide gauges with high sea-level decline are often disbanded. Of the 10 tide gauges that measured the largest interannual sea-level decline before 1910, 9 were discontinued between 1930 and 1940 and the last one in 1970. Of the tide gauges that show the highest interannual sea-level rise before 1910, only 6 were discontinued and most of them were discontinued later (1921, 1927, two in 1979, 1987 and the last one in 2000), the other 4 of them are still operational.

On the other hand the selective placement of tide gauges is also true. Old tide gauges were more often placed in developed countries and a lot of effort has been put in creating a network of tide gauges with a more representative coverage.

Figure 4.5: Reconstruction of global sea-level rise using Equation 4.5 using tide gauges from different time periods. Confidence intervals represent the 95% confidence interval of the broken regression lines. The switch point is in year 1987.

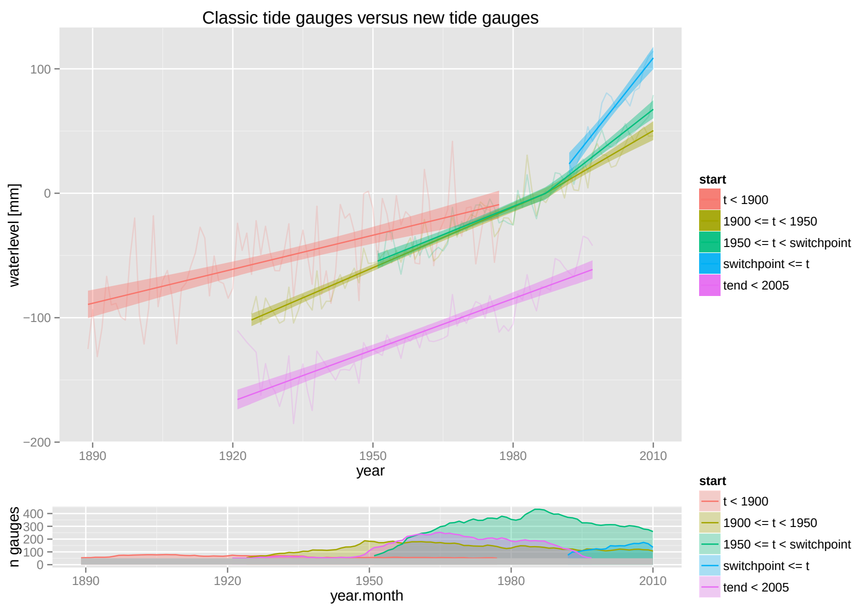

Global absolute sea level

The phases found at the tidal stations are compared with the phases found in nearby measurements from altimetry satellites for verification. This dataset was obtained from the CSIRO website and consists of sea surface heights with inverse barometer (IB) correction, seasonal signal removed and glacial isostatic adjustment (GIA) corrected. Because satellite data is only available for one lunar nodal period, the results are susceptible to other influences and thus not yet stable. The global phase variation is plotted in Figure 4.6. Tidal gauge and satellite measurements show a reasonable correspondence in the Atlantic but not in the Pacific Ocean. The canonical correlation between amplitude and phases of stations and nearby satellites is 0.21, which is low yet statistically significant ($p < 0.05$).

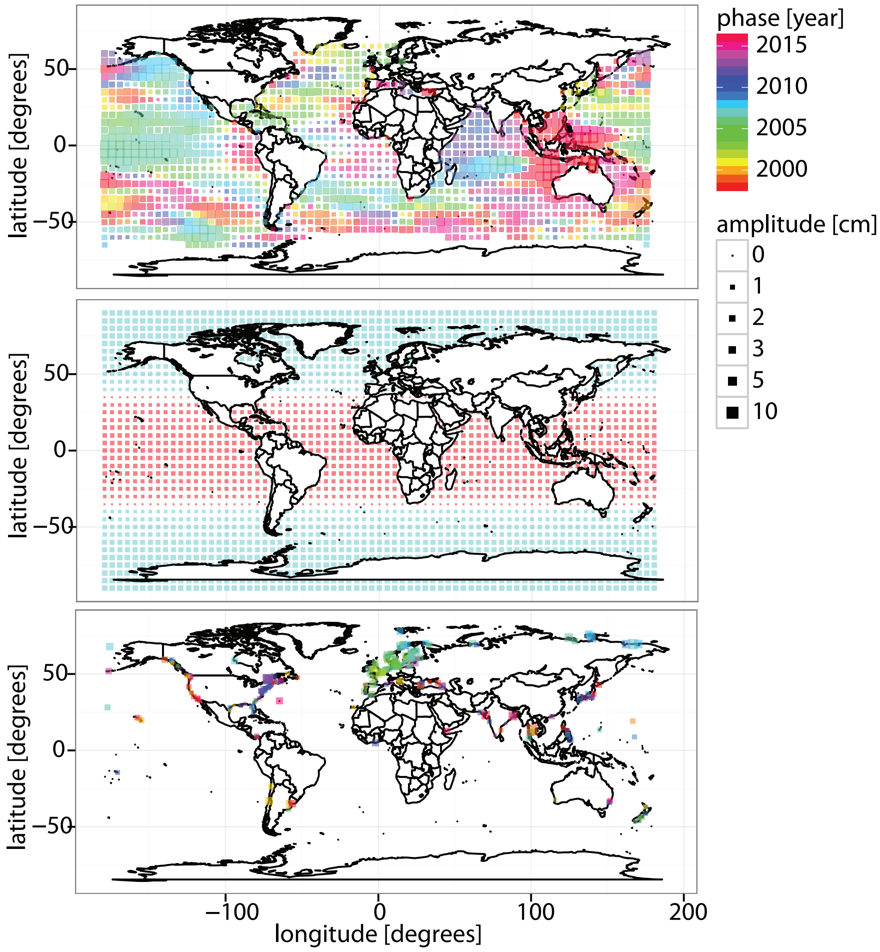

Figure 4.6: Nodal cycle, estimated using Equation 4.2. Amplitudes in cm (size of circles) and phases in years (colour) of the lunar nodal cycle. *Top figure*: tide gauges with at least 57 years of measurements *Middle figure*: altimetry satellites. *Bottom figure*: equilibrium.

When to include the nodal cycle

The two extra parameters, the amplitude and phase, can result in a less accurate estimate of the sea-level rise parameter. One way to approach this is by determining if the variance explained by the combination of the two extra parameters is statistically significant (using an ANOVA with two degrees of freedom). An alternative is here is to use the Akaike Information Criterion (AIC).

We use another simulation to find out what would be a good period for including a nodal cycle in regional sea level. For this we assume sea-level rise equal to 0.2 cm yr^{-1}, a nodal amplitude of 2.2 cm and a uniform distributed random phase and random error of 2.5 cm. By varying the time period and comparing the root mean square error of the estimate of nodal fit and linear fit, we find that it is useful to include the nodal cycle terms starting for periods from 14 years and longer. This time period, for which it is advisable to include the nodal cycle, becomes longer as the ratio between the random error and the amplitude of the nodal cycle increases. A similar discussion can be found in Blewitt and Lavallée [2002] for the comparable problem of fitting geodetic velocities.

This answers Question 3.5.2.

If the goal is to get an unbiased local estimate of the sea-level rise parameter, the simplest approach is to use timeseries of multiples of 18.6 years + 9.3 years (integer plus a half). When the goal is to get a good estimate of the level or acceleration, this approach can not be used.

This is a rule of thumb, the optimal lengths of timeseries run up from 1.43 *through* $N + 0.5$

The aim of including the nodal tide is to fit the nodal cycle and not other decadal cycles. Therefore when including the nodal cycle, it should be checked if 18.6 year is within the modal frequency bin of the multi-year spectrum. Finally it is advisable to check for the reliability of the fit, for example splitting up the tidal signal into two separate parts should yield the same nodal cycle phase. If the estimate of the nodal cycle is based on satellite measurements it should be verified using local tide gauges.

4.1.3 *Conclusions*

Coastal management requires estimates of sea-level rise. The trends found locally for the Dutch coast, are the same as have been found in the last fifty years [Deltacommissie, 1960; Dillingh et al., 1993]. Even though, after including the nodal cycle, it was more likely that high-level scenarios would have become apparent, no acceleration was found. The higher recent rise [van den Hurk et al., 2007] coincides with the up phase of the nodal cycle. For the period 2005 through 2011 the Dutch mean sea-level is expected to drop due to the lunar cycle down phase. This shows the importance of including the 18.6 year cycle in regional sea-level estimates. Not doing so on a regional or local scale for decadal length projections leads to inaccuracies.

It was found that the local sea-level shows no sign indication of sea-level acceleration. Although we do find a significant trend break in 1987, in the commonly used tide gauge reconstruction from Church and White [2011], it is not the most obvious trend break given the data and it is not confirmed by the analysis of individual tide gauges

[Houston and Dean, 2011b]. Part of the trend break that does occur can be explained by extra corrections that have been applied in the reconstruction [Church and White, 2011]. In addition, we have found that the *classic* tide gauges are significantly different from *new* tide gauges. New tide gauges are more often placed in areas with higher sea-level rise and tide gauges with sea-level decline are more likely to be removed.

In Section 2.3 we saw that the forecasts of accelerated sea-level [van den Hurk et al., 2007] rise initiated a change in coastal policy. We now know that the observed local trend was overestimated and that the higher scenario, if it would have been set in motion, would likely have been observed. Also the suggested recent global acceleration seems more likely to be connected to a changing "tide gauge population" than a change in climate. Should this put us back to the drawing board, reconsider the costs and benefits of our actions based on these scenarios?

Of course it affects the confidence we have in the forecasts, as will be discussed in Chapter 7. However, the methods used in this study also have their limitations. We therefore suggest to continue making different types of forecasts, as discussed in Baart et al. [2012d].

There is a difference between the nodal cycle phase expected from equilibrium and the nodal cycle phase found in tidal records. This is inconsistent with results from Trupin and Wahr [1990], possibly due to the difference between the stacking approach and the harmonic approach. It is similar to the differences found by Cherniawsky et al. [2010]. The cause for the difference between the observed nodal cycle and the equilibrium nodal cycle is not known. It could be a physical effect, but could also be the result of the way our mean sea levels are measured and computed.

On the nodal cycle we can state that whatever the cause may be, if there is a known decadal signal in the sea-level records, it should be taken into account. This can give better estimates of local sea-level rise, but one should carefully check that the nodal fit is clearly present.

Although the nodal tide does not affect the true global mean sea level, it can affect global mean sea level estimates. In sea-level trends from satellites, if one would assume the equilibrium nodal phase, one would expect a small nodal cycle in the mean due to the phase distribution in combination with the limited spatial coverage of the altimetry satellite. The sea-level trends based on tide gauges can also be affected by the nodal cycle due to irregular spatial sampling of tide gauges. The observed nodal cycle shows a more east-west pattern than the equator-poles pattern of the equilibrium. The nodal cycle can thus be safely ignored for global mean sea-level estimates based on satellites. For global mean sea-level estimates based on tide gauges, the distribution of nodal cycles phases could be checked for approximate circular uniforminess.

It was shown that globally the 18.6 year cycle is observable in one fourth of the selected tidal stations, with a varying phase. The phases found based on tidal records and satellite data, show a weak canonical correlation, probably due to the short period of the satellite measurements. It is not yet possible to give an accurate estimate of the effect of the cycle across the globe. Just like a sea-level rise trend can be very sensitive to the window of observation, an estimate of a cycle is highly sensitive to peaks. Without removing such effects, for example El Niño-Southern Oscillation, short series like the satellite measurements are not very representative of the effect of the nodal cycle. A logical follow-up on this research would be to simulate the effect of the nodal cycle using a global tide model.

This answers Question 3.5.

4.2 DESIGN LIFETIME: STORMINESS TREND

One of the aspects to take into account when planning interventions at the coast is the possibility of a change in storminess. This is relevant because many of the forces that directly influence the dunes (waves, surge) are storm related. This section describes gives an overview of changes in coastal storm occurrence for the Netherlands. Both observed trends in storminess as well as expected climate change impacts on future storm occurrence are examined.

In different studies different measures are used to quantify "storminess". A storm can be characterised by intensity, frequency and duration of characteristic storm properties like wind speeds. In some studies proxies are used, for example pressure tendencies, surface air pressure and storm surge. Other studies examine wind speeds directly. An overview of different proxies and research methods for determining storminess changes can be found in Carnell et al. [1996]; Smits et al. [2005]; Bijl et al. [1999].

Here coastal storminess is assumed to be an underlying variable representing both frequency and intensity of storms directed at the coast. Change in storminess is operationalized [see Bridgman, 1950, chap. 1] as the relative changes in the annual number of storm events.

The availability of data determines the frequency of storms that can be investigated. Low frequency storms require a long period of measurements. For the Netherlands, sets of continuous measurements are available since the 1960's. This is just enough to notice big changes in storminess for infrequent (twice per year) events. In case the trend changes in storminess are small, they can only be observed over longer timespans or for higher frequent events.

We will first examine wind observations at coastal stations over the last decades. These results will be compared with previous analysis of surge levels. Storminess in the context of climate change will be examined using results from scenario studies and reanalysis studies.

The relative changes in the annual number of storm events can be examined using decadal length time series of wind speeds collected by weather stations or by proxies of these like pressure measurements. The most important dataset for examining storminess changes in the Netherlands resides at the KNMI. The KNMI measures wind speeds at different stations in the Netherlands. Because direct station measurements of storm occurrence and intensity are available, studies doing reanalysis of proxy data [for example Sterl and Caires, 2005] will not be considered as the measure for describing observed changes in storminess. Comparisons between these studies can be found in for example van den Hurk et al. [2006].

Smits et al. [2005] analysed the wind dataset of the KNMI for 13 stations, both coastal as well as inland stations over the period 1962 through 2002. As an indicator for frequency they used the annual number of independent wind events that last for several hours, for intensity the observed hourly peak wind speeds. The study makes an ordinal categorization of storms where weak events occur on average 30 times per year, moderate wind events are defined as winds which occur on average 10 times (windspeed 6 Bft to 7 Bft), and strong events have an occurrence rate of 2 times per year (windspeed 7 Bft to 8 Bft). For each storm frequency (number of storms per year), the trend over 40 years was analysed. It was found that moderate to strong events do not show statistically significant decrease nor increase.

Longer timeseries (100 years), using storm surges as a proxy, were analysed by Bijl et al. [1999]. Here the focus is on the stations Hoek van Holland and Vlissingen stations. The authors define a storminess factor for each station, using four different storm frequencies, by splitting the timeseries in groups of 10 years. For each decade an expected $^1/_{10000}\text{yr}^{-1}$ storm surge is computed. The expected $^1/_{10000}\text{yr}^{-1}$ storm surge over the whole 100 years is subtracted from the decadal storm surge. This is what the authors call the "storminess factor". This analysis of 100 year storm surge variations also showed no significant trend for both stations.

An example of the effect of climate change on future storminess is given by Winter et al. [2012]. They propagated the storminess into a wave climate and found that the wave climate is not projected to differ between 1961-1990 and 2071-2100.

The wind data of the KNMI combined with historic records is also used as a source for the climate change scenarios described in van den Hurk et al. [2006]. This study extrapolates expected wind occurrence using numerical weather prediction models and 4 different climate scenarios. In a similar study van den Hurk et al. [2006] used four climate scenarios, varying on two factors: air circulation patterns (constant, increased) and temperature increase (1°, 2°), and found an increase in two scenarios, a decrease in one scenario and non change in the last based on the outcome of annual maximum wind speed.

Another common way to analyse the storminess change is to use the combination of historic records and numerical simulations in the form of a reanalysis. This approach was used by Vautard et al. [2010] who found a slight decrease in surface wind speeds in the Northern Hemisphere.

The statistical power of most observed datasets is not enough to show differences in the lower frequency storms. While one series of observations alone does not provide enough statistical power to test hypotheses on the decadal trends, doing a meta-analysis over several European countries can. This meta-analysis was performed in the Morphological Impacts and COastal Risks induced by Extreme storm (MICORE) project. There was no relation found between storminess changes and global climate change. [Ciavola et al., 2011a]. This can be seen in Figure 4.7. One could argue that this study is not a "meta-analysis" but a merely a "systematic review". For example, the Dictionary of Epidemiology [Porta, 2008] gives the definitions below. The lack of suffient similarity (mainly the lack of reported statistical measures and inconsistent quantification of "storminess") makes it hard to come to an overall quantified statement.

SYSTEMATIC REVIEW The application of strategies that limit bias in the assembly, critical appraisal, and synthesis of all relevant studies on a specific topic.

META-ANALYSIS A statistical analysis of results from separate studies, examining sources of differences in results among studies, and leading to a quantitative summary of the results if the results are judged sufficiently similar to support such synthesis.

Thus only a qualitative statement can be made, that the study confirmed the general picture of no positive storminess trend, as for each trend of increased storminess a trend of decreased storminess was found.

This answers Question 3.4.1.

4.3 POLICY ANALYSIS: EROSION TRENDS

This section describes the decadal scale variation of coastal erosion along the Dutch coast, with a focus on the Egmond location. Coastal erosion is another quantity that is relevant for coastal maintenance, and just as in the previous section it is quantified using a trend estimate.

The relevant quantities depend on the goal of their analysis. The process of selecting good "quantities of interest" for morphodynamic analysis is described by van Koningsveld and Mulder [2004].

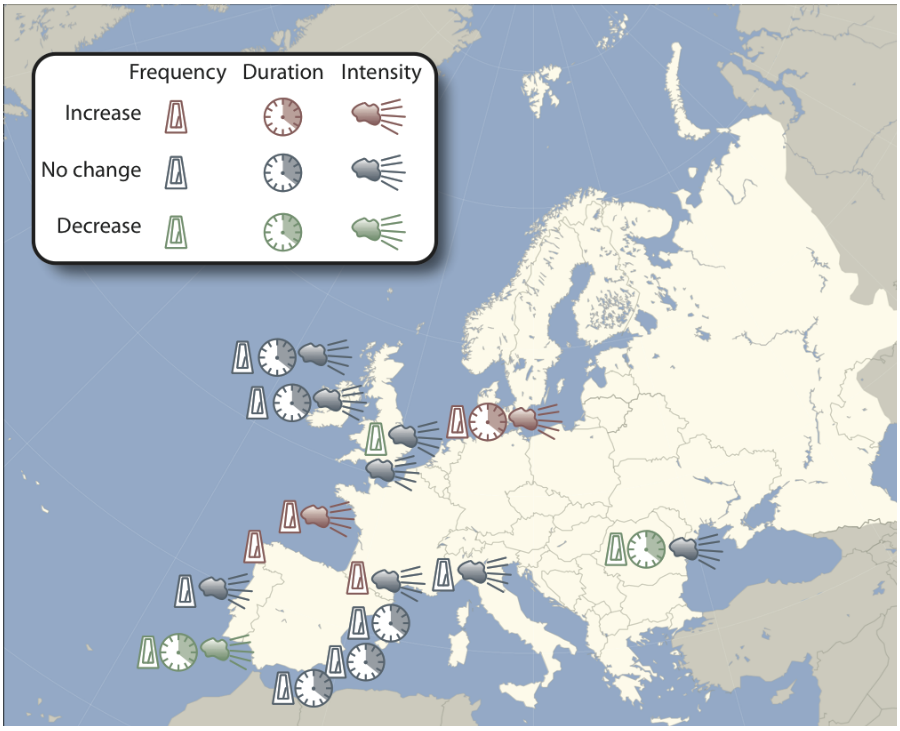

Figure 4.7: Meta-analysis of trends in coastal storminess. Based on Table 2 from [Ciavola et al., 2011b]

The quantities that are in used in the analysis of the Dutch coast are traditional morphometric quantities. Traditional morphometric quantities measure one aspect of the coast such as beach width, dune volume, beach volume, beach slope. An alternative is to look at the whole shape, often based on features, distinctive points that are present in all measurements. This approach was initiated by Thompson [1917] (Figure 4.8). Examples of features for a dune coast are the dune top, dune foot and the high water line. While the classic morphometric quantities allow comparison of dunes based on physical quantities, morphological changes are often expressed in the form of feature and shape changes. Expressing morphological change in the form of feature or shape change is part of the field of modern morphometrics [Claude, 2008].

Besides the traditional morphometric and the modern morphometric view, we can look at the dataset from a geological point of view. From a geological perspective one would prefer to look at the history of the coast. This can be shown using a geological profile plot. A geological profile plot is made by assigning years to layers of sediments that are present in the current year, but not in the year before. This plot is generated sequentially from the last measurement to the first measurement, resulting in a cumulative area plot with a timestamp assigned to each area (Figure 4.9).

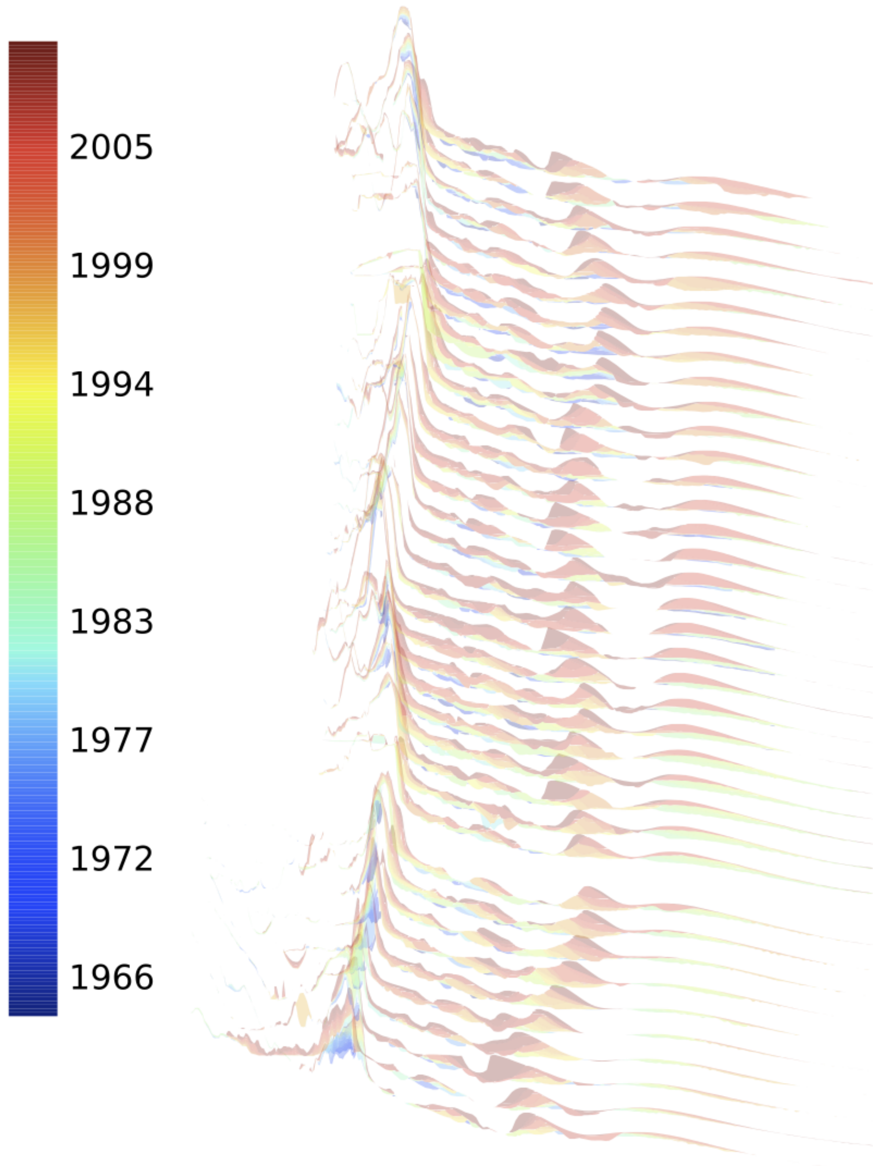

Figure 4.9: Geological map of the coast near Egmond. The colour shows the date when the bathymetry and topography were last measured at that location. An older bathymetry indicates that the sand at that location has been measured the first time in the year indicated by the colour and has since then not moved or has been replaced by other sand.

Just as for sea level the quantitity of interest for erosion is expressed in a trend. These trends are used to make local, short-term (years ahead) forecasts. They can also be used to test hypotheses. For example, the hypothesis that the change in nourishment strategy did not have an effect on the coastline trend. This is a relevant topic since the nourishment strategy changed in the 1990, and there is now enough data available to test the effectiveness. Different measures are used to test the effectiveness of the strategy change. A linear trend analysis of the Dune Erosion Point (DEP) and Momentary Coast Line (MKL) van Koningsveld and Lescinski [2007] suggested that the policy change overshot its objective, "the operational objective was to maintain the coastline at a position not landward of the 1990 reference, not to move it seaward". They estimated the long-term nourishment effectiveness to be around 20%, where the nourishment effectiveness was quantified as a volume percentage based on the total nourishment volume and the retaining volume.

One of the assumptions of a trend fitted using a linear regression is that the errors are uncorrelated. Southgate [2011] showed that the assumption of uncorrelated errors is invalid for the coastal erosion trends. He found that a linear trend predicts worse than assuming the MKL stays constant, thus that the last beach state is a much better predictor.

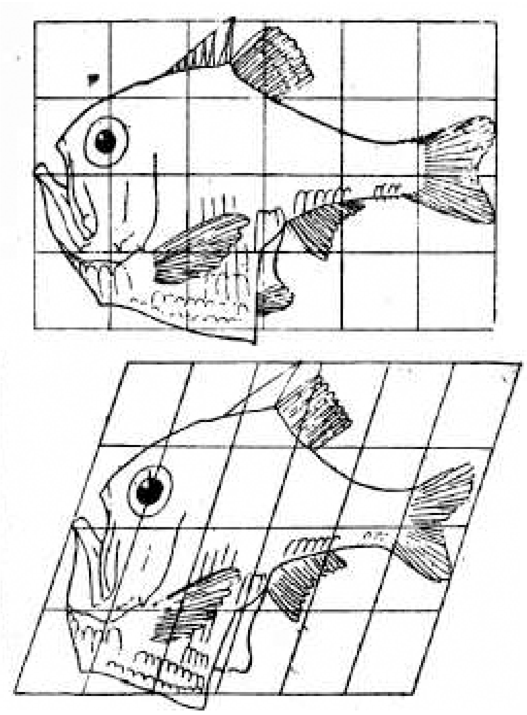

Figure 4.8: Example of a morphometric analysis on fish shapes [from Thompson, 1917]

Here we combine both methods and show how to include the confidence interval. Van Koningsveld and Lescinski [2007] estimated the effect of change in coastal policy in the 1990's using a segmented linear regression model (sometimes called a broken linear regression model). The fitted linear model is given in Equation 4.6, where mkl is the MKL position at time t in years, a_1 is the intercept for the regression line fitted up to 1990, β_1 is the slope of the regression line fitted up to 1990, a_2 is the intercept for the period after 1990, β_2 is the slope for the period after 1990 and ϵ_t is the residual. This model uses four coefficients, two slopes and two intercepts.

$$mkl(t) = \begin{cases} a_1 + \beta_1 t + \epsilon_t & \text{if } t < 1990 \\ a_2 + \beta_2 t + \epsilon_t & \text{if } t \geqslant 1990 \end{cases} \tag{4.6}$$

For our example we will use the interaction of time versus policy to reduce the number of parameters to three (see Equation 4.7), here a is the intercept, β_1 is the slope for the period up to 1990, β_2 is the slope increase for the period after 1990 and policy is a dummy variable (a dichotomous variable with 0 for the period up to 1990 and 1 for the period from 1990. Reducing the number of variables increases the statistical power, the likelihood that we will detect the effect of a changed policy, if it were present.

$$mkl(t-1990) = a + \beta_1(t-1990) + \beta_2(t-1990) * \mathrm{policy} + \epsilon_t \quad (4.7)$$

The same Dutch Annual Coastal Measurement (JARKUS) dataset as described in Chapter 3 was used. This dataset describes the yearly measurements with a resolution of approximately 250 m alongshore by 10 m cross-shore.

Here we apply Equation 4.7 to the same coastal position but including the recent measurements. The effect of including the $\mathrm{policy} \times t$ interaction variable is that the trend switches in the year 1990 from β_1 to $\beta_1 + \beta_2$. The fitted equation is $mkl(t-1990) = 116.8 + 0.3 \times t + 2.4 \times \mathrm{policy} \times t$, from which we can conclude that before 1990 the average MKL growth was $0.3 \pm 0.4\,\mathrm{m\,yr^{-1}}$ and after the policy change in 1990 the average MKL growth increased with $2.4 \pm 0.8\,\mathrm{m\,yr^{-1}}$. For this location that is a significant change ($t = 2.9$). The confidence intervals, based on standard error of slope, intercept and interaction are shown in Figure 4.10.

The confidence interval of the policy effect parameter is so small that we can conclude that we would not have found such a large effect if there was no policy change. This shows how we can use the confidence intervals to test how effective a policy change is. If we ignore the methodological error of not considering auto and spatial correlations, we can conclude that the period before and after 1990, corresponding to the policy change, resulted in positive seaward trend of the momentary coastline moved seaward of $2.4\,\mathrm{m\,yr^{-1}}$ in addition to the already positive trend of $0.3\,\mathrm{m\,yr^{-1}}$. Of course including the confidence intervals does not give extra information on the causality, other factors might also cause these kind of variations in trends.

As Southgate [2011] suggested, it is sometimes a good idea to include the autocorrelation. Several textbooks discuss the differences between deterministic trends versus stochastic trends and the difference between stationary and non-stationary time series [for example Cryer and Chan, 2008, Chapter 5]. A simple way to think of the difference between a stationary and non-stationary time series is "what would be the forecast for the first future time step if the last time step showed a sudden drop?". In a linear regression, the forecast for $t+1$ would be predicted value of t plus the trend, where for an autoregressive model we would predict the observed value of t plus the trend. One can check for such properties using a test for the unit root, such as the Dickey-Fuller test [see Said and Dickey, 1984, for details].

From the two methods proposed by Southgate [2011] we choose the auto-regression approach. This method takes into account the tempo-

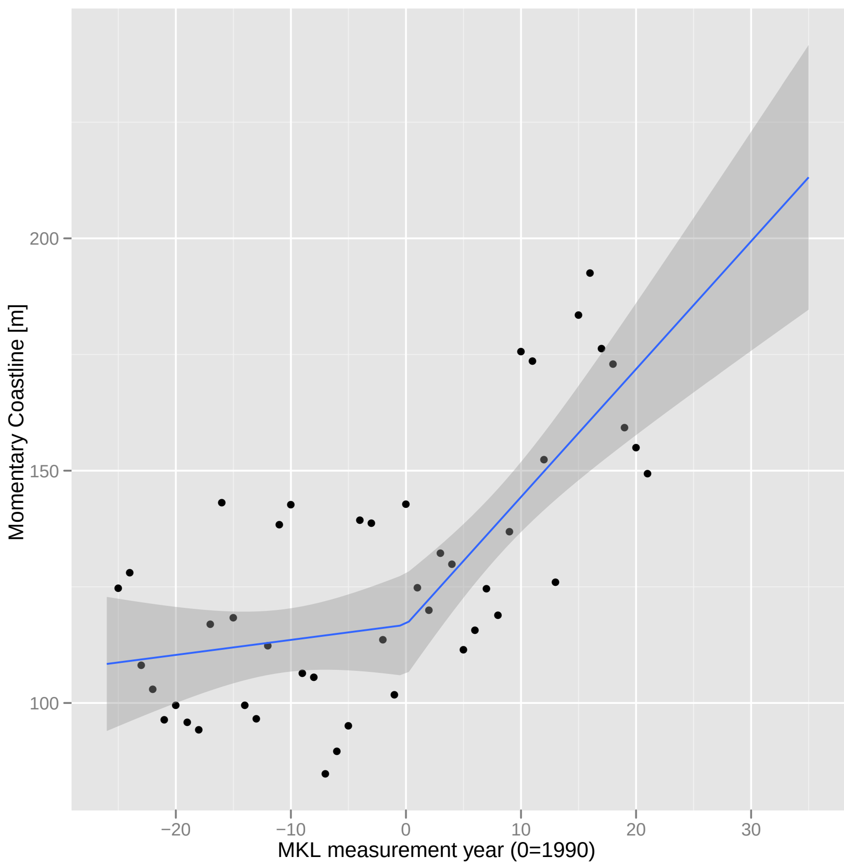

Figure 4.10: Segmented linear model including policy effect for the Egmond location (Jarkus transect 7003800)

ral correlation in the time series. This is appropriate here because the residuals from the fit using Equation 4.7 are non-stationary, as tested using the augmented Dickey-Fuller test ($p < 0.05$). Here we extend the approach to include the effect the policy change. Including for the effect of policy is done using the same way as for the linear model. In the context of auto-regressive models this extra term is referred to as an external regressor.

The fitted model is given by Equation 4.8, where α_i is the coefficient for the ith autoregressive term, β is the coefficient for the external regressor policy, μ is the mean and ϵ_t is the residual.

$$\begin{aligned} mkl(t) = &\alpha_1 mkl(t-1) + \alpha_2 mkl(t-2) + \alpha_3 mkl(t-3) \\ &+ \beta(t-1990) * policy + \mu + \epsilon_t \end{aligned} \tag{4.8}$$

Confidence intervals for autoregressive models are a bit more complex than for linear models. They are rarely presented for hindcast periods. Figure 4.11 shows the confidence intervals computed using Kalman Filtering [Durbin et al., 2001] as implemented in R [R Development Core Team, 2009].

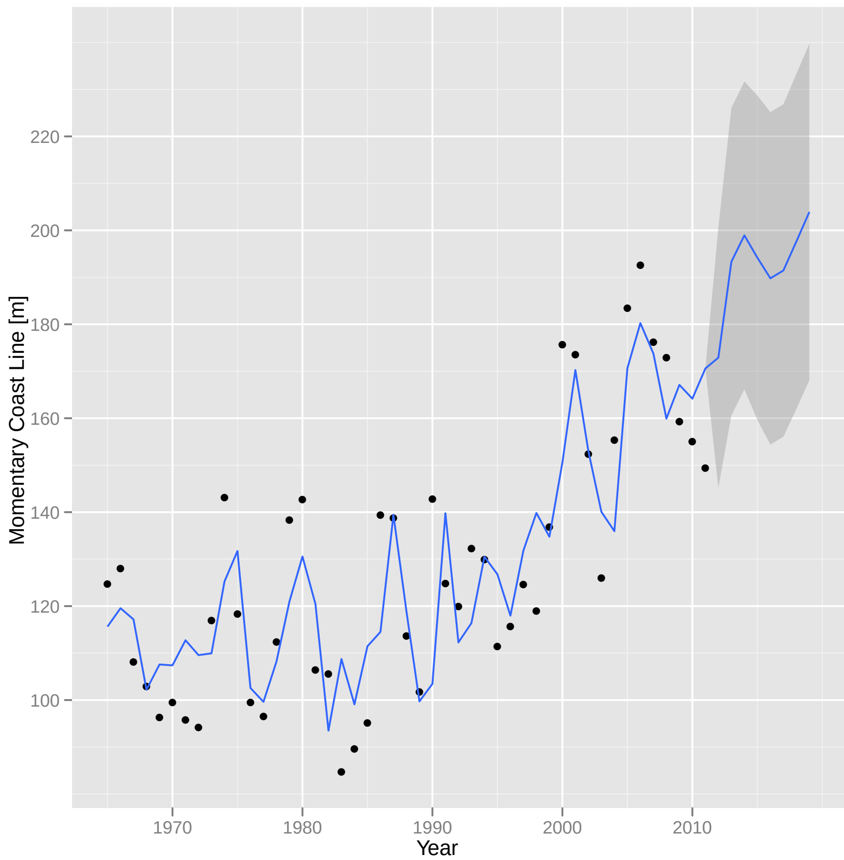

Figure 4.11: ARIMA (3,0,1) including the policy effect and intercept for the Egmond location (Jarkus transect 7003800)

Including the autocorrelation into our statistical model does not result in a more narrow confidence interval. We do not "increase" our confidence, but it can be assumed that our confidence estimate is more valid, as we no longer assume that the errors (ϵ_t in Equation 4.7) are independent and identical distributed.

The application of these models to the whole Dutch coast is shown in Figure 4.12. The major part of the coast shows the positive (blue) effect of coastal policy.

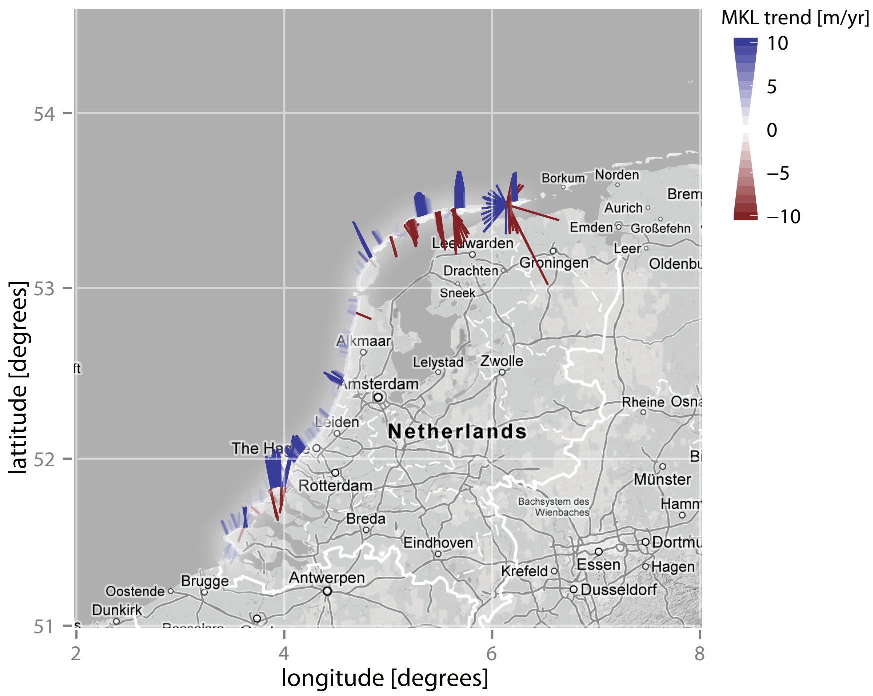

Figure 4.12: Momentary coastline positions trends based on the sum of the drift and policy effect.

We can conclude that the policy change did co-occur with a significant change in the trend of the MKL position (old trend is significantly different lower than new trend). In fact, one could state, that the trend has now shifted to a significant positive trend. The effect of a local "hold the line" strategy is a dune volume growth along the major part of the Holland coast.

This answers Question 3.6.1 and 3.7.

Part II

PREPARATION

Part i focussed on forecasts for the mitigation phase. This Part presents forecasts for the preparation phase. For this purpose the operational forecast system for the Dutch coast is extended with quantities that describe changes in coastal morphology and with confidence intervals. The aim of the forecasting system is to provide coastal managers with timely, accurate, precise and relevant information. This information can be used to make appropriate decisions when a coastal storm is imminent. Chapter 5 describes the design considerations of the extensions of the coastal forecasting system with morphological quantities. Chapter 6 focusses on the extension of the operational forecasting system with confidence intervals.

5

A MORPHOLOGICAL FORECASTING SYSTEM

Contents

This chapter first evaluates the need for a preparation approach. After that the focus switches a discussion on the setup an operational morphological forecasting system. The next chapter discusses the extension of the forecasting system by introducing confidence intervals around operational morphological forecasts.

As we have seen in the Chapter 1 a safety approach consists of four phases (mitigation, preparation, response and recovery). If it is a good practice to setup a preparation approach for coastal management, what would this entail? Where mitigation relates to the activities required to prevent or reduce the effect of a negative event, the preparation approach relates to influencing the behaviour of people involved in a disaster.

Examples of a preparation approach in coastal context are warning people of possible events, making available sandbags or other temporal defences for short term protection and for example setting up evacuation plans and emergency supplies. An interesting but unadvisable example of a preparation approach is the lowering of ships in front of the shore with the goal to reduce the wave impact to the coast [Walstra and Bos, 2009].

Figure 5.1: Example of a preparation approach, simulation of sinking ships in front of the coast as a last minute preparation before a storm [Walstra and Bos, 2009]

One thing to consider, before we look at the implementation of a preparation approach for dune based coasts, is how to evaluate the optimal balance of investments between the two complimentary approaches: preparation and mitigation. Should we not spend all our efforts into making the dunes as safe as possible? How do we find an optimal balance between the two? Several considerations can be used as arguments to justify or dispute the investments into a preparation approach.

EFFECTIVENESS OF WARNINGS One of the main considerations is that the effectiveness of a warning system is usually limited. We have already seen the example of the Xynthia case where there was a warnings given, but it did not give the relevant information (information of probability of flooding was absent). Another well-described shortcoming of warning systems is that they are prone to introduce a "cry wolf" effect [see for example Breznitz, 1984]. In the 2011 tsunami many people delayed evacuating or ignored warnings because over the years many false positive tsunami alerts were given [Normile, 2012]. Many victims knew the waves were coming but could not escape or did not try until it was too late [Normile, 2011]. The question is also if one is able to give a timely warning, with enough confidence so that people can act in time. Chapter 6 discusses this further.

ETHICAL Another aspect that is relevant is the risk perception bias [see for example Starr, 1969]. A society is willing to allow a much higher risk if the risk is voluntary. We can apply this to an operational coastal forecasting system. Let's assume we provide the public with a warning of an expected coastal flooding. This allows people to evacuate or seek higher grounds and this would transform the risk when they do not evacuate from an involuntary risk to a voluntary risk. Could we then lower the safety level? Answering this question raises some ethical questions.

If we have the technical capability to warn people about possible negative consequence events, do we also have the responsibility to warn them? Arceneaux and Stein [2006] studied the relation between disasters and voter behaviour. They found that after a disaster, in hindsight, the local and national government are held responsible for the whole chain of mitigation, preparation and response. It was found that the amount of personal control in the situation and the amount of knowledge about the government's working methods were the important factors in the amount of blame put on the government. The first point confirms the study by Starr [1969], in that risks are more acceptable if people are "self proficient" and that indeed, the public expects these warnings. The second point indicates that the decisions made in the context of cost effectiveness, what is defended and what not, should be communicated clearly. As we have seen in the description of the Xynthia storm (Section 1.1), lack of communication of risk can cause dramatic effects.

It lack of communication of risk can also be reason for conviction as seen in the recent trial in Italy, where 6 scientists were found guilty of manslaughter. They were accused of giving out giving out "inexact, incomplete and contradictory information". The public communication officer had translated their forecast into "the scientific community tells us there is no danger ..." [NewScientist, 2012], which turned out not to be true as the earthquake in L'Aquila caused 297 casualties.

EXPECTED UTILITY One could dispute if it is cost efficient to have a preparation approach ready for areas where the probability of an event is lower than once in a lifetime. An example calculation for Dordrecht, an area prone to river flooding was made, and showed that including the preparation approach on top of a mitigation approach with a low probability safety level is not cost effective [Hoss et al., 2011]. Another approach to look at the benefit of information is given by the value of information theory [see for example Howard, 1966]. This theory describes how one can assess the value of added information, in this case information of a warning about the breaching of a dune. Howard [1980] later came up with the idea to use "micromorts" as a more easy to use currency for valuing life versus other benefits.

In practice one will find that one of the safety links is already in place. For areas with a high probability of erosion or inundation one will be more experienced in getting the relevant information on imminent natural hazards. Inhabitants of areas with high frequency flooding commonly have a boat ready to evacuate and boards to put in front of their doors to prevent water from entering their homes. In areas where the probability of dune failure is small, such as the Dutch dune coast, the preparedness effort is relatively small. Most of the effort is put into improving the mitigation link.

This focus on one link rather than the whole chain is understandable if one considers that the safety chain does not adhere to the physics of ordinary chains. In contrary to most chains, the safety chain is (at least) as strong as the strongest link [Jongejan et al., 2008]. If either of the safety links is fully effective it prevents the hazard to develop into a disaster.

This answers Question 4.2.4 .

In the context of the preparation approach we will focus on setting up a coastal morphological warning system. As we have seen, providing the public and authorities with a warning gives a high sense of control and it is a relatively low cost effort. For the usefulness of a coastal morphological warning system in areas where the probability of events is low (say smaller than once in ten years) the forecasting system should aim to serve multiple purposes. One cannot expect for a system to work if the operators and designers of such a system will have a lower than once a career opportunity to use it. Therefore a system aimed to predict coastal morphological changes in an operational context should be multi purpose, also including purposes that are relevant at least once a year. In the next section we will discuss several use cases for a coastal forecasting system.

5.2 USE CASES FOR A COASTAL FORECASTING SYSTEM

The first step in setting up a coastal forecasting system, or any other system, is making an inventory of the requirements of the system. Examples of requirements for a coastal forecast system are functional requirements (what should it predict?), architectural requirements (which components should it be composed of?) and performance requirements (how fast should it produce results?).

The definition of the functional requirements of a system is a task that is conducted together with potential stakeholders and end users of the system. In the case of a coastal forecasting system the end users consist of local and regional authorities that are responsible for the maintenance of the coast and the safety of the people living and recreating near the coast. The requirements for system are often gathered in a standardized form. For software requirements the requirements are often formulated in the form of use cases or user stories [Beck and Fowler, 2001]. For coastal management questions a common way to formulate the "customer" and "functional" requirements is through the frame of reference method [van Koningsveld et al., 2005]. This method was applied across nine coasts in Europe [Ciavola et al., 2011a] and this resulted in a number of potential applications of a coastal forecast system.

One of the aspects of the frame of reference method is the Quantitative State Concept (QSC), the quantity that the system should be able to predict for different coastal management tasks. Based on the discussions with the potential end users of the coastal forecasting systems the following states were defined, [see also Ciavola et al., 2011a].

DUNE MONITORING Likelihood map with locations for high-water events.

PROTECTION OF IMMOBILE PROPERTY Risk maps (time and space) with expected economical damage in the coastal strip (that contains houses, shops, etc.).

PROTECTION OF MOBILE PROPERTY Run-up timeseries (e.g. extracted from beach morphodynamic model).

CONSERVATION OF NATURAL AREAS Run-up and maximum flooding cross-shore and longshore extension (marine water ingression limit).

SWIMMER SAFETY Space-time map of areas that are unsafe for swimming, covering at least the most used areas.

EVACUATION PREPARATION Providing coastal inhabitants with information of the effect of storms, three days ahead.

If we focus on the physical quantities they are comparable to the quantities that we have seen in the mitigation part. The difference here is mainly the time scale. The water level is important but at a time scale of hours. Also the extreme water level, the maximum run up is important and the morphological change of the dunes are important because the dunes are under heavy loads and failure mechanism of dune erosion can cause the dune to fail. In this thesis we will not analyse the run up estimates because we do not have accurate measurements to compare with.

This answers Question 4.1 .

Now that we have a definition of some of the requirements of the coastal forecast system, we will focus on setting up a morphological forecasting system for a specific locations, in this case the Dutch coast and with a main focus on the use case of predicting morphological changes during the storm of a magnitude corresponding to the safety level discussed in Chapter 3.

5.3 THE EUROPEAN EFFORT TOWARDS A COASTAL FORECASTING SYSTEM

The remainder of this Section 5.3 through 5.5 were published as "Real-time forecasting of morphological storm impacts: a case study in the Netherlands" [Baart et al., 2009a]. The text and figures have been edited, extended and improved for consistency and to incorporate new insights.

Recent events like the Sumatra tsunami and Hurricane Katrina have reminded the world of the vulnerability of coastal areas to extreme events. Despite hydraulic engineering measures to minimise failure probability of coastal defence structures, a probability of failure, albeit small, remains. To assist local authorities and the population in their response to extreme events, timely access to relevant information of sufficient accuracy regarding impending natural threats is crucial. Current real-time systems do not include all relevant physics (e.g. morphodynamic response). This section describes the efforts in the framework of the Morphological Impacts and COastal Risks induced by Extreme storm (MICORE) project to develop such an improved real-time system for the prediction of storm impacts. This section addresses the proposed system architecture and some preliminary results and some aspects of the development environment that may be of more general interest than to this project alone.

The years 2004 and 2005 were characterised by a number of large coastal disasters around the world (i.e. the Sumatra tsunami in December 2004 and Hurricane Katrina in the US in August 2005). These powerful natural events have raised awareness that the coastal areas are vulnerable to natural disasters. The near miss of New Orleans by hurricane Gustav in August-September 2008, only three years after hurricane Katrina, made it clear that although extreme events by definition have a low probability of occurrence this does not mean that they could not in fact happen a number of times within a short period of time.

The exposure of Europe to comparable extreme events was demonstrated by European windstorm Kyrill, which hit in January 2007. It was a mild winter in most of Europe when Kyrill caused severe loss of human lives, great property loss and infrastructure damage. Kyrill was a medium strength storm, which made landfall on the German and Dutch coasts on the afternoon of January 18th, affecting 8 countries causing the loss of 47 human lives and many small properties. The storm losses greatly affected insurance companies. The estimated damage in Germany alone was €4.7 billion [Alovisi et al., 2007].

The preparation approach has received increased attention in more recent times. The European Union (EU) Seventh Framework Programme (FP7) Project MICORE analysed current storm response approaches in nine European countries and concluded that amongst others, the study sites could by improved by implementing operational, quasi real-time, coastal risk assessment methods. Only two European countries have operational systems available predicting storm surge levels [Ferreira et al., 2008]. No real-time systems taking into account morphodynamics were available. It was the main objective of MICORE to develop such a system. It is the main objective of the next sections to describe the architecture of the system and the implementation for the Dutch coast.

The MICORE project has considered the main end users of a real-time system to be local authorities that are responsible for emergency response and last-minute mitigation in case of an upcoming extreme event. In order to support their efforts they need:

1. timely access
2. relevant information
3. sufficient accuracy and precision

Timely access is essential, given the limited time available for (organizing and executing) response activities. This has consequences on the available model runtime, bringing up the issue of weighing accuracy versus being on time. Timely access in this context is at least three days ahead. Both authorities and people should be able to respond. In practice this is not possible if a warning time is two days or less [Kolen, 2010].

Relevant information in this case regards expected coastal hazards such as overtopping, overwashing, beach and dune erosion, dune breach and localized flooding. With this information responsible authorities may better allocate their scarce resources, e.g. allocating levee and dike patrol, selecting locations for emergency repairs, indicating safe areas for residents to evacuate to, etc.

Figure 5.2: Aeolian transport during the November 2011 storm. Src: pzc.nl, Photo: Dirk-Jan Gjeltema

Real-time information on water levels is available in the Netherlands. This information is taken as a trigger to take preparation actions. However, in most, if not all, cases water levels alone are not enough to predict events like overtopping, overwashing, beach and dune erosion, dune breach and localized flooding at the desired level of detail. Merely adding waves to the equation is not enough. Especially during extreme storm events the morphodynamic response of the coastal system can be significant. Depending on this response the influence of water levels and waves in turn may also be affected significantly. The aeolian transport during storms can also affect coastal safety, positively, by strengthening dunes (see Figure 5.2), and negatively, when the lack of visibility hinders evacuation attempts. The extension of the morphological model with aeolian transport [Baart et al., 2012a] is not part of this thesis.

In recent years similar systems have been setup for other countries. A noticeable example is the operational forecast system that predicts coastal regimes a few days ahead [Plant and Holland, 2011a].

Besides including the relevant physics in the model system and producing the proper output, the aggregation of model output data into information relevant for end users is of great importance. Examples of such aggregated results could be maps indicating not only areas of erosion and sedimentation but also separating areas of moderate erosion of those with severe erosion. Which parameters to choose is not a trivial matter, i.e. allocating emergency repair capacity the areas of erosion rates are of interest while indicating safest areas for evacuation whereas one might look at areas of no erosion.

5.4 THE ARCHITECTURE OF A COASTAL MORPHOLOGICAL FORECAST SYSTEM

Now that the use cases and requirements are established, it is possible to define a general architecture for the morphological forecasting system. As there are many comparable forecasting systems existing systems are used for inspiration. For each of the components the design considerations will be discussed in detail.

5.4.1 *Global forecasting systems*

Several operational models are currently active for operational forecasting weather related quantities such as pressure and precipitation. Two major global systems are the Global Forecast System (GFS) by National Oceanic and Atmospheric Administration (NOAA) and the Integrated Forecast System (IFS) by European Centre for Medium-Range Weather Forecasts (ECMWF). A complex computer system, such as these weather models, consists of different parts. Based on the documentation [for example Howard and Ward, 2011] we can identify the following components: *i*) Runner of tasks and jobs *ii*) Gathering of datasets from online sources, such as satellite and measurement stations *iii*) Converting data into boundary conditions for the numerical model. *iv*) Data assimilation and other statistical routines for filtering and predicting missing data. *v*) In most complex systems the physical models are split up by physical processes, for example modules for cloud coverage, ocean waves. *vi*) Inter model communication is needed because most models are too big to run on single computers. By parallelizing over physical processes and over domains (subsections of the numerical grid) multiple computers or processors can be put to work simultaneous. *vii*) Some systems include the possibility to run scenarios or experiments. These scenarios often have the form of perturbations of input or of what-if scenarios. *viii*) After the models have ran output is generated. The output is provided to end users of different levels.

A major difference between the global models is the scale and number of end users of the system. The global systems are used by numerous end user applications, resulting in better quality. This results in a solid push for quantity. Making all the results and source publicly available, as is done in the GFS, increases this even more, according to the mantra “given enough eyeballs, all bugs are shallow” [Raymond, 1999], although another explanation for the quality improvement is that when source and data are public, there is no rug to sweep under.

5.4.2 *Local forecasting systems*

The same approach that is used for global forecasting systems is also used for local weather forecasting systems, such as Weather Research and Forecasting (WRF) [Michalakes et al., 2004] and HIgh Resolution Limited Area Model (HIRLAM). Systems more closely related to the morphological coastal warning system are the hydrodynamic and hydrological forecasting systems. These systems are more local and more specific in their physical processes. Examples for the Dutch coast are the hydrodynamic model train described by Gerritsen et al. [1995] and Verlaan et al. [2005] for the North Sea and the Delft Flood Early Warning System (FEWS) system for the river forecasts [Werner et al., 2009]. The FEWS system is different because of a different architecture and a different approach to inter model communication. It is based on a client-server architecture, with a central relational database for model results, whereas the model results of most Numerical Weather Prediction (NWP) systems are stored on the internet with metadata inside of the datasets. Another aspect is that it does not incorporate a fixed set of models, but requires models to be adapted to a FEWS specific interface. This allows for new models to be incorporated.

5.4.3 *The morphological forecasting system*

The architectural requirements follow from the potential use cases from the system. The following components and tasks can be identified from the QSC above and the corresponding benchmark states [see Ciavola et al., 2011a] and the discussion of the global local forecasting systems.

MODEL SETUP Model setup and establishment of input parameters.

DATA COLLECTION Reading basic data (wind data, pressure data, bathymetric data etc.) from data sources.

PRE-PROCESSING Converting the downloaded basic data to the proper input formats for the model engines.

RUNNING MODEL ENGINES Running the numerical implementations of the physical processes to generate predictions.

running scenarios Running scenarios to incorporate for emergency measures or what if scenarios

post-processing Processing and aggregating the raw model output.

publishing Transform the modeling results into information that can be used by end-users.

The challenge in setting up of a system architecture is not only in defining the correct components but also in keeping the components independent. One might be tempted to generate a train of programs that are all dependent on the outcome of each other (Figure 5.3). This would make the publishing of results directly dependent on the model runs and this does not follow the good design principles [Fowler, 2003] of keeping user interface and the result of the models independent. Good points of introducing inversion of control in the architecture of a forecasting system are after the model run and after the data collection. In practice this means that the publishing component should ask for data (don't call us, we'll call you), as should the pre-processing task.

Regarding the performance requirements, some of the QSC's most of the states require information in a time window of days, either real time (swimmer safety) or a few days ahead. These performance requirements need to be matched with the numerical models, because these are usually the performance bottlenecks in a physical model based forecasting system. Another aspect that is important for performance is the connection between data, models and user interfaces. The information required for running simulations persists within different institutes and is transferred through the internet. To be able to have a fast responding, independent system, having an optimal exchange of datasets through the internet is thus essential.

5.5 The implementation of a coastal morphological system for the Dutch coast

To illustrate the practical implementation of the steps described above their concrete implementation for a Dutch case is discussed. The system has been further expanded to a broader spatial scale and other areas, such as the California coast.

The real-time system is set up in such a way that components of the system can be easily replaced. New bathymetric data that is entered into the database can trigger updates to the model bathymetry used. Also, in the context of the MICORE project regular improvements may be expected to the open-source modeling package XBeach. Using subversion for keeping track of versions, it will be relatively straightforward to replace that part of the real-time model train.

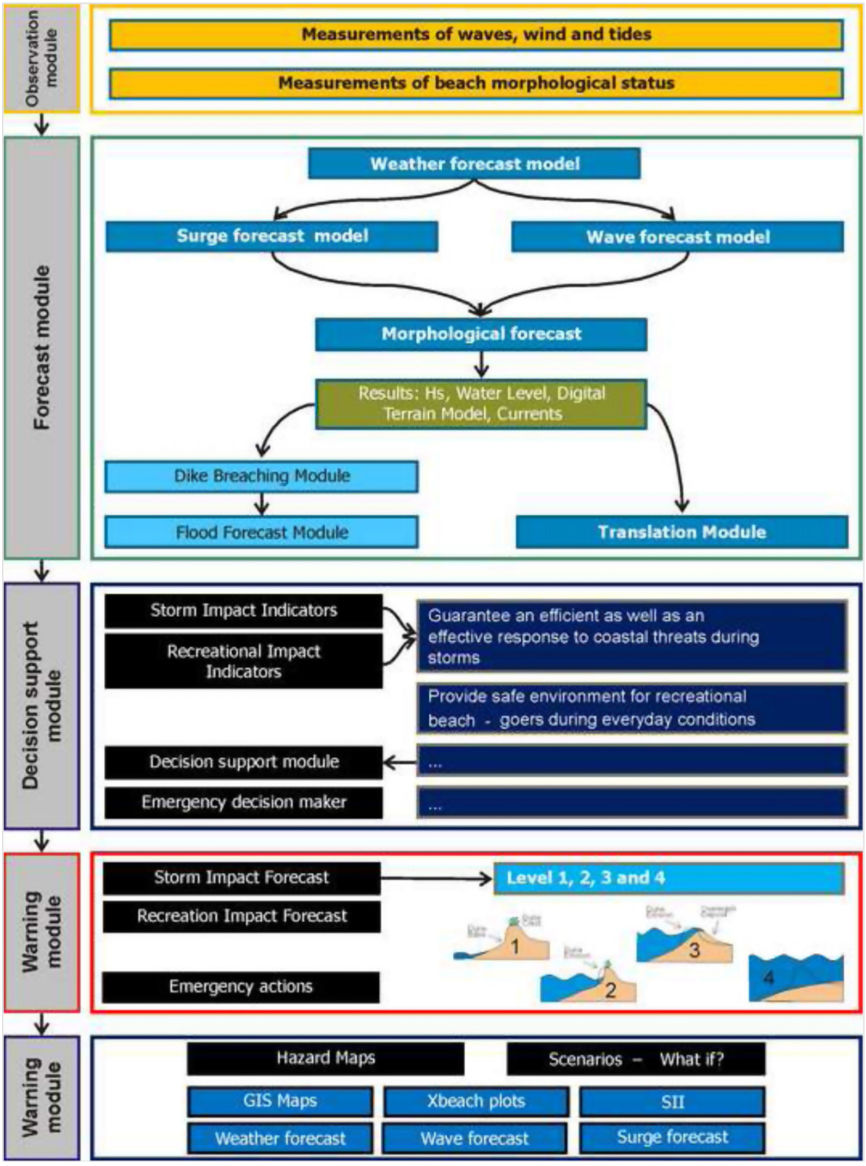

Figure 5.3: General architecture of the coastal forecasting systems setup in MICORE [Ciavola et al., 2011a], the last row indicates the visualization module.

Reproducing forecasts with changing data, models and tools is prone to errors or subjective decisions. Keeping track of the whole process, fully automating all changes from initial datasets to results, is a guarantee for reproducibility. Using a scripting language is a good way to automate processes like this. Automating also allows for errors to be corrected by simply rerunning the scripts which were used to create results.

To allow for freedom to reuse, adapt, inspect and replace components, open source and open standards are used as much as possible. By publishing source code and keeping track of history, quality and accountability is improved.

5.5.1 *Model setup*

One of the challenges in setting up the model domains is to incorporate the correct physics, while maintaining computational efficiency. This is especially challenging because the relevant processes occur at a wide variety of spatial and temporal scales, as we have seen in Figure 2.1. The same processes that were used for the safety level in Chapter 2 are relevant here, but at a time scale of days.

This answers Question 4.2.1 .

There are several approaches to this. Some numerical applications allow for local refinements. This is the case for implementations based on non equidistant grids and implementations based on domain decomposition. Another approach that is used for the Dutch case is to use nesting where the numerical models run on different resolutions, exchanging information either internally by making local refinements in the grid [see for example Borthwick et al., 2001], one directional (the coarser model feeds the finer model) or two directional (two way exchange between two models).

In the coastal morphological model we start with the transformation astronomical tides in combination with predicted wind and pressure fields into predicted current, water levels and waves. This is a large scale model ($O(1000x1000km)$), which may be part of the coastal model train, however, in some cases such models are already run by other organisations and tapping into these results using them as boundary conditions may be considered. Next a regional model ($O(100x100km)$)is needed to transfer the overall current, water levels and wave patterns towards the coastal region of interest. An additional refinement in the near shore area ($O(10x10km)$) is generally needed to generate input of sufficient spatial resolution to properly drive the local model ($O(1x1km)$) that resolves the detailed hydro- and morphodynamic processes that are of interest for decision makers dealing with response to extreme events. Depending on the modelled area the number of models needed may increase or decrease. The major advantage of using this nested model approach is that the models at different scales can be used for other purposes as well.

Also there is no need to make a single purpose numerical grid, other than the nested local grids. Creating a local grid often involves some local knowledge. By having the local grids as pluggable elements in the system they can be easily replaced by new models, once local reconsideration is needed.

In the Dutch case developed for the MICORE project four model schematisations of increasing resolution describe the hydrodynamic, wave and morphologic processes: 3 Delft3D models and 1 XBeach model. Figure 5.4 shows the schematisations.

The three coarsest schematisations cover the North Sea, the Dutch coast and the Dutch coast near Egmond and are based on the Dutch Continental Shelf Model [Gebraad and Philippart, 1998]. Domain decomposition is used to connect the hydrodynamic processes whereas nesting is used to connect the wave processes. The schematisation with the highest resolution, covering the Egmond beach area, is used to describe the morphological processes.

5.5.2 *Data collection*

The following datasets are used for the operational morphologic predictions.

1. The online windfield predictions from the HIRLAM NWP forecast system. The latest predicted windspeed and wind direction are used.

2. The online waterlevel predictions from the Multifunctional Access Tool foR Operational Oceandata Services (MATROOS). The MATROOS system provides daily forecasts of waterlevels.

3. The network of directional wave buoys of Rijkswaterstaat. The network of directional wave buoys is used to compare predicted to observed wave heights.

4. The annual transects of the JARKUS dataset [Rijkswaterstaat, 2008]. This dataset has a goal to evaluate annual changes in the coastline. The dataset covers both topography and bathymetry of the nearshore area. The latest bathymetry and topography is used from this dataset.

This answers Question 4.2.3 .

5.5.3 *Pre-processing*

The wind fields and water level predictions use the same schematisation for the coarsest grids and can be used directly as input for the combined wave/flow model run. The wave spectra and significant wave heights are used as boundary conditions.

For the three coarser schematisations the bathymetry of the Dutch Continental Shelf Model is used as a fixed bathymetry while the

Figure 5.4: Schematisations of the operational model. From top to bottom, left to right: Wave Watch 3, Contintental Shelf Model, Kuststrook Fijn

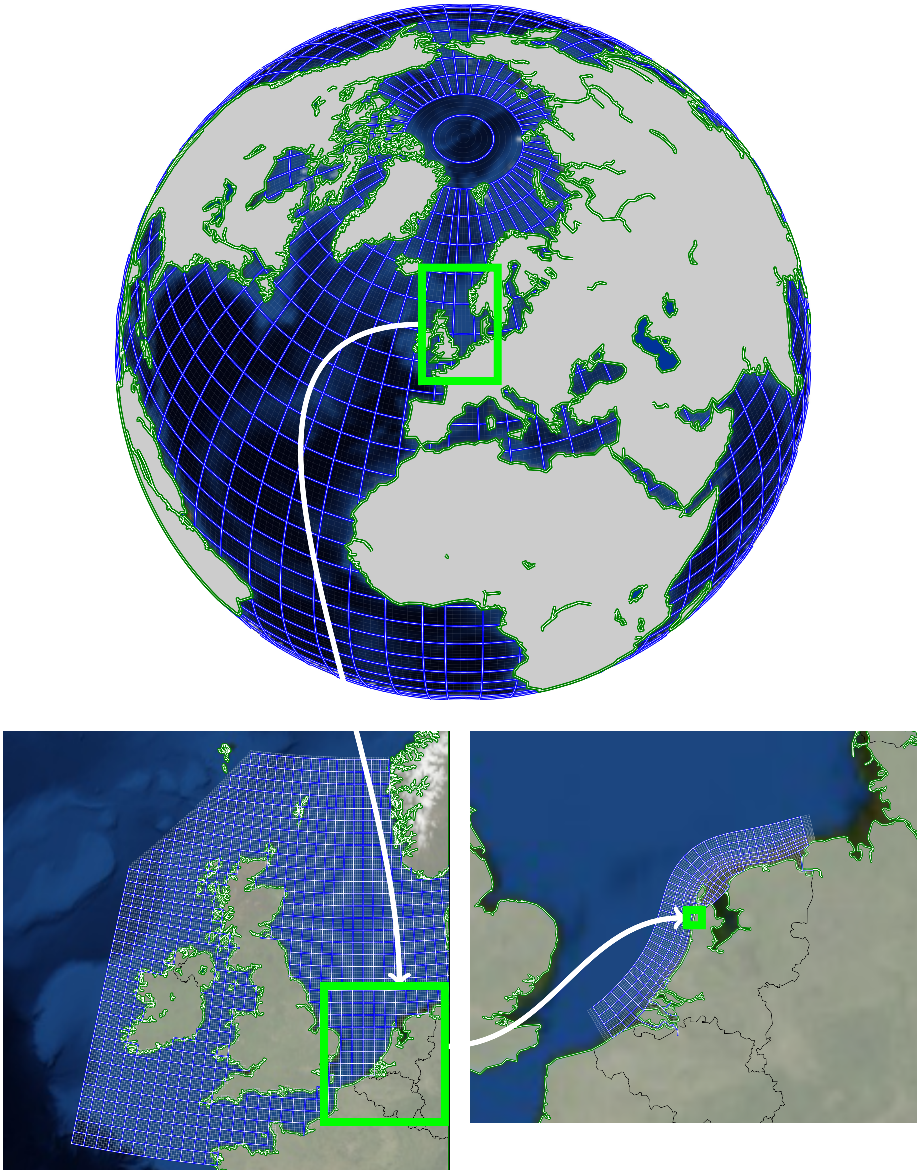

Egmond beach area uses the measurements from the JARKUS data. The predicted bathymetry is not used as input for the next prediction but the bathymetry is reset to the JARKUS observations at each run. Using an updated bathymetry of known precision will be an improvement.

5.5.4 *Model components*

The hydrodynamics, waves and morphological processes were simulated with different model engines. The hydrodynamic and the wave models ran online (output exchanged bidirectional). The morphologic model was coupled offline (output exchanged unidirectional) with the hydrodynamic model.

1. Hydrodynamic processes were simulated using the Delft3D-FLOW software (3.27) [Stelling, 1984].
2. Wave processes were simulated using the SWAN software (4051AB) [Booij et al., 1999].
3. The morphodynamic processes were simulated using XBeach [Roelvink et al., 2007]. XBeach is a two-dimensional model that is used for sediment transport and morphological changes of the nearshore area, beaches, dunes.

The most relevant output variables for storm events, viz. water levels, significant wave height and bathymetry are saved with a 10 minutes interval.

This answers Question 4.2.2 .

5.5.5 *Post processing*

In this step of the process normally the physical model results would be aggregated to present proper information for decision-makers. Information one could think of are: sedimentation erosion maps, inundation maps, maps pointing out suitable and non-suitable spots for emergency evacuation etc. Ciavola et al. [2011a] gives an overview of indicators that were used in the MICORE project. For the Egmond case we converted the model results into potential safe and unsafe evacuation areas, based on the human stability studies from Abt et al. [1989]; Jonkman et al. [2005]; Jonkman and Penning-Rowsell [2008].

Forecasts of coastal erosion in the Dutch coast at Egmond were produced between July 2008 and October 2010. After the MICORE project ended the running of operational forecasts stopped due to lack of maintenance.

By limiting the calculation time which is required for timely predictions, a balance is needed between model accuracy and speed. This requires to limit the number of processes taken into account and the

Figure 5.5: Egmond model showing erosion (bottom image), water level + waves (transparent surface), bathymetry (solid surface)

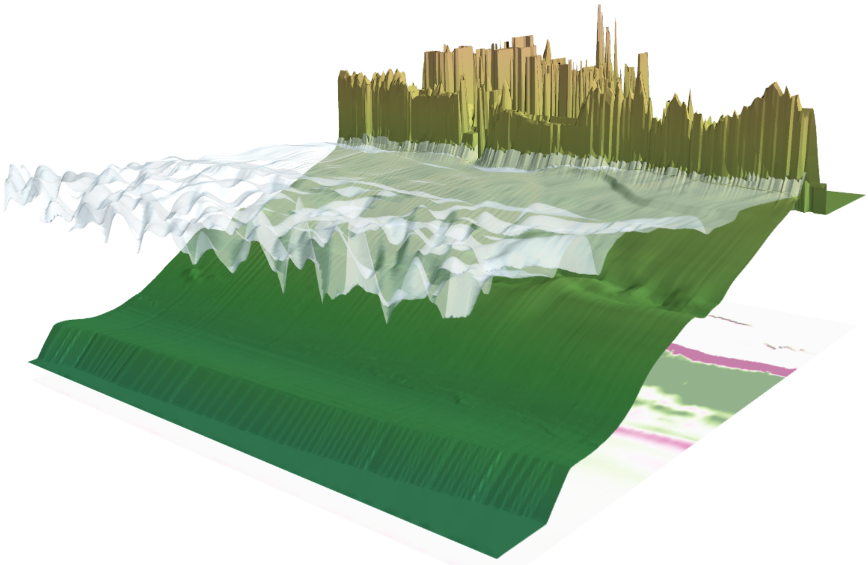

detail of the schematisation used. Because we are limiting the accuracy of the model, it is important to present the results with known information about the precision and accuracy of the predictions. This will be the topic of Chapter 6.

5.5.6 *Publishing*

The results of forecast systems models were traditionally stored in safe data centers. Only the very communities that run these models were able to access the data produced by these models. Currently there are two trends that endeavor to make these results available on the internet for a larger audience than these communities themselves. In Baart et al. [2011b] and Baart et al. [2012b] we analysed different methods for publishing results from numerical models through the internet. The Open-source Project for a Network Data Access Protocol (OPeNDAP) approach is currently used to publish the results of the numerical models that forecast the morphological change.

This answers Question 4.2 .

6

CONFIDENCE IN REAL-TIME FORECASTING OF MORPHOLOGICAL STORM IMPACT

Contents

In the previous chapter a coastal forecasting system was presented. A forecast of coastal change should be presented with a confidence intervals. This chapter presents the final example of how to extend a forecasting system with confidence intervals. From the three methods discussed in Baart et al. [2011c], two methods are examined in detail. This chapter shows the skill of the forecasting system as a function of forecast lead time, to answer the question "How many days ahead can we make a morphological forecast?".

This section was submitted as "Confidence in real-time forecasting of morphological storm impact" to the journal Weather and Forecasting

6.1 INTRODUCTION

Coastal areas are exposed to natural disasters of marine origin. Providing warnings is one of the ways to reduce the risk to human life and to allow for property to be protected [Day et al., 1969]. Although these warnings are not always effective [Normile, 2012], when a disaster is imminent people expect to be warned [Arceneaux and Stein, 2006].

In order for a coastal warning to be helpful it needs to be relevant, timely, accurate (Section 5.3) and with a confidence interval [Baart et al., 2011c]. Previous studies have worked on providing relevant warnings by extending operational hydrodynamic forecast models with forecasts of morphological change [Section 5.3, Plant and Holland, 2011a; Vousdoukas et al., 2011]. Adding morphodynamic processes to a coastal warning system is relevant because the failure modes of coastal dunes depend on the morphological change [Sallenger, 2000; Mai et al., 2007].

Setting up a warning system that takes into account coastal morphology was part of a broader European effort [Ciavola et al., 2011b]. Here we expand on this effort by showing how accurate, precise and timely we can forecast coastal changes during a storm surge. We show how accurate and timely the forecasts are by analysing the Forecast Skill Score (SS) and Mean Squared Error (MSE) of the forecasts as a function of forecast lead time.

The forecast of the morphological effects of a storm is at the end of a chain of nested numerical models. The last four parts of the chain, which are used to forecast the coastal morphology, are shown in Figure 6.1. Each of these models is based on assumptions, schematisations and reductions of the real world [Oreskes et al., 1994] and can only explain a certain proportion of variance of the quantity for the next link. Unexplained variance propagates through the chain of models, making the forecasts of the models down the chain weaker and weaker.

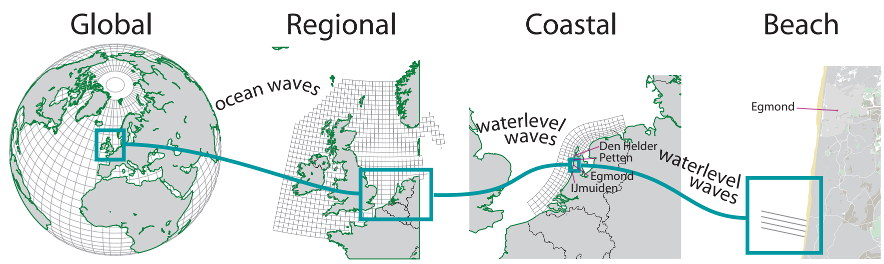

Figure 6.1: Schematisations of the operational model.

This raises the question "How many days ahead can we still rely on operational morphological forecasts?". An important question, because it determines the feasibility of different response actions.

6.1.1 *How many days ahead?*

The quality of the forecast of morphological change depends on the quality of the other forecasts in the chain. We will first examine how many days ahead we can predict the indirect and direct input of the morphodynamic model. The indirect inputs include pressure fields, wind fields and ocean waves. These are used to compute the direct inputs: coastal waves and water levels. The variables are assimilated in the model chain up to the morphodynamic model and thus part measurement and part model. The output and input of the model is the bathymetry and topography from −20 m to the dunes.

At the start of the model chain are the pressure fields that are used to generate wind and surge. The most common representation is the 500 hPa geopotential height, because it represents the long atmospheric waves that influence the dynamics of the weather at the ground. To determine how many days ahead pressure fields can be predicted the Anomaly Correlation (AC) is used. The AC is a measure of potential skill [see Wilks, 2011, and Equation 6.6] that is used for continuous field forecasts, such as pressure fields. Detailed explanations about the SS, AC and how they relate to MSE can be found in Murphy and Epstein [1989]; Wilks [2011].

The second input to the model chain is the wave height. The coastal waves consist of long ocean waves that enter at the continental shelf boundary and of local generated wind waves within the regional domain. The ocean waves are based on the winds caused by pressure field anomalies. Figure 6.2 shows that the ACs of the ocean waves are lower than the pressure fields, 60% versus 70% for the 7 days ahead forecast and 92% versus 98% for the 3 days ahead forecast. In general, the consequent coupling of the models reduces the explainable variance down the chain, which is a probable cause of this skill reduction.

The third and most important input to the morphological forecast is the water level forecast from the regional model. The water level is forecast by the regional and coastal model, which have the global pressure and wave forecasts as input. De Vries [2009] found that the skill of the forecasts of surge is quite variable. The skill for water level forecast is lower than the skills for the wave and pressure forecasts. This water level skill is computed using the Brier Skill Score (BSS), a skill score for probability forecasts. The probability forecast used for the Brier Score (BS) is the probability of exceeding the local warning thresholds under 60% for forecasts up to 3.5 days ahead. This is in line with the assumption of a reduction of explained variance through

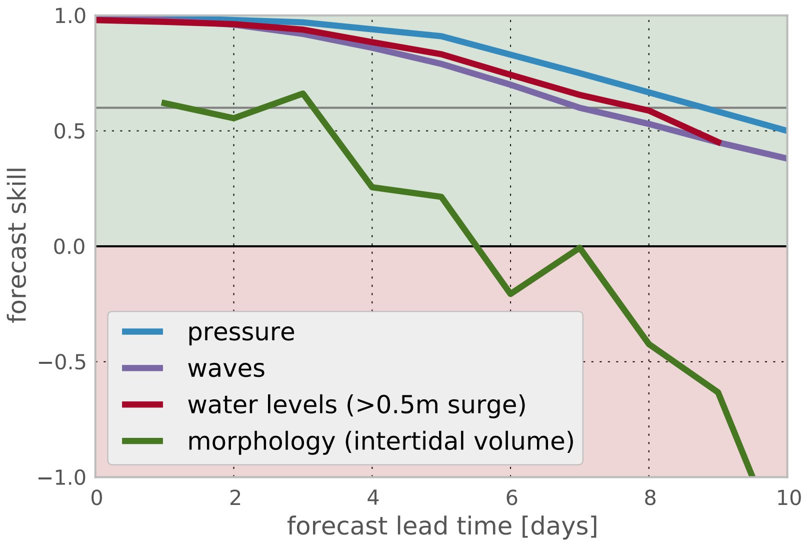

Figure 6.2: Skills for pressure, waves, waterlevels and morphology as a function of forecast lead time. Pressures are Anomaly Correlation (AC) for the European Centre for Medium-Range Weather Forecasts (ECMWF) 500 hPa forecasts [European Centre for Medium-Range Weather Forecasts, 2010], waves are Anomaly Correlation (AC) for the European Centre for Medium-Range Weather Forecasts (ECMWF) significant wave height forecasts [European Centre for Medium-Range Weather Forecasts, 2010]. Water levels are the Forecast Skill Score (SS) for the water levels for the regional model, data de Vries [2009], skill computed in this paper. Morphology SS for the intertidal beach volume, this paper.

the chain. In this study we recalculate the water level SS and MSE for the same time windows as the morphological skill in order to make them better comparable.

This subsequential reduction of skill shows that less variance is explained as we propagate through the chain of models up to the morphological model. At this stage it is unclear how much we can still explain with the morphological model. How many days ahead can we still make a skillful forecast of storm induced morphological change?

6.1.2 *Creating confidence intervals*

A forecast should not only be presented with information on skill, but also with information on precision. This helps in making cost effective decisions [for example Johnson and Holt, 1997]. How a confidence interval can influence a decision can be illustrated by a simple example: Suppose we have terrace inventory on the beach, with a worth of 10000EUR. Assume it costs 100EUR to move the inventory to safety. A deterministic forecast for 1 day ahead might give an outcome that the beach will not erode up to the property and the terrace is safe. The best approach would be to keep the inventory on the beach. With a forecast including the confidence interval one could have a probability of erosion, resulting in the loss of the terrace, of 10%. In that case one would move the terrace away from the beach. The expected loss of 1000EUR can now be reduced to 100EUR. This example shows that with the inclusion of confidence intervals around the forecast the most cost effective decision can be made.

Including confidence intervals can be done in different ways. One import assumption is how one considers measurements: are the measurements "true" or do we assume the "truth" to be somewhere in the middle of the observations and model results? In this study we assume the observations are "true", which can be done if one expects the measurement errors to be an order of magnitude smaller than the model errors. Other choices to be made are the sources of variations that are considered. Here we consider two different sources of variation out of the three discussed in Baart et al. [2011c]:

MORPHOLOGICAL ERRORS Based on records of morphological forecasts, the expected forecast error is calculated. The distribution of these errors is assumed to be representative for future errors. This method requires a history of morphological forecasts and measurements and is the least computational intensive, it does not require any additional model runs.

ENSEMBLES Ensembles are propagated through the regional model and used as a boundary condition for the beach model. This does not require any record of old forecasts but is the most computational intensive because it requires multiple hydrodynamic and morphological model runs.

The question here is methodological, what is the best method to include confidence bands around the morphological forecasts? In Baart et al. [2011c] we discussed that when one takes into account the computational time the morphological errors method is preferred. Here we define "best" as which method produces the most accurate confidence interval [O'Connor and Lawrence, 1989]. A 95% confidence interval is accurate when it covers 95% of the parameter of interest in the population.

This answers Question 4.3.3..

6.2 METHODS & DATASETS

In order to estimate our skill and confidence in the operational morphological forecast, we select storm events and collect relevant datasets. To study accuracy and timeliness of the forecasts, the skill and MSE as a function of forecast lead time are calculated, based on previous events. The forecast lead time is the interval between the time when the forecast was issued and the occurrence time of the forecast phenomena.

We include information about the precision of our forecast by including confidence intervals around the morphological forecasts as described in [Baart et al., 2011c]. In a statistical context, precision is defined as the reciprocal of the variance [pp 245 Gauss, 1809] and the confidence interval width is a function of the variance.

6.2.1 *Model setup*

The model chain used to forecast coastal change (Figure 6.1) is described in detail in Section 5.3. The model chain consists of a global wave model (schematisation: Wave Watch, processes: waves, model: Wave Watch 3 (WW3)), with a nested regional (Dutch continental shelf model (DCSM), hydrodynamic and waves, Delft3D) and coastal model (Dutch "Kuststrook Fijn", hydrodynamic and waves, Delft3D).

The last link is the beach model (Egmond profiles, hydrodynamics, waves and morphodynamics, XBeach). The beach model is schematised using 1D profiles instead of a 2DH bathymetry. The main reason for this is to reduce calculation time. It is believed that for this part of the coast a 1D approach is also sufficient [den Heijer et al., 2012]. The variability in profiles near Egmond is shown in Figure 4.9. For areas with more complex foreshores a 2D approach is thought to be more appropriate [van Geer and Boers, 2012].

The water level forecasts are generated by the setup as described by De Vries [2009] (Delft3D replaced by the similar SIMONA model), which provides a history of ensemble forecasts.

6.2.2 *Study site Egmond (the Netherlands)*

The model chain is applied to the Egmond study site, located in the Bergen municipality in the Netherlands has been used in numerous publications [for example Aagaard et al., 2005]. The video measurement stations have generated before and after storm bathymetry measurements over the last decade, essential for computing the morphologic skill and validating the morphological confidence bands. The stations at IJmuiden, Petten and Den Helder provide measurements of waterlevels and waves, required for estimating the hydrodynamic skill. The morphodynamic forecasts are relevant for the town of Egmond aan Zee, as it is an area with a high risk of dune erosion [den Heijer et al., 2012].

6.2.3 *Storm selection*

To answer the question how many days ahead the morphological effect of a storm can be forecast, multiple storms are considered. The forecast system is setup to predict extreme events. For a representative sample, one would prefer a large number of high return period storms ($\geqslant$ 10 yr). But as only a decade of data is available, this is not possible. The water level records from the Petten tide gauge (20 km north of Egmond) give a good selection criterion, as it is the closest tide gauge to the Egmond study site. A peak search for the highest water levels, with a window of three days, results in the selection of five storm events (see Table 6.1).

Date	Pre	Post
2007-11-09	2007-01-01 – 2007-01-06	2007-11-10 – 2007-11-14
2006-11-01	2006-10-26 – 2006-10-30	2006-11-02 – 2006-11-07
2007-01-18	No data	No data
2008-03-01	2008-02-27 – 2008-02-29	2008-03-02 – 2008-03-07
2007-03-18	2007-03-14 – 2007-03-17	2007-03-19 – 2007-03-24

Table 6.1: Selection of pre and post storm profiles for the five storms that resulted in the highest water level at Petten, the Netherlands.

Besides a high water level, availability of morphologic and hydrodynamic data is important. No intertidal morphologic estimates have been made for the 2007-01-18 storm, due to unavailability of the Argus video camera system, which was setup in the CoastView project [Davidson et al., 2007]. Therefore, this storm is only used to determine the hydrodynamic forecast error and skill as a function of forecast lead time.

6.2.4 *Boundary conditions*

Water level observations are collected by three stations near the Egmond site, at IJmuiden, Petten and Den Helder (locations in Figure 6.1). Operational forecasts, including ensembles, are available only for the IJmuiden and Den Helder location. As a boundary condition for our morphodynamic model we need an estimate for the water level, either based on observations or forecasts, for the Egmond location.

To estimate the water level at a location where no tide gauge or forecast is available one would normally use a hydrodynamic model that includes tidal forces and that is calibrated on the observed water levels of several nearby tide gauges. An alternative that can be used for both observations and forecasts, is to compute the water levels in Egmond based on an interpolation of the stations IJmuiden and Den Helder.

For the calculation of the water levels, one could be tempted to simply reconstruct an estimate of the tide gauge by computing some weighted mean (by for example inverse distance) over the two nearby gauges. Such an approach underestimates the amplitude of the tide, because adding two sines with a slightly shifted phase reduces the amplitude. Interpolating the tidal constituents and the surge separately does not suffer from this effect. Here we use constituents, including the nodal factor, based on the tables available in the t-tide software package (based on the xtide dataset) [Pawlowicz et al., 2002; Flater, 2012].

Equation 6.1 computes the water level H in Egmond (egm) as a function of t in year $year$, based on the arithmetic mean amplitude A and the circular mean phase θ of location IJmuiden (ijm) and Den Helder (dh). The amplitude A and phase θ for station Egmond are combined and summed over constituents i through C by combining them with the nodal factor (N) amplitude and phase speed (f) for the year and constituent. The datum and surge can be computed by regular averaging, as there is no phase difference. This interpolation gives a water level for the Egmond location that can be used as a boundary condition.

$$A_{egm} = \left(\frac{A_{ijm} + A_{dh}}{2}\right) \tag{6.1}$$

$$\theta_{egm} = \angle\left(\frac{\exp(i\theta_{ijm}) + \exp(i\theta_{dh})}{2}\right) \tag{6.2}$$

$$datum_{egm} = \frac{datum_{ijm} + datum_{dh}}{2} \tag{6.3}$$

$$surge_{egm} = \frac{surge_{ijm} + surge_{dh}}{2} \tag{6.4}$$

$$H_{egm}(t) = \sum_{i}^{C}\left(N_{i,year}A_{egm,i} * \cos((f_i t + \theta_{eq,year} - \theta_{egm})\frac{\pi}{180\circ})\right) + datum_{egm} + surge_{egm} \tag{6.5}$$

The normal operational setup allows the use of wave forecasts from the coastal model. There is no archive of the coastal wave forecasts with ensembles. The wave time series, as observed at the "IJmuiden munitie depot" station, provide us with a reasonable alternative to use as a boundary for the beach model. Based on our understanding of storm impact on dunes in the Netherlands, it is expected that the water level is the most important input [see for example van de Graaff, 1986] and that the wave observations are reasonably representative for the offshore wave boundary conditions [Van Thiel de Vries, 2009], since both are located at a depth of −20 m. This could lead to overconfident confidence intervals around the morphological forecasts, because no wave errors are taken into account.

Two datasets provide information for the bathymetry and topography. The Dutch Annual Coastal Measurement (JARKUS) dataset [Rijkswaterstaat, 2008] provides the base bathymetry and topography. Pre- and post storm intertidal bathymetry is obtained from the Automated Shoreline Mapper (ASM) archive [Uunk et al., 2010], a process for extracting shorelines from the Argus video camera system.

The ASM measurements only cover the intertidal zone. This is not the most interesting area when one wants to study the storm impact on dunes. Erosion mainly sets in above the dune foot. Along the Dutch coast, the sand that erodes from the dune is transported through the intertidal zone towards the sea. After a storm, part of the sand that eroded remains in the intertidal zone, causing the volume of the intertidal zone to temporary increase. As the intertidal shorelines are the only available real time measurement source, it is still the best approach to use here. In the ongoing analysis we make the assumption that the volume changes in the intertidal zone are representative, or at least a proxy for the storm impact above the dune foot. More specific, it is assumed that the volume changes in the intertidal area have the dune as a source. Morphological errors are expressed as a function of distance from the dune top, because as the dunes grow, the position varies from year to year.

Adjustments were made to the process described by Uunk et al. [2010]. The shorelines generated by the ASM showed intra-day inconsistencies, which required an extra manual selection step. In the context of an operational system, a manual selection step is unsatisfying because it requires human intervention. The overview of selected days for each storm event can be found in Table 6.1. A possible overestimated point is the 2 meter observation in Figure 6.3 (profile 4, 2007-03-18). It is likely too high, although without other measurement sources we cannot confirm this. We choose not to "fix" these issues by taking longer bathymetry averages, or by interpolating. The dry spots that cause these overestimates are typical features that are not captured by the processes and settings in the 1D XBeach model. Leaving them in, results in an underestimate of our potential skill, but it does give a good estimate of the skill that we would expect for new forecasts and it gives a direction for improving our numerical model, schematisation and measurement techniques.

A summary of the time windows used for the model runs can be found in Figure 6.4. The morphological forecasts are made with XBeach (revision 2892) using a "morstart" and "morstop" that starts and ends with the start time of the bathymetry interpolation time windows.

6.2.5 *Forecast skill*

To assess the SS (Equation 6.10 and 6.11) we run deterministic morphological model runs for the four storm periods. We start the forecasts based on the original deterministic model runs of the water level forecasts. The forecasts were made with a lead time from 10 up to 1 day. Both forecasts and measurements are required to assess the skill. These are available at the IJmuiden and Den Helder station. The SS for water level is computed with the astronomical tide as a reference forecast (`ref`). When this SS goes below 0, the astronomical tide is a better forecast than the model forecast. We use the high and low tide estimates and ignore any errors in forecast time.

The SS for morphological change is computed with the initial bathymetry as a reference forecast. When this forecast skill goes below 0, the initial bathymetry is a better forecast than the model forecast. We apply this skill for the total intertidal volume change.

Here we do not use the term BSS, which relates to the skill of probability forecast. Probability forecasts have the form of "the probability that it will rain tomorrow is 70%". An example of a continuous forecast is "it will rain 10 mm tomorrow". For the probability forecasts, the outcome is a probabilitiy for dichotomous events, and the BS can be computed. In coastal literature the term BSS is sometimes mistakenly used to refer to continuous forecast skill [for example van Rijn et al., 2003; Sutherland et al., 2004].

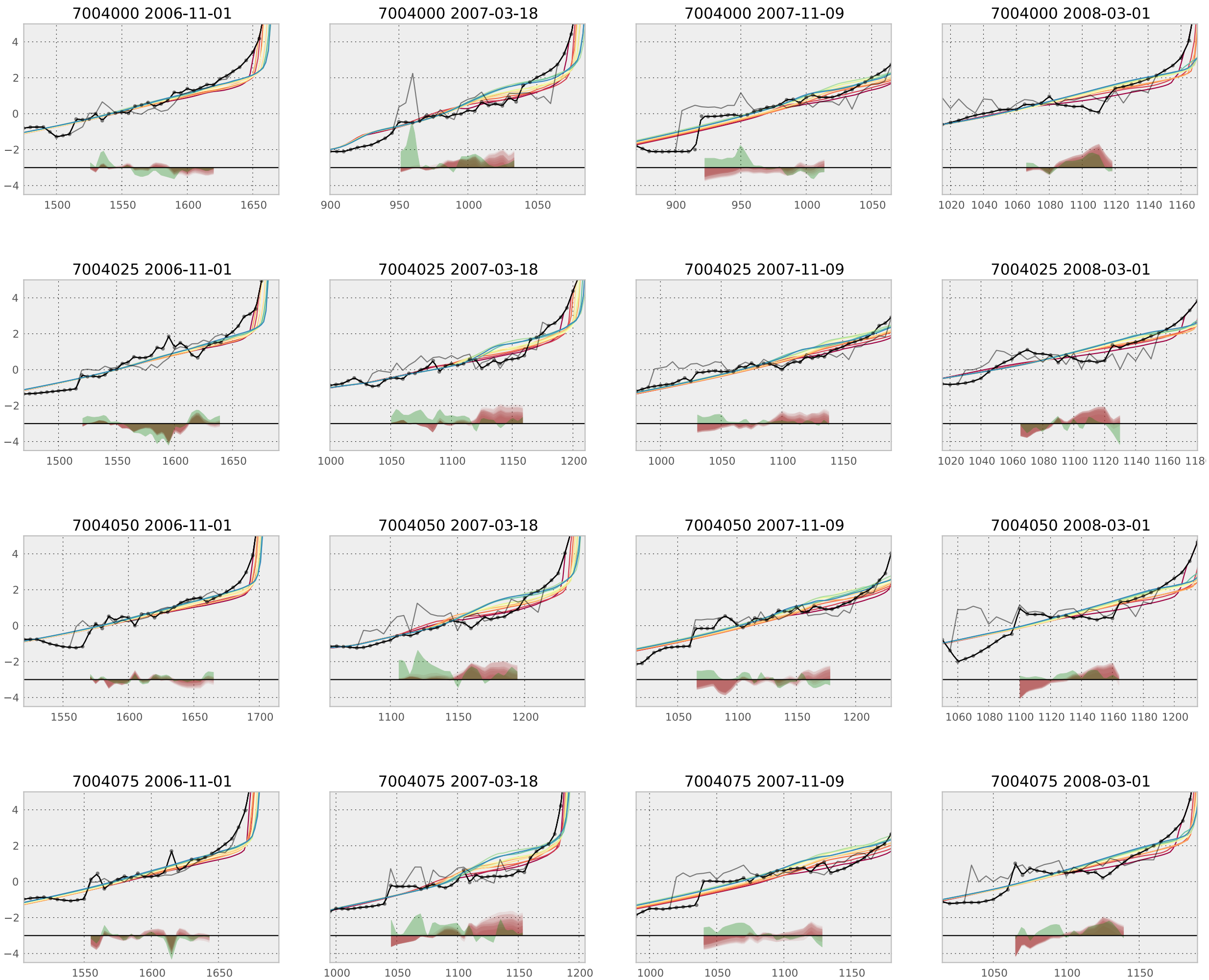

Figure 6.3: Observed and modelled pre and post storm profiles for the four different profiles and the four different storms. Black dots: observed pre storm profile. Black solid line: initial model bathymetry. Gray line: observed post storm profile. Coloured lines: forecasts from 10 days ahead (red) to 1 day ahead (blue). Green area with origin at -3: observed bathymetry change. Brown area with origin at -3: forecast bathymetry changes.

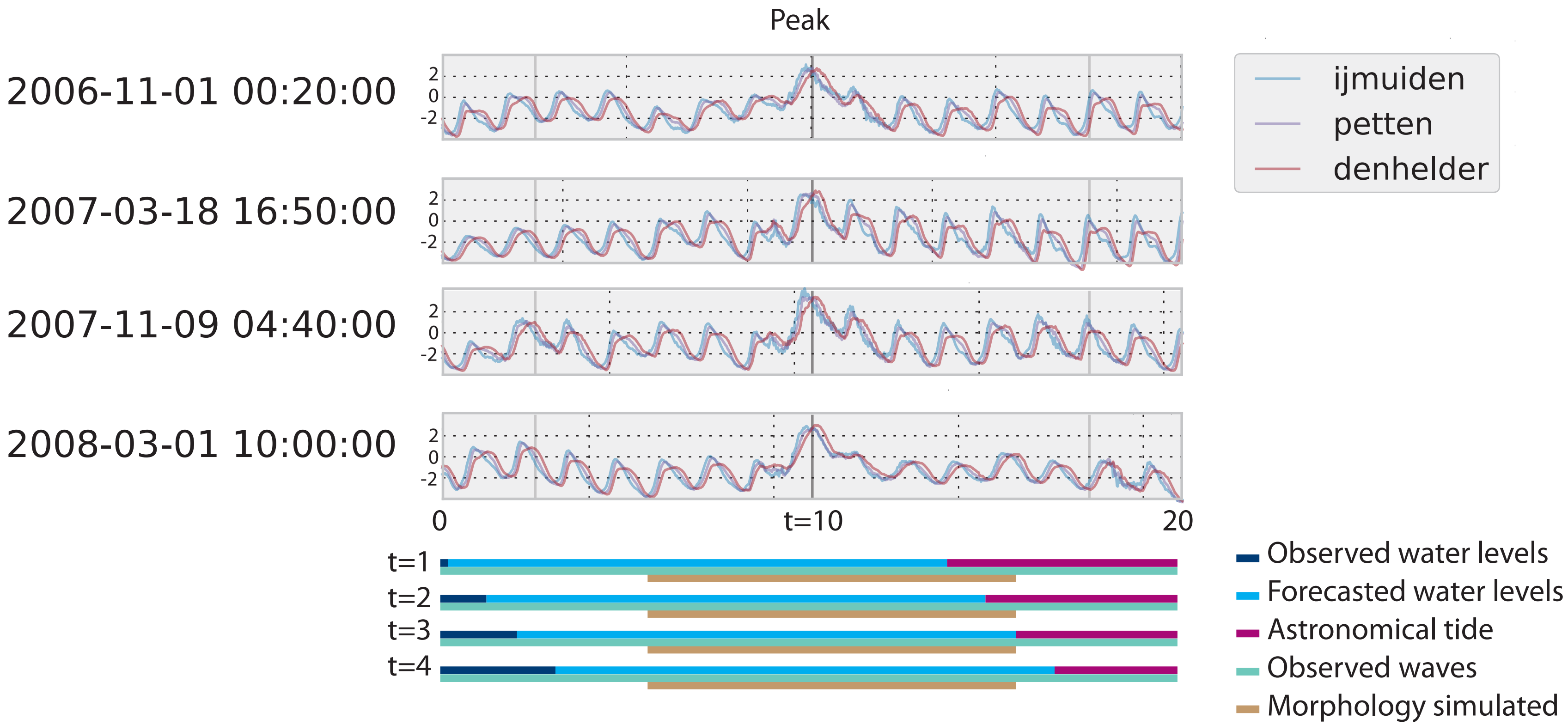

Figure 6.4: Overview of the time windows for the model runs. All simulations start at t=-10, morphology updates are turned on at the start of the pre storm morphology measurement and turned off at the start of the post storm measurement. Water level boundary conditions are left padded with observed water levels and right padded with tide forecasts. For wave boundary conditions only observations are used (see text).

Verification calculations were done using the National Center for Atmospheric Research (NCAR) R Project for Statistical Computing (R) verification package [Gilleland, 2010].

The statistical measures that are used in this paper are listed in Equations 6.6 through 6.13. These include Anomaly Correlation (AC) based on forecast y, observations o and climate c, a number of n forecast, observation pairs with index k, Mean Squared Error (MSE), the Root Mean Square Error (RMSE), the Forecast Skill Score (SS), the Brier Score (BS) and the Brier Skill Score (BSS).

$$AC_{uncentered} = \frac{\sum_{k=1}^{n}(y_k - c_k)(o_k - c_k)}{\sqrt{\sum_{k=1}^{n}(y_k - c_k)^2}\sqrt{\sum_{k=1}^{n}(o_k - c_k)^2}} \tag{6.6}$$

$$MSE = \frac{1}{n}\sum_{k=1}^{n}(y_k - o_k)^2 : o \in \mathbb{R} \tag{6.7}$$

$$\sigma_{\text{observed}} = \sqrt{\frac{1}{N}\sum_{i=1}^{N}(o_i - \mu_{\text{observed}})^2} \tag{6.8}$$

$$RMSE = \sqrt{MSE} \tag{6.9}$$

$$SS_{bathymetry} = 1 - \frac{MSE_{\text{model}}}{MSE_{\text{initial bathymetry}}} \tag{6.10}$$

$$SS_{waterlevel} = 1 - \frac{MSE_{\text{model}}}{MSE_{\text{astronomical tide}}} \tag{6.11}$$

$$BS = \frac{1}{n}\sum_{k=1}^{n}(y_k - o_k)^2 : o \in \{0, 1\} \tag{6.12}$$

$$BSS = 1 - \frac{BS}{BS_{ref}} \tag{6.13}$$

6.2.6 *Error sources for the confidence intervals*

The two different methods to compute the confidence bands (ensembles, morphological errors) require different error sources. For the water level ensembles, we use the ensembles that are generated by the Royal Netherlands Meteorological Institute (KNMI) operational forecast system. For the extrapolation of morphological errors, the storms of March 2006, March 2007 and November 2008 generate error estimates. The confidence band generated from these errors are validated using the November 2007 storm. This storm is used, because it is the storm with the highest surge. For the ensemble method only one profile is used, again to reduce computation time and because the deterministic runs did not show a noteworthy differnece between the profiles. The profile that is closest to the Argus video camera station is used, as it has the highest pixel/m^2 ratio and thus, assumably, the lowest measurement errors.

6.3 RESULTS

6.3.1 *Days ahead hydrodynamics*

The hydrodynamic forecast skill over the whole month, starting from two weeks before and ending two weeks after the storm (Figure 6.2), shows that for all the time windows the SS is positive, even for forecasts 10 days ahead. The skill is over 0.6 [in coastal research often used as a criterion for a good forecast van Rijn et al., 2003] for seven days. The conditional errors (given that there is a storm in the next ten days) are shown in Figure 6.5a. As can be seen from the white lines, when a storm is about to occur, longer forecast lead times result in a positive forecast errors. An observed positive surge minus a near zero surge forecast give a positve forecast error. As an alternative to the 0.6 SS criterion, the $RMS_{error} > \sigma_{observed}$ threshold also gives an indication that a forecast is beyond a "useful" lead time.

The hydrodynamic ensemble forecast errors for the November 2007 storm are shown in Figure 6.5c. These are comparable to the deterministic forecast errors.

This answers Question 4.3.1.

6.3.2 *Days ahead morphology*

Based on the deterministic water level forecast, the observed waves and the interpolated bathymetry, we hindcast the morphological model starting from 10 days to 1 day before the storm. The morphological forecast skill (Figure 6.2) shows that the forecast skill is positive up to five days ahead and over 0.6 for three days.

The results from the determinstic model runs are shown in Figure 6.3. The first thing to note is that in the forecast bathymetries the sand is deposited closer to the dunes than observed. This can be seen in the brown patches that are higher than the green patches near the dunes and the green patches that are higher than the brown patches near the intertidal area −1.5 m to 1.5 m, representing forecast and observed bathymetry changes. The intertidal volume change is not very sensitive to errors in beach angles. If a coastal state indicator [van Koningsveld et al., 2005] was chosen based on individual points, it would result in a lower skill.

The morphological errors are shown in Figure 6.5b. Comparable to the hydrodynamic forecast errors, the deterministic morphological forecast errors show an increased average error (white line going up) for longer forecast times. As the storm approaches the inter tidal volume change forecasts are more close to the observed volume changes. The ensemble errors, shown in Figure 6.5d, are computed for the profile closest to the camera. The errors for this profile are larger than for the average of the average of the four deterministic profile runs in Figure 6.5b.

This answers Question 4.3.2.

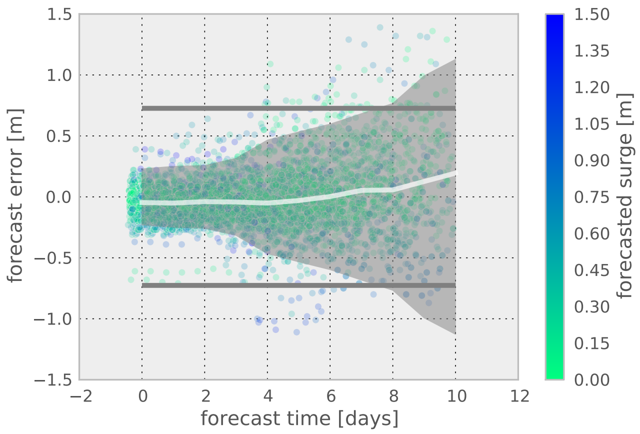

(a) Hydrodynamic deterministic forecast errors as a function of forecast lead time.

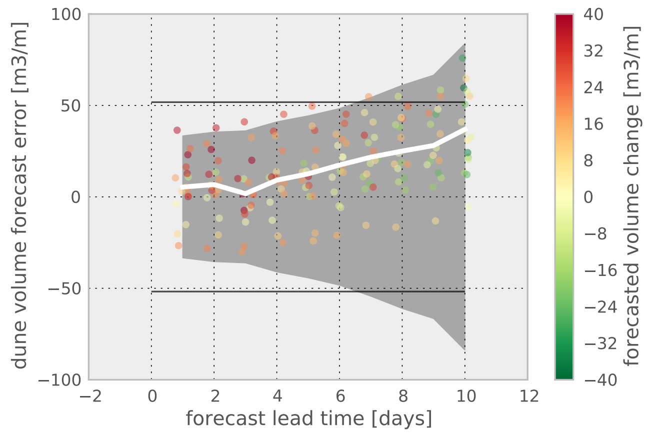

(b) Morphological deterministic forecast errors (intertidal volume change) as a function of forecast lead time.

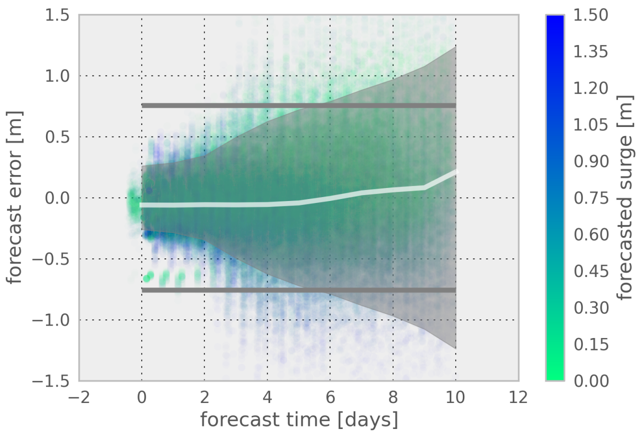

(c) Hydrodynamic ensemble forecasts errors as a function of forecast lead time.

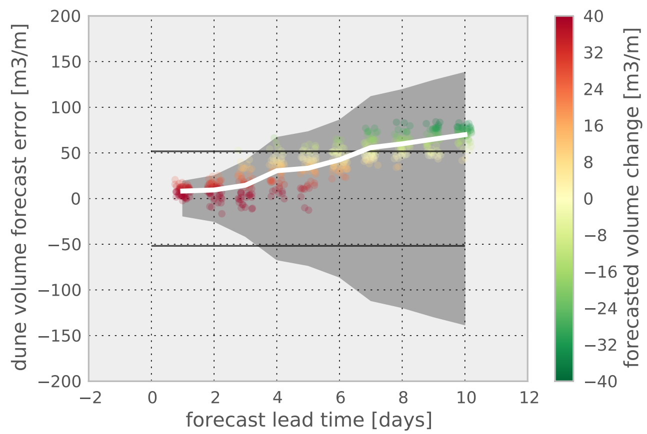

(d) Morphological ensemble forecast errors (intertidal volume change) as a function of forecast lead time for ensemble forecasts.

Figure 6.5: Errors for hydrodynamic and morphological forecasts (deterministic and ensembles) as a function of forecast lead time for the 10 days before the storm surge peaks. White line shows the mean forecast error for inter tidal dune volume change. Gray area shows the $1.96 * \mathrm{RMS}_{\mathrm{error}}$ interval. The grey lines show $1.96 * \sigma_{\mathrm{observed}}$ for dune volume change and surge.

6.3.3 *Confidence intervals*

The two confidence intervals methods were tested as a 1D field forecast (individual points in the profile, not shown in figures). Both methods applied created invalid confidence intervals. The morphological errors method resembled the validation storm errors most closely.

MORPHOLOGICAL ERRORS The morphological errors from the storms in November 2006, and March 2007 and 2008 were used to determine the expected confidence for forecast bathymetry changes as a function of distance from the dune top. The confidence interval for these intervals were confirmed using the November 2007 storm. This showed that the confidence intervals created using the historic forecast errors are slightly under-confident as the confidence interval entails 100% of the volume differences. An accurate confidence interval contains 95% of the parameter of interest if a new sample is drawn from the same population.

ENSEMBLES The confidence interval for the individual points in the profile based on the ensemble propagation, without assimilation, entails only 18% of the observed intertidal bathymetry changes making the confidence interval overconfident. This is caused by the structural beach slope difference between the observed and modelled post-storm bathymetry.

This answers Question 4.3.4.

6.4 CONCLUSION

We have seen that the nested hydrodynamic and morphological models can predict water levels up to ten days ahead and volume changes in the intertidal zone with a skill over 0.6 up to three days ahead at the Egmond location under storm conditions.

The system is nearing the skill level needed to predict coastal breaches with enough lead time to act, but it is not there yet. A lead time of three days is just enough for a warning of possible breaching to trigger a preparation effort. From the three days the calculation time of several hours needs to be subtracted. An extra margin (over the 0.6 SS level) should be included to account for the negative effect of providing false warnings [Breznitz, 1984]. This leaves us with a morphological forecast with a too low skill, just a few hours late to provide a useful warning for preparation purposes.

The lower skill for the morphological forecasts is in line with what one would expect from a basic error propagation theory, where the explainable variance reduces when one makes longer chains of models. This can be countered by assimilating at multiple steps along the chain. However this shifts the morphological model from a "process based" model to a "statistical model". The generalizability that we hope to achieve using the process based model is lost to the "the sample is representative subset of the population" assumption of the statistical assimilation model.

Several approaches can be used to improve on these results. The statistical models used here all assume that the measurements represent a true value, without error. The non-intertidal measurements are only measured once per year and have a limited representability for the current bathymetry using the storm. The Argus measurements did not show the expected precision when used in an operational setting. The automated analysis of video data still has some room for improvement. So in hindsight it makes more sense to include these sources of variance into the statistical model. In fact this is an ongoing activity, for example by van Dongeren et al. [2008].

Another alternative is to replace the morphological model by a statistical model [Plant and Holland, 2011a] trained on numerical simulations. This would have the advantages of the greatly reduce computation times and it would make the separation between the statistical model and the numerical model more explicit. One of the current disadvantages of the Bayesian Network approach [as used by Plant and Holland, 2011a,b] is that continuous variables are treated as nominal variables resulting in a large number of parameters. By moving to a probabilistic graphical model that include continuous variables, for example a Marcov Chain Monte Carlo (MCMC) model [Gelman et al., 2004], the number of parameters can be reduced, allowing for a greater generalizability. To generalize from mild storms, for which the model can be trained, to large storms, for which the model should predict, requires a parsimonuos statistical model.

This answers Question 4.3.

There are also efforts to improve the numerical models and schematisations used. As a result of these efforts, over the last years the water level forecasts skill increased [Verlaan et al., 2005]. Operational models, similar to the one discussed here, have been setup accross Europe, also resulting in a better set of default parameters for the XBeach model [Ciavola et al., 2011a]. In this study we have used four year old bathymetry measurement techniques and four year old hydrodynamic forecasts. As our knowledge, measurement and modeling skills have progressed over the last four years, a logical step would be to repeat this activity for the later and coming storms in order to assess our progression.

This study shows that it is important for forecasting systems to keep a record of historic forecasts in order to determine forecast errors. The preferred way, if data storage is limited, is to store output of the models at locations where measurements are also available. An alternative, and in itself advisable, is to keep track of the exact versions of the software, input data, schematisations with which the model was run. This allows to recreate old forecasts.

As discussed in Baart et al. [2011c] the different methods of confidence interval creation, each have their own characteristics and advantages. It was found that to estimate a confidence interval we can use our record of old forecasts. In this example this gave much better results then using the ensemble based method, because it allows to match the skewed errors. The morphological error and hydrodynamic error approaches work as long as we don't upgrade our schematisation and numerical models. After an upgrade the whole history of forecasts has to be recreated to get new expected errors. The apparent advantage of reduced calculation time only works as long as we can assume that errors from old forecasts are representative for future errors.

For verification of beach profiles it would make sense to work towards a goodness of fit measure that takes into account the different type of errors that can be made when estimating a 1D beach profile, such as slope errors, horizontal errors and vertical errors, analogue to the work for 2D field verification [Gilleland, 2010]. This study assumes that the skill of the intertidal volume changes is representative for the volume changes in the dunes. The coastal state indicator of tidal beach volume is not the most appropriate, but the only indicator that provided enough data for validation purposes.

Part III

DISCUSSION AND CONCLUSION

7

DISCUSSION

Contents

The question that this thesis started with, "How can we show and improve our confidence in coastal forecasts?", is a methodological question. This chapter first addresses confidence in a broader methodological context before going into the statistical techniques that were used to show and improve confidence intervals The last section of this chapter addresses the other main question, "For which phases of coastal safety management are coastal forecasts relevant?", by giving an overview of the differences and intersections between the mitigation and preparation phases.

Especially for low lying countries, the different forecasts that were analysed in this thesis are of great importance. They are used to determine how public money is spent and how safe people living behind the coastal defence are.

This thesis discusses one aspect of confidence in forecasts, namely the confidence intervals, which relate to the precision. To have a more general confidence in forecasts one would require more than just statistical confidence.

One could use many definitions of confidence. Probabilistic terminology is used inconsistently and is not always well defined, especially not across different fields of study. For example, the word reliability has a different meaning in statistical terms where it is basically the same as precision, whereas in engineering it is used for the probability of non-failure. The term confidence was recently introduced with a new meaning in climate research, relating to the combination of high inter-scientist agreement and "high evidence" [Mastrandrea et al., 2010]. This is a very limited view and can also be wrong for an inter-scientist agreement can also be the result of a failing scientific system. Here we propose to use confidence as the combination of reliability and validity (in the statistical context [see for example Wilkinson, 2005]). Table 7.1 provides a more detailed overview of what makes one confident in a forecast, based on the work on the quality of tests [Cronbach and Meehl, 1955, and follow-up research] and the partial list of Wilks [2011].

When we compare this list with the forecasts that are made in this thesis it is obvious that for each forecast not all aspects of confidence are studied or reported. As an example we'll go over a few of them. For most of the forecasts the *reproducibility* was studied, but only by the author. When setting up a numerical model in particular, a lot of subjective choices are made. It is likely that the forecasts made for the $1/10000 \text{yr}^{-1}$ storm surge and the operational morphological forecasts would be different if reproduced by different researchers. The estimates of the storm surge were also *sensitive* to the type of distribution that was chosen. The *stability* was not studied in any of the forecasts. A common way to do this to see if the results change if the floating point precision is changed. For all the calculations this is only practically possible for the coastal model that was used in the prediction of the water levels.

An example of a lack of *convergent* validity can be seen in the sea-level forecasts. We have seen that numerical models consistently predict a sea-level acceleration, whereas statistical models, based on long running tide gauges, predict a constant sea-level rise.

One thing that was explicitly left out of the operational forecasts was the check for *concurrent* validity, it was only checked if the height

Reliability degree to which the forecast is consistent.

- Reproducible does the forecast change when it is recreated?
- Intra forecaster does the forecast change when it is created by someone else?
- Sensitive does the forecast depend on perturbations of input variables or parameters?
- Stability does the forecast magnify numerical approximation errors?

Validity degree to which the forecast corresponds to the real world and is well founded.

- Predictive does the forecast correlate with measurements?
- Sharpness does the forecast predict uncommon events?
- Concurrent does the forecast predict the event at the correct time?
- Spatial does the forecast predict the event at the correct location?
- Discriminant does the forecast produce different outcomes when the measurements are different.
- Construct does the forecast predict the intended quantity?
- Calibrated was the forecast calibrated?
- Content does the forecast predict a representative sample of the domain of interest?
- Resolution does the forecast predict at a high enough resolution to describe the features of interest?
- Internal does the forecast depend on causality?
- Integrity is the integrity of the forecast system guaranteed?
- External does the forecast system predict in new situations?
- Criterion does the forecast correlate with related quantities?
- Convergent does the forecast correlate with other forecasts made by other models?
- Skill does the forecast do better than a reference forecast?
- Persistent does the forecast do better than a persistent forecast?
- Face does the forecast appear to predict what it should?

Table 7.1: Checklist for confidence in forecasts.

of the surge forecast was correct, not if it was an hour late, which could have dramatic consequences.

Comparing the forecasts made in this thesis to the list of confidence requirements shows that it is understandable to have a lack confidence in the forecasts. The forecasts made in this thesis can be seen as a representative sample from forecasts used in coastal research in general. Assuming this is true, we can ask the question: how can we gain more confidence in the forecasts made in coastal research?

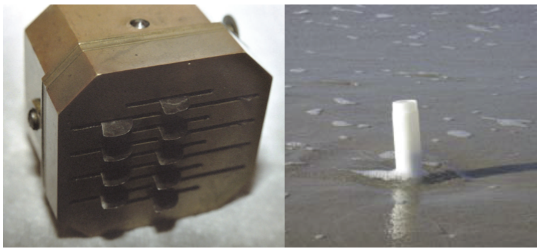

Figure 7.1: Left: a scarificator used for bloodletting (photo by D.R. Ingham). Right: Pressure Equalizing Modules (PEM) module at the Egmond beach, used for waterletting (photo by Rijkswaterstaat).

The answer lies in improving the research methods used in the field. Platt [1964] showed, by comparing different fields of research, that the common applied methods are important for the quality and progress of a field as a whole. When we compare the coastal research methods to methods used in other fields some differences are noticeable.

The nature of the forecasts between for example medical research and psychology is of course different, but one can see the parallel between "is this a successful therapy?" and "is this a successful coastal intervention?". One major difference is that, where there is a large focus on *evidence based practice* in medical research and social sciences, for coastal forecasts there are relatively few requirements or guidelines to conduct research.

The 20th century brought several improvements to the scientific method [see Kagan, 1999, for a partial overview], shown in Figure 7.2.

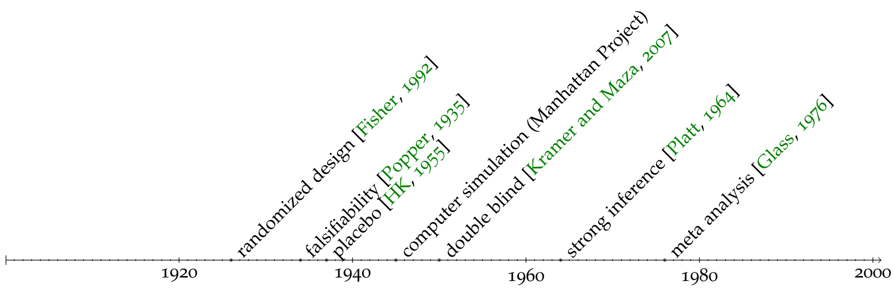

Figure 7.2: Developments in the scientific method in the 20th century.

The use of computer simulations followed from the technical innovation and is popular in coastal research. Other improvements, such as falsfiability and strong inference followed from philosophical developments. These are used to a certain extent in coastal research [as discussed in Baart et al., 2012d].

The improvements that, so far, have not worked their way into coastal research are those that originate from the assumption that the scientist should be treated as biased. The 20th century also saw the introduction of the randomized design, (double) blind studies, and placebo control designs and meta-analysis studies, all with the aim to help the, assumed biased, researchers to reach sound conclusions. In the coastal research practice this assumption is missing.

Where in social sciences fierce debates arise when researchers use only qualitative methods, goals in coastal research are often formulated qualitatively ("to gain insight into the systems behaviour we vary the input of this numerical model ") without any frowns from the community. The common use of numerical models gives the sense that something difficult and therefore correct is done [see for example the discussion in Ågren and Bosatta, 1990], even though only few of the points that determine "confidence" in forecasts are addressed.

Should the recent popularity of the evidence based practice [Sackett et al., 1996] also gain more traction in coastal research? Is testing the effect of bloodletting on patients that different from testing the effect of waterletting on the beach (Figure 7.1)? A step forward in the methodological practices would certainly help increase the confidence and progress in coastal research. Translating the philosophy behind evidence based practice to assessing the effect of coastal interventions would mean that:

1. Coastal interventions should be based on effect studies.
2. Effect studies are selected based on norms (disregard theoretical and qualitative studies).
3. Effect studies are combined using meta-analysis, resulting in the current evidence.

In fact, the movement towards an evidence based coastal management is already ongoing.

If we follow the medical practice, the coastal manager can be considered the doctor of the beach, with a wide variety of interventions at his or her disposal. Effect studies are already common practice, albeit without the assumption of the biased scientist.

Efforts are made to define norms and to standardize effect studies [Sutherland et al., 2004; van Koningsveld and Lescinski, 2007]. It is up to the scientific community to determine if it adheres to quality standards, as this is part of the peer process.

After standardized effect studies become common practice, the synthetic, summarizing studies can develop into meta-analyses, providing the coastal manager with the possibility of a practice based on the current evidence.

7.2 Creating confidence intervals

Back to the narrow statistical definition of confidence intervals. This thesis presents examples of including confidence intervals in the topics safety level (Chapter 3), analysis of policy and design lifetime

(Chapter 4) and operational forecasts (Chapter 6). For each of these confidence intervals examples are given on how to improve the interval, which does not always have to be a reduction. Examples were presented on how to combine these intervals with cost estimates. An overview of all the estimates is given in Table 7.2. The analysis of the storminess quantity (Section 4.2 did not result in a confidence interval.

	Variance source	Method	Improve
1/10000yr^{-1} water level (Section 3.1)	observed and reconstructed annual maximum water level and their estimated return period	peak over threshold and annual maximum [Coles and Stephenson, 2010]	increase number of observations (reconstruction from paintings), different probability density function
sea-level rise (Section 4.1)	difference between observed and modelled mean water level	linear regression, bayesian MCMC	include extra parameter (nodal cycle)
erosion trend (Section 4.3)	difference between observed and modelled coastal volume	Autoregressive integrated moving average (ARIMA) and linear regression	include autocorrelation
operational water levels and beach volume (Chapter 6)	difference between observed and modelled beach volume and water levels	ensembles, previous forecast errors	extend numerical model with statistical model

Table 7.2: Overview of different methods used to create confidence intervals

Table 7.2 shows that there are different approaches one can take for creating and improving confidence intervals. The method to create a confidence interval depends on the variance source and the assumed statistical model of this variance source. In this thesis different methods were used ranging from general linear, autoregressive and Marcov Chain Monte Carlo (MCMC) models to more specific extreme value methods and ensemble methods. The list of items that improve confidence in our forecast (Table 7.1) can also be used to improve the quality of the confidence interval of the forecasts. For example, by including the autocorrelation terms in the erosion trends the confidence interval matches the observations better and thus the *predictive* validity is increased.

Another example is the inclusion of the nodal cycle in the sea-level estimates, this improves the confidence interval by increasing the *con-*

tent validity, as now eustatic sea-level rise and tidal sea-level rise can be separated. This reduces the unexplained variance and makes the confidence interval smaller and allows for a higher chance to detect acceleration. As a final example the reliability of the confidence interval of the $1/10000 \text{yr}^{-1}$ storm was increased. This was done by increasing the sample size, which makes the estimate less likely to change when repeated and thus more *reproducible*.

Of course confidence intervals are not the goal itself, they are a way of presenting the probabilistic density function of the quantity of interest in a uniform fashion. Some of the following techniques and guidelines can help to assist in this.

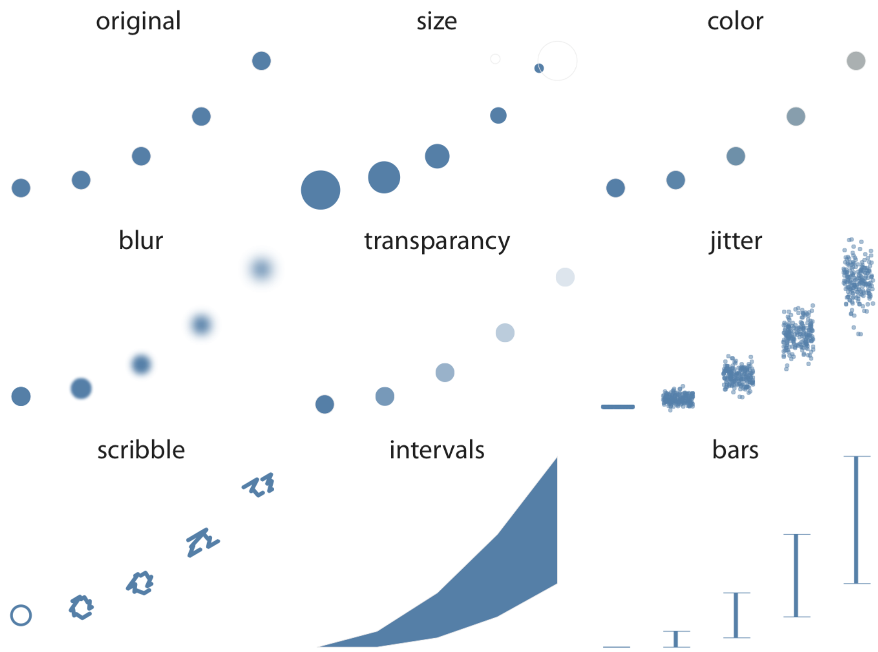

Figure 7.3: Using different style elements and graph types to plot confidence.

SOURCE OF VARIANCE Make clear which data are used. The source of the variation should be explicitly specified. Explain what makes the data a valid source of variance.

MODEL Make explicit which distribution and parameters and statistical methods are used. In some confidence intervals in literature it is not clear how the confidence interval was computed. Some confidence intervals are based on bootstrap methods, others on fitted normal distributions. There are only a few cases where the 95% interval is not preferred over alternative intervals (standard deviation, 90%). As uniformity is the goal, feeling uncomfortable to present results with a really large interval is not an excuse to turn down the percentage knob. Of course there is always the debate whether we should use the Bayesian (credibility) or the frequentist (confidence) approach, but luckily this century we can use both [Efron, 2005].

PRESENTATION Gardner and Altman [1986] gives an overview on how to report confidence intervals in textual notation. Wilkinson [2005, Chapter 15.3] gives an overview of how blur, transparency and size intervals can be used to represent the confidence in information. Examples of visual elements and chart types are presented in Figure 7.3.

This answers Question 1.

7.3 SCALES AND CHAINS

The confidence section (7.2) showed that the way we deal with confidence is not different for forecasts used for the mitigation and preparation phases. The major distinction, which we used to separate the two, is the temporal scale and spatial scale. In the mitigation phase the temporal scale of interest is decadal. In the preparation phase the scale of interest is in the order of days. This requires us to look at different physical causes for the same processes at different spatial scales. In the preparation phase one prepares for the local effects of a storm and not for the global effects of storminess change. In the mitigation phase one prepares for decadal scale changes in the Northern Atlantic Ocean and the North Sea.

People commonly work on either mitigation (the climate type of forecasts) or preparation (the operational forecasts). The two fields can learn from each other on several subjects.

The field of forecast verification, testing the quality of the forecasts, is well developed in the operational forecast field, where in climate forecasts it is often a lacking item. In fact most climate projections can not be considered forecasts, as they are mere expert judgments regarding plausible future [Moss et al., 2010].

The cooperation of the different fields (biology, economics, ecology, geophysics) benefited greatly from the boost in climate research since the 1990's. The climate forecasts have strongly developed integrated approaches, where the effect of human induced changes is calculated through a the chain of numerical and statistical models, covering topics from the effect of climate change on the local worm population [Briones et al., 2007] through to the supply of your favourite coffee bean [Gay et al., 2006]. The operational model chains are also increasing in length, but often end at quantities within the physical domain. This is also the case for our extension of the coastal operational forecast system with information about morphology. Would it make sense to extend it take the operational chain even further?

If we could have some confidence in the forecast chains created by these integrated approaches, it would result in a major step forward in science as we would increase our predicting coverage of the world. Although people who use models are more often right [Tetlock, 2005], one could argue that hooking up these type of models is resulting in integronsters rather than science [Voinov and Shugart, 2012]. The lack of skill that we have seen by adding operational morphology shows that we can't just keep adding models to a chain. One could patch up the skill at every link in the chain by assimilating with data, but this transforms the chain of numerical models to a de facto statistical model that does not have the required generalizability to forecast the unseen storms that the system was designed for. It would make little sense, at this stage, to extend the model chain with models that use the morphology as input. Based on basic rules of error propagation, resulting in a degrading skill in the chain, this just could not result in a confident forecast.

8

CONCLUSION

Contents

8.1 MOST IMPORTANT STATEMENTS

This thesis gives examples of common types of coastal forecasts using a variety of numerical and statistical models. These examples include several common use cases, such as safety assessment, design lifetime estimates, falsification, policy analysis and early warnings. Using these examples it is shown that coastal forecasts can be improved by extending the forecasts with confidence intervals. The improvement can be found in that coastal decisions can be made more cost effective. The confidence intervals in operational forecasts provide an extra level of information on which people can act, giving them a higher level of self-proficiency. It is not the goal to reduce the size of the confidence interval, but to get an accurate estimate of the interval. In fact, contrary to common belief, reducing the size of the confidence interval will result in exactly the same cost estimate if the cost function is linear.

Both in the mitigation phase and in the preparation phases, coastal forecasts are relevant. Although the temporal and spatial scales for these two phases are different, the methods to create the confidence in the forecasts are common. It is argued that the movement towards improving the confidence in coastal forecasts is part of the more general movement towards an evidence based practice. The development of coastal research and related fields could accelerate if the methodological practice becomes a specific research topic.

8.2 IMPLICATIONS

In Chapter 3 historical records were used to get a better estimate of the $1/10000 \mathrm{yr}^{-1}$ storm. This showed that the larger storms seen in the 18th century resulted in greater storm surges than we have seen in this century. This is in line with the results discussed in Section 4.2, where in Europe there was no indication of an overall increase in storminess. This reduces the need to take into account extra storminess in the calculation of an optimal safety level.

In Section 4.1 including the nodal cycle resulted in a more valid estimate of recent sea-level rise. It was shown that if there would be a high-end sea-level rise, that it would already be visible. The inclusion of high end scenarios for coastal constructions should be reconsidered. The structural over-projection of sea-level rise in the last decades is an indication of a publication bias and should be evaluated.

In Section 4.3 the effect of policy change in coastal nourishments shows that the coastal nourishment strategy is locally "overshooting" the objective.

Part ii showed that current coastal warning systems do not include forecasts of the breaching of the coastal dunes. For coastal safety this is one of the more relevant processes as the failure mechanisms of dune breaching is caused by storm induced erosion. The extension of the warning system with morphological change is relevant but at the moment the forecast lead time of three days is not enough to reevaluate the non-evacuation decision.

8.3 LA FAUTE-SUR-MER

How could these results have helped the citizens of the town of La Faute-sur-Mer? Let's assume that the Dutch findings are generalizable to the French coast.

Figure 8.1: A demonstration for the construction of protective dikes. Photo: Xavier Leoty, Source: 20minutes.fr

Re-evaluating the cost benefit analysis by including confidence intervals would result in a different cost estimate. Not because of including the intervals but because the number of inhabitants and the economical value increased behind the sea defence since it was constructed. On the other hand the costs of a new coastal defence might have risen at the same rate, resulting in a constant safety level. The constant storminess would not require a further update of the safety level. The study of sea-level rise showed that sea-level rise has occurred over the 20th century. This would require at least a reanalysis if the coastal defence is past the design lifetime.

With the extension of the forecast system with a breaching probability, people could have been provided with information that a breach could occur. They could have had the chance to evacuate. The coastal forecast system currently does not have enough skill to give warnings without causing the "cry wolf" effect, so it would perhaps not reduce the number of casualties. It would however increase the self-proficiency of the inhabitants and thereby reduce the perceived effect of the storm.

Of course in hindsight the weighing of risks and the perception of hazards changes [Parker, 2010]. Fortunately, nobody listened to the journalist who wrote that the next storm will not occur before the year 12010 [Brosset, 2010], based on the estimated 10000yr return period. It was decided that spatial planning is the solution for this area. Black zones are defined where houses will be destroyed. From the 702 homes in the zones, 575 were evacuated or bought by the government [AFP, 2012], except for one small group of indomitable French that still hold out against the water (Figure 8.1).

ACRONYMS

AC	Anomaly Correlation
AIC	Akaike Information Criterion
AHN	Actueel Hoogtebestand Nederland
ARIMA	Autoregressive integrated moving average
ASM	Automated Shoreline Mapper
BSS	Brier Skill Score
BS	Brier Score
DCSM	Dutch continental shelf model
DEP	Dune Erosion Point
ECMWF	European Centre for Medium-Range Weather Forecasts
EU	European Union
EOF	Empirical Orthogonal Function
FEWS	Delft Flood Early Warning System
FP7	Seventh Framework Programme
GEV	Generalized Extreme Value
GIA	Glacio Isostatic Adjustment
GFS	Global Forecast System
GPD	Generalized Pareto Distribution
HIRLAM	HIgh Resolution Limited Area Model
IFS	Integrated Forecast System
IPCC	Intergovernmental Panel on Climate Change
JARKUS	Dutch Annual Coastal Measurement
KNMI	Royal Netherlands Meteorological Institute
MATROOS	Multifunctional Access Tool foR Operational Oceandata Services
MCMC	Marcov Chain Monte Carlo

MICORE	Morphological Impacts and COastal Risks induced by Extreme storm
MKL	Momentary Coast Line
MSE	Mean Squared Error
NAP	Normaal Amsterdams Peil (Amsterdam Ordnance Datum)
NCAR	National Center for Atmospheric Research
NOAA	National Oceanic and Atmospheric Administration
NWP	Numerical Weather Prediction
OPeNDAP	Open-source Project for a Network Data Access Protocol
PEM	Pressure Equalizing Modules
PSMSL	Permanent Service for Mean Sea Level
QSC	Quantitative State Concept
RMSE	Root Mean Square Error
R	R Project for Statistical Computing
rlr	revised local reference
SS	Forecast Skill Score
TNO	Nederlandse Organisatie voor Toegepast-Natuurwetenschappelijk Onderzoek
USGS	United States Geological Survey
WRF	Weather Research and Forecasting
WW3	Wave Watch 3

BIBLIOGRAPHY

Aagaard, T., Kroon, A., Andersen, S., Møller Sørensen, R., Quartel, S., and Vinther, N. Intertidal beach change during storm conditions; Egmond, The Netherlands. *Marine Geology*, 218(1-4):65–80, 2005. ISSN 0025-3227. URL http://dx.doi.org/10.1016/j.margeo.2005.04.001. (Cited on page 118.)

Abt, S., Wittier, R., Taylor, A., and Love, D. Human stability in a high flood hazard zone. *JAWRA Journal of the American Water Resources Association*, 25(4):881–890, 1989. ISSN 1752-1688. URL http://dx.doi.org/10.1111/j.1752-1688.1989.tb05404.x. (Cited on page 108.)

AFP. La faute-sur-mer (vendée) - deux ans après xynthia, l'attente des familles de victimes. 2012. URL http://www.20minutes.fr/article/887461/deux-ans-apres-xynthia-attente-familles-victimes. In French. (Cited on page 146.)

Alovisi, J., Souch, C., and Toothill, J. Windstorm Kyrill: A glimpse into the future? *Catastrophe risk management*, pages 26–28, 2007. URL http://www.rms.com/newspress/CRM_WindstormKyrill_0407.pdf. (Cited on page 99.)

Anziani, A. Xynthia: les leçons d'une catastrophe. Rapport d'Information 554, Sénat, 2010. (Cited on page 21.)

Arceneaux, K. and Stein, R.M. Who is held responsible when disaster strikes? the attribution of responsibility for a natural disaster in an urban election. *Journal of Urban Affairs*, 28(1):43–53, 2006. ISSN 1467-9906. URL http://dx.doi.org/10.1111/j.0735-2166.2006.00258.x. (Cited on pages 96 and 113.)

Author, U. *Extract van verschyde brieven, uyt Frederik-stad, Hamborg, Embden, Hanover, Essens in Oost-Friesland, Bremen enz. Behelsende een verhaal, van de groote schade aldaar en elders veroorsaakt: door den schrikkelyken storm, en opgehoorden hoogen water-vloet op den 24. en 25. December 1717*. Unknown Publisher, 1717a. Available at Koninklijke Bibliotheek. (Cited on page 53.)

Author, U. Nette aantekeningen volgens peylingen bevonden hoeveel de zomerpeilen in west-vrieslandt zijn verschillende met ordinair dagelijks getij volzee. Map, 1717b. Available at Koninklijke Bibliotheek. (Cited on page 53.)

Baart, F., Bakker, M.A.J., van Dongeren, A., den Heijer, C., van Heteren, S., Smit, M.W.J., van Koningsveld, M., and Pool, A. Using 18th century storm-surge data from the dutch coast to improve the confidence in flood-risk estimates. *Natural Hazards and Earth System Science*, 11(10):2791–2801, 2011a. URL http://dx.doi.org/10.5194/nhess-11-2791-2011. (Cited on pages 46 and 176.)

Baart, F., den Bieman, J., van Koningsveld, M., Luijendijk, A., Parteli, E., Plant, N., Roelvink, J., Storms, J., de Vries, S., van Thiel de Vries, J., et al. An integrated coastal model for aeolian and hydrodynamic sediment transport. In *EGU General Assembly Conference Abstracts*, volume 14, page 12842. 2012a. URL https://publicwiki.deltares.nl/display/~baart_f/2012/04/28/Aeolian+transport+at+EGU+2012. (Cited on pages 100 and 177.)

Baart, F., de Boer, G., Brouwer, R., van Geer, P., den Heijer, K., van Koningsveld, M., and de Sonneville, B. OpenEarth: an open source system for sharing data, models and tools by marine and coastal scientists and engineers. In *NCK International Symposium*. 2009a. (Cited on pages 99 and 176.)

Baart, F., de Boer, G., de Haas, W., Donchyts, G., Philippart, M., van Koningsveld, M., and Plieger, M. OPeNDAP vs. WCS. In *Free and Open Source Software for Geospatial*. 2011b. URL http://2011.foss4g.org/sessions/opendap-vs-wcs. (Cited on pages 109 and 177.)

Baart, F., de Boer, G., de Haas, W., Donchyts, G., Philippart, M., van Koningsveld, M., and Plieger, M. A comparison between wcs and opendap for making model results and data products available through the internet. *Transactions in GIS*, 16(2):249–265, 2012b. ISSN 1467-9671. URL http://dx.doi.org/10.1111/j.1467-9671.2012.01312.x. (Cited on pages 27, 109, and 176.)

Baart, F. and Donchyts, G. Reducing the invasiveness of modelling frameworks. In *AGU Fall Meeting Abstracts*, IN21B-1333. 2010. URL https://publicwiki.deltares.nl/display/~baart_f/AGU2010. (Cited on pages 27 and 176.)

Baart, F., van Gelder, P., de Ronde, J., van Koningsveld, M., and Wouters, B. The effect of the 18.6 year lunar nodal cycle on regional sea level rise estimates. In *Abstracts Scientific Programme Deltas in Depth*. 2010. URL http://www.climatedeltaconference.org/gfx_content/documents/DELTAS%20ABSTRACTS%2009092010.pdf. (Cited on pages 68 and 177.)

Baart, F., van Gelder, P.H.A.J.M., and van Koningsveld, M. Confidence in real-time forecasting of morphological storm impacts. *Journal of Coastal Research*, (Special Issue 64):1835–1839, 2011c. ISSN

0749-0208. URL http://www.ics2011.pl/artic/SP64_1835-1839_F.Baart.pdf. (Cited on pages 111, 113, 116, 117, 129, and 176.)

Baart, F., van Gelder, P.H.A.J.M., de Ronde, J., van Koningsveld, M., and Wouters, B. The effect of the 18.6-year lunar nodal cycle on regional sea-level rise estimates. *Journal of Coastal Research*, 28(2):511–516, 2012c. URL http://dx.doi.org/10.2112/JCOASTRES-D-11-00169.1. (Cited on pages 65 and 176.)

Baart, F. and de Haan, G. A stereoscopic view on the coast. In *NCK International Symposium*. Baart, F, 2010. URL https://publicwiki.deltares.nl/display/OET/A+stereoscopic+view+on+the+coast. (Cited on page 176.)

Baart, F., van der Kaaij, T., van Ormondt, M., van Dongeren, A., van Koningsveld, M., and Roelvink, J.A. Real-time forecasting of morphological storm impacts: a case study in the netherlands. *Journal of Coastal Research*, Special Issue 56:1617–1621, 2009b. URL http://www.cerf-jcr.org/images/stories/1617.1621_F.Baart_ICS2009.pdf. (Cited on page 176.)

Baart, F., van Koningsveld, M., and Stive, M.J.F. Trends in sea-level trend analysis. *Journal of Coastal Research*, 28(2):311–315, 2012d. URL http://dx.doi.org/10.2112/JCOASTRES-11A-00024.1. (Cited on pages 79, 137, and 176.)

Battjes, J.A. and Gerritsen, H. Coastal modelling for flood defence. *Philosophical Transactions of the Royal Society of London Series A-Mathematical Physical and Engineering Sciences*, 360(1796):1461–1475, 2002. ISSN 1364-503X. URL http://dx.doi.org/10.1098/rsta.2002.1010. Royal-Society Meeting on Flood Risk in a Changing Climate, London, England, Nov 21-22, 2001. (Cited on page 69.)

Cramer von Baumgarten, G.J.F. *De kersvloed van 1717; in gesprekken, ter herinnering van dien verschrikkelijken watersnood, voor 1817*. Schierbeek, Groningen, 1817. URL http://discover.tudelft.nl:8888/recordview/view?recordId=aleph%3A000363835. In Dutch. (Cited on page 53.)

Beck, K. and Fowler, M. *Planning extreme programming*. Addison-Wesley, Boston, 2001. ISBN 0201710919 (pbk.). (Cited on page 97.)

Benard, A. and Bos-Levenbach, E.C. Het uitzetten van waarnemingen op waarschijnlijkheids-papier. *Statistica Neerlandica*, 7(3):163–173, 1953. ISSN 1467-9574. URL http://dx.doi.org/10.1111/j.1467-9574.1953.tb00821.x. (Cited on page 46.)

Bijl, W., Flather, R., de Ronde, J., and Schmith, T. Changing storminess? an analysis of long-term sea level data sets. *Climate Research*, 11(2):161–172, 1999. URL http://www.int-res.com/abstracts/cr/v11/n2/p161-172/. (Cited on pages 80 and 81.)

Bindoff, N.L., Willebrand, J., Artale, V., Cazenave, A., Gregory, J., Gulev, S., Hanawa, K., Le Quéré, C., Levitus, S., Nojiri, Y., Shum, C.K., Talley, L.D., and Unnikrishnan, A. Observations: oceanic climate change and sea level. In S. Solomon, D. Qin, M. Manning, Z. Chen, M. Marquis, K.B. Averyt, M. Tignor, and H.L. Miller, editors, *Climate Change 2007: The Physical Science Basis. Contribution of Working Group I to the Fourth Assessment Report of the Intergovernmental Panel on Climate Change*. Cambridge University Press, Cambridge, United Kingdom and New York, NY, USA, 2007. URL http://www.ipcc.ch/pdf/assessment-report/ar4/wg1/ar4-wg1-chapter5.pdf. (Cited on page 66.)

Blewitt, G. and Lavallée, D. Effect of annual signals on geodetic velocity. *Journal of Geophysical Research*, 107(B7), 2002. URL http://dx.doi.org/10.1029/2001JB000570. (Cited on page 78.)

de Boer, G.J., Baart, F., Bruens, A., Damsma, T., van, P.G., Grasmeijer, B., den, K.H., and van, M.K. Openearth: using google earth as outreach for nck's data. pages 97–103. 2012. URL http://proceedings.utwente.nl/177/. (Cited on page 177.)

Bógaert, A. *De kersvloedt van den jare 1717 vermengt met de gedenkwaardigste vloeden sedert den algemeenen*. Gerrit Bosch, Amsterdam, 1719. URL http://discover.tudelft.nl:8888/recordview/view?recordId=aleph%3A000070365. (Cited on page 53.)

Booij, N., Ris, R.C., and Holthuijsen, L.H. A third-generation wave model for coastal regions 1. model description and validation. *J. Geophys. Res.*, 104(C4):7649–7666, 1999. URL http://dx.doi.org/10.1029/98JC02622. (Cited on page 108.)

Borthwick, A.G.L., Cruz León, S., and Józsa, J. The shallow flow equations solved on adaptive quadtree grids. *International Journal for Numerical Methods in Fluids*, 37(6):691–719, 2001. ISSN 1097-0363. URL http://dx.doi.org/10.1002/fld.192. (Cited on page 105.)

Breznitz, S. *Cry wolf: The psychology of false alarms*. Lawrence Erlbaum Associates Hillsdale, NJ, 1984. URL http://archive.org/details/reflectionsofaph031333mbp. (Cited on pages 95 and 127.)

Bridgman, P. *Reflection of Physicist*. Philosophical Library, New York, 1950. URL http://www.archive.org/stream/reflectionsofaph031333mbp. (Cited on page 80.)

van den Brink, H., Konnen, G., and Opsteegh, J. Uncertainties in extreme surge level estimates from observational records. *Philosophical Transactions of the Royal Society of London Series A-Mathematical Physical and Engineering Sciences*, 363(1831):1377–1386, 2005. ISSN 1364-503X. URL http://dx.doi.org/10.1098/rsta.2005.1573. (Cited on pages 42 and 50.)

van den Brink, H.W., Können, G.P., Opsteegh, J.D., van Oldenborgh, G.J., and Burgers, G. Improving 104-year surge level estimates using data of the ecmwf seasonal prediction system. *Geophys. Res. Lett.*, 31(17), 2004. URL http://dx.doi.org/10.1029/2004GL020610. (Cited on pages 48, 49, and 62.)

Briones, M.J.I., Ineson, P., and Heinemeyer, A. Predicting potential impacts of climate change on the geographical distribution of enchytraeids: a meta-analysis approach. *Global Change Biology*, 13(11):2252–2269, 2007. ISSN 1365-2486. URL http://dx.doi.org/10.1111/j.1365-2486.2007.01434.x. (Cited on page 141.)

Broad, K., Leiserowitz, A., Weinkle, J., and Steketee, M. Misinterpretations of the "cone of uncertainty"in florida during the 2004 hurricane season. *Bulletin of the American Meteorological Society*, 88(5):651–667, 2007. URL http://dx.doi.org/10.1175/BAMS-88-5-651. (Cited on page 24.)

Brosset, T. Une catastrophe comme xynthia tous les 10000 ans. 2010. URL http://www.sudouest.fr/2010/04/21/un-catastrophe-comme-xynthia-tous-les-10-000-ans-71858-4628.php. Accessed on July 5 2011. (Cited on page 146.)

van Brussel, T. *Naauwkeurige beschryving der twee voornaamste watervloeden van de XVIIIe eeuwe, in 1717 en 1775 ...; waarby gevoegd is een kort kronykje van alle watervloeden, van den zondvloed van Noach af, tot op deezen laatsten toe ..* Bom (Gerrit), Amsteldam, 1776. (Cited on page 53.)

Bruun, J.T. and Tawn, J.A. Comparison of approaches for estimating the probability of coastal flooding. *Journal of the Royal Statistical Society: Series C (Applied Statistics)*, 47(3):405–423, 1998. ISSN 1467-9876. URL http://dx.doi.org/10.1111/1467-9876.00118. (Cited on page 44.)

Buisman, J. *Bar en boos: Zeven eeuwen winterweer in de Lage Landen*. Bosch & Keuning, 1984. ISBN 9024644127. In Dutch. (Cited on page 55.)

Buisman, J. and Engelen, A.v. *Duizend jaar weer, wind en water in de lage landen. Dl. 1. Tot 1300*. Van Wijnen, Franeker, 1995. ISBN 90-5194-075-0. In Dutch. (Cited on pages 49 and 53.)

Buisman, J. and Engelen, A.v. *Duizend jaar weer, wind en water in de lage landen. Dl. 2. 1300-1450*. Van Wijnen, Franeker, 1996. ISBN 90-5194-141-2. In Dutch. (Cited on page 49.)

Buisman, J. and Engelen, A.v. *Duizend jaar weer, wind en water in de Lage Landen. Dl. 5. 1675-1750*. Van Wijnen, Franeker, 2006. ISBN 978-90-5194-190-6. In Dutch. (Cited on pages 50 and 51.)

Buisman, J. and Engelen, A.v. *Duizend jaar weer, wind en water in de Lage Landen. Dl. 6. 1750-*. Van Wijnen, Franeker, 2012. ISBN 978-90-5194-190-6. In Dutch. (Cited on page 55.)

Bürger, G. and Cubasch, U. Are multiproxy climate reconstructions robust? *Geophys. Res. Lett.*, 32(23):L23711, 2005. URL http://dx.doi.org/10.1029/2005GL024155. (Cited on page 23.)

Camuffo, D. and Sturaro, G. Sixty-cm submersion of Venice discovered thanks to Canaletto's paintings. *Climatic Change*, 58:333–343, 2003. ISSN 0165-0009. URL http://dx.doi.org/10.1023/A:1023902120717. (Cited on page 50.)

Carnell, R.E., Senior, C.A., and Mitchell, J.F.B. An assessment of measures of storminess: simulated changes in northern hemisphere winter due to increasing co2. *Climate Dynamics*, 12:467–476, 1996. ISSN 0930-7575. URL http://dx.doi.org/10.1007/s003820050121. (Cited on page 80.)

Cartwright, D.E. and Edden, A.C. Corrected tables of tidal harmonics. *Geophysical Journal of the Royal Astronomical Society*, 33(3):253–264, 1973. ISSN 1365-246X. URL http://dx.doi.org/10.1111/j.1365-246X.1973.tb03420.x. (Cited on page 67.)

Cartwright, D.E. and Tayler, R.J. New computations of the tide-generating potential. *Geophysical Journal of the Royal Astronomical Society*, 23(1):45–73, 1971. ISSN 1365-246X. URL http://dx.doi.org/10.1111/j.1365-246X.1971.tb01803.x. (Cited on page 67.)

Charnock, H. Wind stress on a water surface. *Quarterly Journal of the Royal Meteorological Society*, 81(350):639–640, 1955. ISSN 1477-870X. URL http://dx.doi.org/10.1002/qj.49708135027. (Cited on page 57.)

Chauveau, E., Chadenas, C., Comentale, B., Pottier, P., Blanlœil, A., Feuillet, T., Mercier, D., Pourinet, L., Rollo, N., Tillier, I., and Trouillet, B. Xynthia: leçons d'une catastrophe. *European Journal of Geography*, (538), 2011. URL http://dx.doi.org/10.4000/cybergeo.23763. (Cited on page 21.)

Cherniawsky, J.Y., Foreman, M.G., Kang, S.K., Scharroo, R., and Eert, A.J. 18.6-year lunar nodal tides from altimeter data. *Continental Shelf Research*, 30(6):575 – 587, 2010. ISSN 0278-4343. URL http://dx.doi.org/10.1016/j.csr.2009.10.002. (Cited on pages 67, 68, and 79.)

Church, J.A. and White, N.J. A 20th century acceleration in global sea-level rise. *Geophysical Research Letters*, 33(1), 2006. URL http://dx.doi.org/10.1029/2005GL024826. (Cited on pages 66 and 69.)

Church, J.A. and White, N.J. Sea-level rise from the late 19th to the early 21st century. *Surveys in Geophysics*, 32:585–602, 2011. ISSN 0169-3298. URL http://dx.doi.org/10.1007/s10712-011-9119-1. (Cited on pages 69, 74, 75, 78, and 79.)

Church, J.A., White, N.J., Aarup, T., Wilson, W.S., Woodworth, P.L., Domingues, C.M., Hunter, J.R., and Lambeck, K. Understanding global sea levels: past, present and future. *Sustainability Science*, 3(1):9–22, 2008. URL http://dx.doi.org/10.1007/s11625-008-0042-4. (Cited on page 66.)

Ciavola, P., Ferreira, O., Haerens, P., Van Koningsveld, M., and Armaroli, C. Storm impacts along european coastlines. part 2: lessons learned from the micore project. *Environmental Science & Policy*, 14, 2011a. URL http://dx.doi.org/10.1016/j.envsci.2011.05.009. (Cited on pages 82, 98, 102, 104, 108, and 128.)

Ciavola, P., Ferreira, O., Haerens, P., Van Koningsveld, M., Armaroli, C., and Lequeux, Q. Storm impacts along european coastlines. part 1: The joint effort of the micore and conhaz projects. *Environmental Science & Policy*, 14:912–923, 2011b. URL http://dx.doi.org/10.1016/j.envsci.2011.05.011. (Cited on pages 83 and 113.)

Claude, J. *Morphometrics with R*. Springer, New York, 2008. ISBN 978-0-387-77790-0. URL http://dx.doi.org/10.1007/978-0-387-77789-4. (Cited on page 83.)

Coles, S. *An introduction to statistical modeling of extreme values*. Springer Verlag, 2001. ISBN 1852334592. (Cited on pages 41 and 42.)

Coles, S.G. and Stephenson, A. *ismev: An Introduction to Statistical Modeling of Extreme Values*, 2010. URL http://CRAN.R-project.org/package=ismev. R package version 1.35. (Cited on pages 46 and 139.)

Conrad, J. *Verhandeling over de Hondsbossche zeewering*. H. Coster en zoon, Alkmaar, 1864. URL http://discover.tudelft.nl:8888/recordview/view?recordId=aleph%3A000069289. In Dutch. (Cited on page 56.)

Cronbach, L. and Meehl, P. Construct validity in psychological tests. *Psychological Bulletin*, 52(4):281–302, 1955. (Cited on page 135.)

Cryer, J.D. and Chan, K.S. *Time series analysis: with applications in R*. Springer, New York, 2008. ISBN 978-0-387-75959-3. URL http://dx.doi.org/10.1007/978-0-387-75959-3. (Cited on pages 70 and 86.)

Cunningham, A., Bakker, M., van Heteren, S., van der Valk, L., van der Spek, A.J.F., Schaart, D.R., and Wallinga, J. Extracting storm-surge data from coastal dunes for improved assessment of flood risk. *Geology*, 39(11):1063–1066, 2011. URL http://dx.doi.org/10.1130/G32244.1. (Cited on page 56.)

Cunningham, A.C., Wallinga, J., van Heteren, S., Bakker, M., van der Valk, B., Oost, A., and van der Spek, A. Optically stimulated luminescence dating of storm surge sediments: a test case from the Netherlands. In *NCL Symposium Series*, volume 6, pages 1–2. 2009. URL http://www.ncl.tudelft.nl/downloads/2009%20-%20NCL%20symposium%20series%20V6.pdf. (Cited on pages 56 and 57.)

Currie, R.G. The spectrum of sea level from 4 to 40 years. *Geophysical Journal of the Royal Astronomical Society*, 46(3):513–520, 1976. ISSN 1365-246X. URL http://dx.doi.org/10.1111/j.1365-246X.1976.tb01245.x. (Cited on page 68.)

Damsma, T., Baart, F., de Boer, G., Koningsveld, M.V., and Bruens, A. Visualization of coastal data through kml. In *Virtual Globes at AGU*. 2009. URL http://adsabs.harvard.edu/abs/2009AGUFMIN43A1131D. (Cited on page 176.)

van Dantzig, D. Economic decision problems for flood prevention. *Econometrica*, 24(3):276–287, 1956. (Cited on pages 34, 35, 41, 46, and 65.)

Davidson, M., van Koningsveld, M., de Kruif, A., Rawson, J., Holman, R., Lamberti, A., Medina, R., Kroon, A., and Aarninkhof, S. The CoastView project: Developing video-derived Coastal State Indicators in support of coastal zone management. *Coastal Engineering*, 54(6-7):463–475, 2007. ISSN 0378-3839. URL http://dx.doi.org/DOI:10.1016/j.coastaleng.2007.01.007. (Cited on page 118.)

Day, H.J., Bugliarello, G., Ho, P.H.P., and Houghton, V.T. Evaluation of benefits of a flood warning system. *Water Resour. Res.*, 5(5):937–946, 1969. URL http://dx.doi.org/10.1029/WR005i005p00937. (Cited on page 113.)

Deltacommissie. *Rapport Deltacommissie. Dl. 1. Eindverslag en interimadviezen*. Staatsdrukkerij- en Uitgeverijbedrijf, 's-Gravenhage, 1960. URL http://repository.tudelft.nl/file/1219694/382018. In Dutch. (Cited on pages 34, 41, 65, and 78.)

Deltacommissie. Working together with water. Technical report, Deltacommissie, 2008. (Cited on pages 23, 36, and 66.)

Dillingh, D., Baart, F., and de Ronde, J. Do we have to take an acceleration of sea level rise into account? In *EGU General Assembly Conference Abstracts*, volume 14, page 14021. 2012a. URL http://adsabs.harvard.edu/abs/2012EGUGA..1414021D. (Cited on page 177.)

Dillingh, D., Baart, F., and de Ronde, J. Is er al versnelde zeespiegelstijging? *H2O*, 45(14):37, 2012b. In Dutch. (Cited on page 177.)

Dillingh, D., de Haan, L., Helmers, R., Können, G., and van Malde, J. De basispeilen langs de nederlandse kust; statistisch onderzoek. Technical report, Ministerie van Verkeer en Waterstaat, 1993. In Dutch. (Cited on pages 67 and 78.)

Donchyts, G., Baart, F., and Jagers, B. Delftshell-integrated modeling environment with elements of gis, data management and openmi support. In *American Geophysical Union, Fall Meeting 2008*,, H41G-0958. 2008. URL http://adsabs.harvard.edu/abs/2008AGUFM.H41G0958D. (Cited on page 176.)

Donchyts, G., Baart, F., and Jagers., B. Development of the delta shell as an integrated modeling environment. In *European Geophysical Union, General Assembly 2010*, HS8.1. 2010. URL http://adsabs.harvard.edu/abs/2010EGUGA..1215030D. (Cited on page 176.)

Donchyts, G., Baart, F., Jagers, B., and van Putten, H. Open source integrated modeling environment delta shell. In *EGU General Assembly Conference Abstracts*, volume 14, page 13183. 2012a. URL http://adsabs.harvard.edu/abs/2012EGUGA..1413183D. (Cited on page 177.)

Donchyts, G., Baart, F., Jagers, H., and van Dam, A. Functional coverages. *OSGeo Journal*, 10(1):12, 2012b. URL http://journal.osgeo.org/index.php/journal/article/view/196. (Cited on page 176.)

Donchyts, G., Jagers, B., Baart, F., and Geer, P. Delta shell: Integrated modeling by example. *AGU Fall Meeting Abstracts*, 1:1455, 2011. URL http://adsabs.harvard.edu/abs/2011AGUFMIN23B1455D. (Cited on page 177.)

van Dongeren, A.R., Plant, N., Cohen, A.B., Roelvink, J.A., Haller, M.C., and Catalán, P. Beach Wizard: Nearshore bathymetry estimation through assimilation of model computations and remote observations. *Coastal Engineering*, 55(12):1016–1027, 2008. ISSN 0378-3839. URL http://dx.doi.org/10.1016/j.coastaleng.2008.04.011. (Cited on page 128.)

Doodson, A.T. The harmonic development of the tide-generating potential. *Proceedings of the Royal Society of London Series A-Containing Papers of a Mathematical and Physical Character*, 100(704):305–329, 1921. URL http://www.jstor.org/stable/93989. (Cited on page 67.)

Douglas, B.C. Global sea-level acceleration. *Journal of Geophysical Research-Oceans*, 97(C8):12699–12706, 1992. URL http://dx.doi.org/10.1029/92JC01133. (Cited on page 66.)

Durbin, J., Koopman, S., and Atkinson, A. *Time series analysis by state space methods*, volume 15. Oxford University Press Oxford, 2001. (Cited on page 88.)

Economist. Accentuate the negative. 2010. URL http://www.economist.com/blogs/newsbook/2010/07/bias_and_ipcc_report. (Cited on page 36.)

Efron, B. Bayesians, frequentists, and scientists. *Journal of the American Statistical Association*, 100(469):1–5, 2005. URL http://dx.doi.org/10.1198/016214505000000033. (Cited on page 141.)

Eijgenraam, C.J.J. and Zwaneveld, J. Second opinion kosten-batenanalyse waterveiligheid 21e eeuw. Notitie, Centraal Planbureau, 2011. In Dutch. (Cited on page 35.)

European Centre for Medium-Range Weather Forecasts. Annual report. Technical report, European Centre for Medium-Range Weather Forecasts, 2010. (Cited on page 115.)

Ferreira, O., Ciavola, P., and Armaroli, C. Report on risk definition for each study site. Technical report, Micore, 2008. Project 202798. (Cited on page 99.)

Fisher, N. *Statistical analysis of circular data*. Cambridge University Press, Cambridge, UK, 1993. ISBN 0-521-35018-2. (Cited on page 69.)

Fisher, R. The arrangement of field experiments. In S. Kotz and N. Johnson, editors, *Breakthroughs in Statistics*, Springer Series in Statistics, pages 82–91. Springer New York, 1992. ISBN 978-0-387-94039-7. URL http://dx.doi.org/10.1007/978-1-4612-4380-9_8. (Cited on page 137.)

Flater, D. Xtide. 2012. URL http://www.flaterco.com/xtide. (Cited on page 119.)

Fowler, M. *Patterns of enterprise application architecture*. Addison-Wesley Professional, 2003. ISBN 978-0321127426. (Cited on page 103.)

Gardner, M.J. and Altman, D.G. Confidence intervals rather than p values: estimation rather than hypothesis testing. *BMJ*, 292(6522):746–750, 1986. URL http://dx.doi.org/10.1136/bmj.292.6522.746. (Cited on page 141.)

Gauss, C.F. *Theoria Motus Corporum Coelestium in Sectionibus Conicis Solem Ambientum*. Hamburgi, Sumtibus Frid. Perthes et I.H. Besser, 1809. URL http://books.google.nl/books?id=ORUOAAAAQAAJ. (Cited on pages 23 and 117.)

Gay, C., Estrada, F., Conde, C., Eakin, H., and Villers, L. Potential impacts of climate change on agriculture: A case of study of coffee production in veracruz, mexico. *Climatic Change*, 79:259–288, 2006. ISSN 0165-0009. URL http://dx.doi.org/10.1007/s10584-006-9066-x. (Cited on page 141.)

Gebraad, A.W. and Philippart, M.E. The Dutch Continental Shelf Model, DCSM98: calibration using altimeter data. Werkdocument RIKZ/OS- 98.121x, RIKZ, 1998. In Dutch. (Cited on page 106.)

van Geer, P. and Boers, M. Assessing dune erosion: 1d or 2dh? the noorderstrand case study. In W. Kranenburg, E. Horstman, and K. Wijnberg, editors, *NCK-days 2012 : Crossing borders in coastal research*, pages 229–233. University of Twente, Enschede, the Netherlands, 2012. URL http://dx.doi.org/10.3990/2.203. (Cited on page 117.)

van Gelder, P.H.A.J.M. A new statistical model for extreme water levels along the dutch coast. *Stochastic Hydraulics*, 7:243–251, 1996. (Cited on pages 51 and 58.)

van Gelder, P.H.A.J.M. *Statistical methods for the risk-based design of civil structures*. Ph.D. thesis, Delft University of Technology, 2000. URL http://www.library.tudelft.nl/ws/search/publications/search/metadata/index.htm?docname=088270. (Cited on page 52.)

Gelman, A., Carlin, J.B., Stern, H.S., and Rubin, D.B. *Bayesian data analysis*. Texts in Statistical Science. Chapman & Hall/CRC, Boca Raton, Fla., 2nd ed edition, 2004. ISBN 158488388X (alk. paper). URL http://www.loc.gov/catdir/enhancements/fy0646/2003051474-d.html. (Cited on pages 69 and 128.)

Gerritsen, H. What happened in 1953? - the big flood in the netherlands in retrospect. *Philosophical Transactions of the Royal Society A-Mathematical Physical and Engineering Sciences*, 363(1831):1271–1291, 2005. URL http://dx.doi.org/10.1098/rsta.2005.1568. (Cited on page 35.)

Gerritsen, H., de Vries, J.W., and Philippart, M. *Quantitative Skill Assessment for Coastal Ocean Models*, chapter The Dutch Continental Shelf Model. American Geophysical Union, 1995. ISBN 0-87590-261-8. URL http://www.agu.org/books/ce/v047/. (Cited on page 102.)

Gilleland, E. *verification: Forecast verification utilities.* NCAR - Research Application Program, 2010. URL http://CRAN.R-project.org/package=verification. R package version 1.31. (Cited on pages 124 and 129.)

Glass, G.V. Primary, secondary, and meta-analysis of research. *Educational Researcher*, 5(10):3–8, 1976. URL http://dx.doi.org/10.3102/0013189X005010003. (Cited on page 137.)

Gottschalk, M. *Stormvloeden en rivieroverstromingen in Nederland. Dl. 1. De periode voor 1400*, volume 1. Van Gorcum, Assen, 1971. ISBN 9789023207177. In Dutch. (Cited on page 49.)

de Graaf, H., Elberink, S.O., Bollweg, A., Brügelmann, R., and Richardson, L. Inwinning droge jarkus profielen langs nederlandse kust. Technical Report AGI-GAM-2003-40, Rijkswaterstaat, 2003. (Cited on pages 54 and 57.)

van de Graaff, J. Probabilistic design of dunes - an example from the Netherlands. *Coastal Engineering*, 9(5):479–500, 1986. URL http://dx.doi.org/10.1016/0378-3839(86)90009-8. (Cited on pages 34 and 120.)

Gratiot, N., Anthony, E.J., Gardel, A., Gaucherel, C., Proisy, C., and Wells, J.T. Significant contribution of the 18.6 year tidal cycle to regional coastal changes. *Nature Geoscience*, 1(3):169–172, 2008. URL http://dx.doi.org/10.1038/ngeo127. (Cited on page 67.)

Gumbel, E. and Lieblein, J. *Statistical theory of extreme values and some practical applications: a series of lectures*. US Govt. Print. Office, 1954. (Cited on page 42.)

de Haan, L. Fighting the arch–enemy with mathematics'. *Statistica Neerlandica*, 44(2):45–68, 1990. ISSN 1467-9574. URL http://dx.doi.org/10.1111/j.1467-9574.1990.tb01526.x. (Cited on pages 41 and 44.)

de Haan, L. and Ferreira, A. *Extreme value theory: an introduction*. Springer Verlag, 2006. ISBN 978-0-387-34471-3. (Cited on pages 44 and 45.)

Haartsen, T., Ligtendag, W., and Steenhuisen, F. Historische reconstructie dieptelijnen Nederlandse kust. Technical report, Rijksuniversiteit Groningen, Arctisch Centrum, 1997. In Dutch. (Cited on page 57.)

Hass, H. Northern Europe climate variations during late holocene: evidence from marine Skagerrak. *Palaeogeography, Palaeoclimatology, Palaeoecology*, 123(1-4):121–145, 1996. URL http://dx.doi.org/10.1016/0031-0182(95)00114-X. (Cited on page 61.)

den Heijer, C., Baart, F., and van Koningsveld, M. Assessment of dune failure along the dutch coast using a fully probabilistic approach. *Geomorphology*, 143-144(0):95–103, 2012. ISSN 0169-555X. URL http://dx.doi.org/10.1016/j.geomorph.2011.09.010. (Cited on pages 117, 118, and 176.)

HK, B. The powerful placebo. *Journal of the American Medical Association*, 159(17):1602–1606, 1955. URL http://dx.doi.org/10.1001/jama.1955.02960340022006. (Cited on page 137.)

Holgate, S.J. On the decadal rates of sea level change during the twentieth century. *Geophysical Research Letters*, 34(1), 2007. URL http://dx.doi.org/10.1029/2006GL028492. (Cited on page 66.)

Holthuijsen, L. *Waves in oceanic and coastal waters*. Cambridge Univ Pr, 2007. ISBN 0521860288. (Cited on page 57.)

Hoss, F., Jonkman, S., and Maaskant, B. A comprehensive assessment of multilayered safety in flood risk management – the Dordrecht case study. In *Proceedings of the 5th International Conference on Flood Management*. Tokyo, Japan, 2011. (Cited on page 96.)

Houston, J.R. and Dean, R.G. Accounting for the nodal tide to improve estimates of sea level acceleration. *Journal of Coastal Research*, 27(5):801–807, 2011a. URL http://dx.doi.org/10.2112/JCOASTRES-D-11-00045.1. (Cited on pages 67, 68, and 69.)

Houston, J.R. and Dean, R.G. Sea-level acceleration based on U.S. tide gauges and extensions of previous global-gauge analyses. *Journal of Coastal Research*, pages 409–417, 2011b. URL http://dx.doi.org/10.2112/JCOASTRES-D-10-00157.1. (Cited on pages 66, 69, and 79.)

Howard, K. and Ward, J. Running global model parallel experiments. Technical report, NOAA/NWS/NCEP/EMC Global Climate and Weather Modeling Branch, 2011. URL http://www.emc.ncep.noaa.gov/GFS/doc.php. (Cited on page 101.)

Howard, R. Information value theory. *Systems Science and Cybernetics, IEEE Transactions on*, 2(1):22 –26, 1966. ISSN 0536-1567. URL http://dx.doi.org/10.1109/TSSC.1966.300074. (Cited on page 96.)

Howard, R. On making life and death decisions. In R.C. Schwing and W.A. Albers, editors, *Societal Risk Assessment*, pages 89–113. Plenum Press, New York, 1980. ISBN 0-306-40554-7. (Cited on page 96.)

Hunter, J.D. Matplotlib: A 2d graphics environment. *Computing In Science & Engineering*, 9(3):90–95, 2007. (Cited on page 181.)

van den Hurk, B., Tank, A.K., Lehderink, G., van Ulden, A., van Oldenborgh, G.J., Katsman, C., van den Brink, H., Keller, F., Bessembinder, J., Burgers, G., Komen, G., Hazeleger, W., and Drijfhout, S. New climate change scenarios for the Netherlands. *Water Science and Technology*, 56(4):27–33, 2007. ISSN 0273-1223. URL http://dx.doi.org/{10.2166/wst.2007.533}. 2nd International Conference on Climate Change and Water Management, Amsterdam, Netherlands, Sep 25-27, 2006. (Cited on pages 65, 72, 78, and 79.)

van den Hurk, B., Tank, A.K., Lenderink, G., van Ulden, A., van Oldenborgh, G.J., Katsman, C., van den Brink, H., Keller, F., Bessembinder, J., Burgers, G., Komen, G., Hazeleger, W., and Drijfhout, S. KNMI climate change scenarios 2006 for the Netherlands. Scientific report, KNMI, De Bilt, 2006. (Cited on pages 36 and 81.)

Izuma, K. and Adolphs, R. The brain's rose-colored glasses. *Nat Neurosci*, 14(11):1355–1356, 2011. URL http://dx.doi.org/10.1038/nn.2960. (Cited on page 35.)

Jakubowski-Tiessen, M. *Sturmflut 1717: die Bewältigung einer Naturkatastrophe in der frühen Neuzeit*, volume 24. Oldenbourg Wissenschaftsverlag, 1992. In German. (Cited on page 53.)

Jelgersma, S., Stive, M., and van der Valk, L. Holocene storm surge signatures in the coastal dunes of the western netherlands. *Marine Geology*, 125(1-2):95 – 110, 1995. ISSN 0025-3227. URL http://dx.doi.org/10.1016/0025-3227(95)00061-3. (Cited on pages 44 and 49.)

Jevrejeva, S., Moore, J.C., Grinsted, A., and Woodworth, P.L. Recent global sea level acceleration started over 200 years ago? *Geophysical Research Letters*, 35(8), 2008. URL http://dx.doi.org/10.1029/2008GL033611. (Cited on pages 50 and 66.)

Johnson, S. and Holt, M. *Economic value of weather and climate forecasts*, chapter 3: The value of weather information. Cambridge Univ Pr, 1997. ISBN 0-521-43420-3. (Cited on page 116.)

Jongejan, R., Vrijling, H., and Jonkman, B. Bestuurders geboeid door de veiligheidsketen. *Openbaar Bestuur*, 2:2–3, 2008. In Dutch. (Cited on page 97.)

Jonkman, S., Kelman, I., and Bain, V. A physical interpretation of human stability in flowing water. In *Proceedings of the International Symposium on Stochastic Hydraulics*. International Association of Hydraulic Research, Nijmegen, the Netherlands, 2005. (Cited on page 108.)

Jonkman, S. and Penning-Rowsell, E. Human instability in flood flows1. *JAWRA Journal of the American Water Resources Association*, 44(5):1208–1218, 2008. ISSN 1752-1688. URL http://dx.doi.org/10.1111/j.1752-1688.2008.00217.x. (Cited on page 108.)

Jonkman, S. and Vrijling, J. Loss of life due to floods. *Journal of Flood Risk Management*, 1(1):43–56, 2008. ISSN 1753-318X. URL http://dx.doi.org/10.1111/j.1753-318X.2008.00006.x. (Cited on page 22.)

Kabat, P., Fresco, L.O., Stive, M.J.F., Veerman, C.P., van Alphen, J.S.L.J., Parmet, B.W.A.H., Hazeleger, W., and Katsman, C.A. Dutch coasts in transition. *Nature Geoscience*, 2(7):450–452, 2009. URL http://dx.doi.org/10.1038/ngeo572. (Cited on pages 36 and 65.)

Kagan, Y.Y. Is earthquake seismology a hard, quantitative science? *pure and applied geophysics*, 155:233–258, 1999. ISSN 0033-4553. URL http://dx.doi.org/10.1007/s000240050264. (Cited on page 137.)

Kahneman, D. and Tversky, A. Prospect theory: An analysis of decision under risk. *Econometrica: Journal of the Econometric Society*, pages 263–291, 1979. URL http://www.jstor.org/stable/1914185. (Cited on page 35.)

Katsman, C., Sterl, A., Beersma, J., van den Brink, H., Church, J., Hazeleger, W., Kopp, R., Kroon, D., Kwadijk, J., Lammersen, R., et al. Exploring high-end scenarios for local sea level rise to develop flood protection strategies for a low-lying delta the netherlands as an example. *Climatic Change*, pages 1–29, 2011. (Cited on page 66.)

Katsman, C.A., Hazeleger, W., Drijfhout, S.S., Oldenborgh, G.J.v., and Burgers, G. Climate scenarios of sea level rise for the northeast Atlantic Ocean: a study including the effects of ocean dynamics and gravity changes induced by ice melt. *Climatic Change*, 91(3-4):351–374, 2008. URL http://dx.doi.org/10.1007/s10584-008-9442-9. (Cited on page 65.)

Kind, J. Maatschappelijke kosten-batenanalyse waterveiligheid 21e eeuw. Technical Report 1204144-006, Deltares, 2011. (Cited on pages 25 and 35.)

KNMI. Antieke reeksen. 2011. URL http://www.knmi.nl/klimatologie/daggegevens/antieke_wrn/index.html. (Cited on page 56.)

Kolen, B. Zelfredzaamheid bij overstromingen en grootschalige evacuaties. In I. Helsloot and B. van 't Padje, editors, *Zelfredzaamheid Concepten, thema's en voorbeelden nader beschouwd*, volume 1, chapter 6, pages 139–163. Boom Lemma, 2010. In Dutch. (Cited on page 100.)

Kolen, B., Slomp, R., van Balen, W., Terpstra, T., Bottema, M., and Nieuwenhuis, S. Learning from French experiences with storm Xynthia. Technical report, HKV lijn in water and Rijkswaterstaat, Waterdienst, 2010. (Cited on page 21.)

van Koningsveld, M., de Boer, G.J., Baart, F., Damsma, T., den Heijer, C., van Geer, P., and de Sonneville, B. OpenEarth - Inter-Company Management of: Data, Models, Tools & Knowledge. In *Proceedings WODCON XIX Conference*. Beijing, China, 2010. (Cited on pages 27, 55, and 177.)

van Koningsveld, M., Davidson, M.A., and Huntley, D.A. Matching science with coastal management needs: The search for appropriate coastal state indicators. *Journal of Coastal Research*, pages 399–411, 2005. URL http://dx.doi.org/10.2112/03-0076.1. (Cited on pages 98 and 125.)

van Koningsveld, M. and Lescinski, J. Decadal scale performance of coastal maintenance in the netherlands. *Shore and Beach*, 1(Winter 2007):20–36, 2007. (Cited on pages 85 and 138.)

van Koningsveld, M. and Mulder, J.P.M. Sustainable coastal policy developments in the netherlands. a systematic approach revealed. *Journal of Coastal Research*, pages 375–385, 2004. URL http://dx.doi.org/10.2112/1551-5036(2004)020{$[$}0375:SCPDIT{$]$}2.0.CO;2. (Cited on pages 33, 36, 37, and 82.)

van Koningsveld, M., Mulder, J.P.M., Stive, M.J.F., van der Valk, L., and van der Weck, A.W. Living with sea-level rise and climate change: A case study of the Netherlands. *Journal of Coastal Research*, 24(2):367+, 2008. ISSN 0749-0208. URL http://dx.doi.org/{10.2112/07A-0010.1}. (Cited on page 35.)

Kooi, H., Johnston, P., Lambeck, K., Smither, C., and Molendijk, R. Geological causes of recent (~100 yr) vertical land movement in the Netherlands. *Tectonophysics*, 299(4):297–316, 1998. (Cited on page 65.)

de Kraker, A. Reconstruction of storm frequency in the north sea area of the pre-industrial period, 1400–1625 and the connection with reconstructed time series of temperatures. *History of Meteorolology*, 2:51–69, 2005. URL http://www.meteohistory.org/2005historyofmeteorology2/05dekraker.pdf. (Cited on page 50.)

Kramer, L. and Maza, S. *The History of Science, Or, an Oxymoronic Theory of Relativistic Objectivity*, chapter 15, pages 297–318. Blackwell Publishers Inc., 2007. ISBN 9780470998748. URL http://dx.doi.org/10.1002/9780470998748.ch16. (Cited on page 137.)

Kriebel, D.L. and Dean, R.G. Numerical simulation of time-dependent beach and dune erosion. *Coastal Engineering*, 9(3):221 – 245, 1985. ISSN 0378-3839. URL http://dx.doi.org/10.1016/0378-3839(85)90009-2. (Cited on page 34.)

Lang, A. and Homann, J. *Die Weinachtsflut vom 2. Dezember 1717: Erlũterungen zur Lichtdr. ausg. der Karte 'Geographische Vorstellung der Jammerlichen Wasser-Flutt in Nieder-Teutschland' des J.B. Homann von 1718*. Verlag Die Bake, Juist, 1963. In German. (Cited on pages 51 and 53.)

Larson, M., Erikson, L., and Hanson, H. An analytical model to predict dune erosion due to wave impact. *Coastal engineering*, 51(8-9):675–696, 2004. URL http://dx.doi.org/10.1016/j.coastaleng.2004.07.003. (Cited on page 34.)

van Ledden, M., Westra, M.R., Groeneweg, J., Wenneker, I., and Scholl, O. SWAN berekeningen ten behoeve van hr2006 voor de hollandse kust rapportage fase 1. Technical Report 9P8603.A0, Royal Haskoning, 2005. In Dutch. (Cited on page 57.)

Lisitzin, E. The tidal cycle of 18.6 years in the oceans. *ICES Journal of Marine Science*, 22(2):147, 1957. URL http://dx.doi.org/10.1093/icesjms/22.2.147. (Cited on page 67.)

Love, A.E.H. The yielding of the earth to disturbing forces. *Proceedings of the Royal Society of London. Series A, Containing Papers of a Mathematical and Physical Character*, 82(551):pp. 73–88, 1909. ISSN 09501207. URL http://www.jstor.org/stable/92970. (Cited on page 68.)

Macdonald, N., Werritty, A., Black, A., and McEwen, L. Historical and pooled flood frequency analysis for the river tay at perth, scotland. *Area*, 38(1):34–46, 2006. URL http://dx.doi.org/10.1111/j.1475-4762.2006.00673.x. (Cited on page 50.)

Mai, C.V., van Gelder, P., and Vrijling, J. Probabilistic investigation of failure mechanisms of coastal flood defence structures. In *Asian and Pacific Coasts 2007*. September, 2007. (Cited on pages 33 and 113.)

van Malde, J. Historische stormvloedstanden. Technical Report 2003.08.1, Aqua Systems International, 2003. In Dutch. (Cited on pages 50, 51, 52, 53, 56, and 58.)

Maslow, A. A theory of human motivation. *Psychological review*, 50(4):370, 1943. (Cited on page 37.)

Mastrandrea, M., Field, C., Stocker, T., Edenhofer, O., Ebi, K., Frame, D., Held, H., Kriegler, E., Mach, K., Matschoss, P., et al. Guidance note for lead authors of the ipcc fifth assessment report on consistent treatment of uncertainties. Guidance note, Intergovernmental Panel on Climate Change, 2010. (Cited on page 135.)

McInnes, R. Art as a tool in support of the understanding of coastal change. Report, The Crown Estate, 2008. (Cited on page 51.)

Meehl, G., Stocker, T., Collins, W., Friedlingstein, P., Gaye, A., Gregory, J., Kitoh, A., Knutti, R., Murphy, J., Noda, A., Raper, S., Watterson, I., Weaver, A., and Zhao, Z.C. Global climate projections. In S. Solomon, D. Qin, M. Manning, Z. Chen, M. Marquis, K.B. Averyt, M. Tignor, and H.L. Miller, editors, *Climate Change*

2007: The Physical Science Basis. Contribution of Working Group I to the Fourth Assessment Report of the Intergovernmental Panel on Climate Change. Cambridge University Press, Cambridge, United Kingdom and New York, NY, USA, 2007. (Cited on page 66.)

Michalakes, J., Dudhia, J., Gill, D., Henderson, T., Klemp, J., Skamarock, W., and Wang, W. The weather research and forecast model: Software architecture and performance. In *Proceedings of the 11th ECMWF Workshop on the Use of High Performance Computing In Meteorology*, volume 25, page 29. World Scientific, 2004. (Cited on page 102.)

Ministerie van Verkeer en Waterstaat. *3e Kustnota: traditie, trends en toekomst*. Ministerie van Verkeer en Waterstaat, Den Haag, 2000. In Dutch. (Cited on page 37.)

Ministerie van Verkeer en Waterstaat. Nationaal waterplan. Technical report, Ministerie van Verkeer en Waterstaat, 2009. In Dutch. (Cited on pages 36 and 65.)

Molteni, F., Buizza, R., Palmer, T., and Petroliagis, T. The ECMWF ensemble prediction system: Methodology and validation. *Quarterly Journal of the Royal Meteorological Society*, 122(529):73–119, 1996. ISSN 1477-870X. URL http://dx.doi.org/10.1002/qj.49712252905. (Cited on page 23.)

Moss, R.H., Edmonds, J.A., Hibbard, K.A., Manning, M.R., Rose, S.K., van Vuuren, D.P., Carter, T.R., Emori, S., Kainuma, M., Kram, T., Meehl, G.A., Mitchell, J.F.B., Nakicenovic, N., Riahi, K., Smith, S.J., Stouffer, R.J., Thomson, A.M., Weyant, J.P., and Wilbanks, T.J. The next generation of scenarios for climate change research and assessment. *Nature*, 463(7282):747–756, 2010. URL http://dx.doi.org/10.1038/nature08823. (Cited on page 141.)

Murphy, A. and Epstein, E. Skill scores and correlation-coefficients in model verification scores and correlation-coefficients in model verification. *Monthly Weather Review*, 117(3):572–581, 1989. (Cited on page 114.)

Nations, U. Agenda 21. Technical report, UN Department of Economic and Social Affairs, 1993. (Cited on page 36.)

Netwerk. De toekomst van het deltaplan. television, 2007. (Cited on page 36.)

NewScientist. Italian earthquake case is no anti-science witch-hunt. 2012. URL http://www.newscientist.com/article/dn22416-italian-earthquake-case-is-no-antiscience-witchhunt.html. (Cited on page 96.)

Neyman, J. Outline of a theory of statistical estimation based on the classical theory of probability. *Philosophical Transactions of the Royal Society of London. Series A, Mathematical and Physical Sciences*, 236(767):pp. 333–380, 1937. ISSN 00804614. URL http://www.jstor.org/stable/91337. (Cited on page 22.)

NOAA. Storm surge overview. 2013. URL http://www.nhc.noaa.gov/surge/. (Cited on page 44.)

Normile, D. Waves of destruction. *Science*, 331(6023):1376, 2011. URL http://dx.doi.org/10.1126/science.331.6023.1376. (Cited on page 95.)

Normile, D. One year after the devastation, tohoku designs its renewal. *Science*, 335(6073):1164–1166, 2012. URL http://dx.doi.org/10.1126/science.335.6073.1164. (Cited on pages 95 and 113.)

O'Connor, M. and Lawrence, M. An examination of the accuracy of judgemental confidence intervals in time series forecasting. *Journal of Forecasting*, 8(2):141–155, 1989. ISSN 1099-131X. URL http://dx.doi.org/10.1002/for.3980080207. (Cited on page 117.)

Oreskes, N., Shrader-Frechette, K., and Belitz, K. Verification, validation, and confirmation of numerical models in the earth sciences. *Science*, 263(5147):641, 1994. URL http://dx.doi.org/10.1126/science.263.5147.641. (Cited on page 113.)

Pachauri, R. and Reisinger, A. Climate change 2007: Synthesis report. contribution of working groups i, ii and iii to the fourth assessment report of the intergovernmental panel on climate change contribution of working groups i, ii and iii to the fourth assessment report of the intergovernmental panel on climate change. Technical report, Intergovernmental Panel on Climate Change, 2007. (Cited on pages 23 and 24.)

Parisien, L. Xynthia : le maire de la faute-sur-mer mis en examen. 2011. URL http://www.leparisien.fr/nantes-44000/xynthia-le-maire-de-la-faute-sur-mer-mis-en-examen-14-04-2011-1407628.php. (Cited on page 21.)

Parker, T. Southpark episode 14.11 Coon 2: Hindsight. television series, 2010. (Cited on page 146.)

Pawlowicz, R., Beardsley, B., and Lentz, S. Classical tidal harmonic analysis including error estimates in matlab using t_tide. *Computers & Geosciences*, 28(8):929–937, 2002. URL http://dx.doi.org/10.1016/S0098-3004(02)00013-4. (Cited on page 119.)

Peltier, W. Global glacial isostacy and the surface of the ice-age earth: The ice-5g (vm2) model and grace. *Annual Review of Earth and*

Planetary Sciences, 32(1):111–149, 2004. URL http://dx.doi.org/10.1146/annurev.earth.32.082503.144359. (Cited on pages 69 and 74.)

Phien-wej, N., Giao, P., and Nutalaya, P. Land subsidence in Bangkok, Thailand. *Engineering Geology*, 82(4):187 – 201, 2006. ISSN 0013-7952. URL http://dx.doi.org/10.1016/j.enggeo.2005.10.004. (Cited on page 33.)

Philippart, M., Pwa, S., and Dillingh, D. De basispeilen langs de nederlandse kust: de ruimtelijke verdeling en overschrijdingslijnen. Technical report, Rijkswaterstaat, 1995. In Dutch. (Cited on pages 41, 45, 47, and 58.)

Plant, N.G. and Holland, K.T. Prediction and assimilation of surf-zone processes using a bayesian network part i: Forward models. *Coastal Engineering*, 58(1):119–130, 2011a. URL http://dx.doi.org/DOI10.1016/j.coastaleng.2010.09.003. (Cited on pages 100, 113, and 128.)

Plant, N.G. and Holland, K.T. Prediction and assimilation of surf-zone processes using a bayesian network: Part ii: Inverse models. *Coastal Engineering*, 58(3):256 – 266, 2011b. ISSN 0378-3839. URL http://dx.doi.org/DOI:10.1016/j.coastaleng.2010.11.002. (Cited on page 128.)

Platt, J.R. Strong inference. *Science*, 146(3642):347–353, 1964. URL http://dx.doi.org/10.1126/science.146.3642.347. (Cited on page 137.)

Pool, A.D. *Modelling the 1775 storm surge deposits at the Heemskerk dunes*. Master's thesis, TU Delft, 2009. (Cited on page 56.)

Popper, K.R. *Logik der forschung: zur erkenntnistheorie der modernen naturwissenschaft*, volume Bd. 9 of *Schriften zur wissenschaftlichen weltauffassung*. J. Springer, Wien, 1935. (Cited on page 137.)

Porta, M. *Dictionary of epidemiology*. Oxford University Press, USA, 2008. (Cited on page 82.)

Prandi, P., Cazenave, A., and Becker, M. Is coastal mean sea level rising faster than the global mean? a comparison between tide gauges and satellite altimetry over 1993-2007. *Geophysical Research Letters*, 36, 2009. URL http://dx.doi.org/10.1029/2008GL036564. (Cited on page 66.)

Proudman, J. The condition that a long-period tide shall follow the equilibrium-law. *Geophysical Journal of the Royal Astronomical Society*, 3(2):244–249, 1960. URL http://dx.doi.org/10.1111/j.1365-246X.1960.tb00392.x. (Cited on page 67.)

Pugh, D. *Tides, surges, and mean sea-level*. John Wiley & Sons, Chichester, 1987. (Cited on pages 42 and 68.)

R Development Core Team. *R: A Language and Environment for Statistical Computing*. R Foundation for Statistical Computing, Vienna, Austria, 2009. URL http://www.r-project.org. ISBN 3-900051-07-0. (Cited on pages 46 and 88.)

Ågren, G.I. and Bosatta, E. Theory and model or art and technology in ecology. *Ecological Modelling*, 50(1-3):213 – 220, 1990. ISSN 0304-3800. URL http://dx.doi.org/10.1016/0304-3800(90)90051-H. (Cited on page 138.)

Ramachandran, P. and Varoquaux, G. Mayavi: 3D Visualization of Scientific Data. *Computing in Science & Engineering*, 13(2):40–51, 2011. ISSN 1521-9615. (Cited on page 181.)

Ranasinghe, R., Donnelly, C., and Larson, M. Numerical modeling of beach profile change caused by overwash. In *Coastal Dynamics 2005*, pages 1–14. 2005. URL http://dx.doi.org/10.1061/40855(214)56. (Cited on page 44.)

Raymond, E. The cathedral and the bazaar. *Knowledge, Technology & Policy*, 12(3):23–49, 1999. (Cited on page 102.)

Rice, J.A. *Mathematical statistics and data analysis*. Duxbury press, 2007. ISBN 978-0534399429. (Cited on page 24.)

Rijkswaterstaat. De JAaRlijkse KUStmetingen (JARKUS). 2008. URL http://www.watermarkt.nl/kustenzeebodem/. (Cited on pages 106 and 120.)

van Rijn, L.C., Walstra, D.J.R., Grasmeijer, B., Sutherland, J., Pan, S., and Sierra, J.P. The predictability of cross-shore bed evolution of sandy beaches at the time scale of storms and seasons using process-based profile models. *Coastal Engineering*, 47(3):295–327, 2003. (Cited on pages 121 and 125.)

Roelvink, D., Reniers, A., van Dongeren, A., de Vries, J.v.T., McCall, R., and Lescinski, J. Modelling storm impacts on beaches, dunes and barrier islands. *Coastal Engineering*, 56(11-12):1133–1152, 2009. URL http://dx.doi.org/10.1016/j.coastaleng.2009.08.006. (Cited on page 55.)

Roelvink, J.A., Reniers, A.J.H.M., van Dongeren, A.R., van Thiel de Vries, J.S.M., Lescinski, J.M., and Walstra, D.J.R. XBeach Annual Report and Model Description. Modeling of Hurricane Impacts. Technical report, UNESCO-IHE, 2007. (Cited on page 108.)

Roscoe, K. and Diermanse, F. Effect of surge uncertainty on probabilistically computed dune erosion. *Coastal Engineering*, 58(11):1023

– 1033, 2011. ISSN 0378-3839. URL http://dx.doi.org/10.1016/j.coastaleng.2011.05.014. (Cited on page 25.)

Rossiter, J.R. An analysis of annual sea level variations in european waters. *Geophysical Journal of the Royal Astronomical Society*, 12(3):259–299, 1967. URL http://dx.doi.org/10.1111/j.1365-246X.1967.tb03121.x. (Cited on page 67.)

Rozin, P. and Royzman, E.B. Negativity bias, negativity dominance, and contagion. *Personality and Social Psychology Review*, 5(4):296–320, 2001. URL http://dx.doi.org/10.1207/S15327957PSPR0504_2. (Cited on page 36.)

de Ruig, J. Coastline management in the netherlands: human use versus natural dynamics. *Journal of Coastal Conservation*, 4:127–134, 1998. ISSN 1400-0350. URL http://dx.doi.org/10.1007/BF02806504. 10.1007/BF02806504. (Cited on page 54.)

Sackett, D.L., Rosenberg, W.M.C., Gray, J.A.M., Haynes, R.B., and Richardson, W.S. Evidence based medicine: what it is and what it isn't. *BMJ*, 312(7023):71–72, 1996. URL http://dx.doi.org/10.1136/bmj.312.7023.71. (Cited on page 138.)

Said, S. and Dickey, D. Testing for unit roots in autoregressive-moving average models of unknown order. *Biometrika*, 71(3):599–607, 1984. URL http://dx.doi.org/10.1093/biomet/71.3.599. (Cited on page 86.)

Sallenger, A. Storm impact scale for barrier islands. *Journal of Coastal Research*, 16(3):890–895, 2000. URL http://www.jstor.org/stable/4300099. (Cited on pages 33 and 113.)

Schenk, P. *Kennemaria et Westfrisia vulgo et vernacul Noord-Holland, tam in minores quam praecipuas ditiones ..: edita per Nicolaum Visscher Amst: ..* Schenk (Petrus), 1740. URL http://www.library.tudelft.nl/Tresor/webpages/TRL_5_3_1_15.html. (Cited on page 53.)

Settle, A.K. Financing disaster mitigation, preparedness, response, and recovery. *Public Administration Review*, 45:pp. 101–106, 1985. ISSN 00333352. URL http://www.jstor.org/stable/3135004. (Cited on page 21.)

Smits, A., Tank, A., and Konnen, G. Trends in storminess over the Netherlands, 1962-2002. *International Journal of Climatology*, 25(10):1331–1344, 2005. URL http://dx.doi.org/DOI10.1002/joc.1195. (Cited on pages 50, 80, and 81.)

Southgate, H.N. Data-based yearly forecasting of beach volumes along the dutch north sea coast. *Coastal Engineering*, 58(8):749 – 760, 2011. ISSN 0378-3839. URL http://dx.doi.org/10.1016/j.coastaleng.2011.03.011. (Cited on pages 85 and 86.)

Specht, C. *Kaart van 't Graafschap Holland: naauwkeurig afgedeelt in zyne Heemraadschappen, Baljuwschappen en Waarden, nevens verscheide andere mindere afdeelingen en onderhorige landen alsmede de Heerlykheit Utrecht en het grootste gedeelte van Gelderlandt*. Ottens, Amsterdam, 1740. URL http://www.library.tudelft.nl/Tresor/webpages/TRL_5_3_1_05.html. In Dutch. (Cited on page 53.)

Spiegelhalter, D., Pearson, M., and Short, I. Visualizing uncertainty about the future. *Science*, 333(6048):1393–1400, 2011. URL http://dx.doi.org/DOI10.1126/science.1191181. (Cited on page 24.)

Starr, C. Social benefit versus technological risk. *Science*, 165(3899):1232–1238, 1969. URL http://dx.doi.org/10.1126/science.165.3899.1232. (Cited on pages 95 and 96.)

Stelling, G.S. *On the construction of computational methods for shallow water flowproblems*, volume 35 of *Rijkswaterstaat communications*. Rijkswaterstaat, The Hague, The Netherlands, 1984. (Cited on page 108.)

Sterl, A. and Caires, S. Climatology, variability and extrema of ocean waves: The web-based knmi/era-40 wave atlas. 2005. URL http://dx.doi.org/DOI10.1002/joc.1175. International Journal of Climatology. (Cited on page 81.)

Stive, M., De Vriend, H., Cowell, P., and Niedoroda, A. Behaviour-oriented models of shoreface evolution. In *Proceedings Coastal Dynamics*, volume 95, pages 998–1005. 1995. (Cited on page 33.)

Sutherland, J., Peet, A., and Soulsby, R. Evaluating the performance of morphological models. *Coastal Engineering*, 51(8-9):917–939, 2004. URL http://dx.doi.org/10.1016/j.coastaleng.2004.07.015. (Cited on pages 121 and 138.)

Tetlock, P.E. *Expert political judgment: How good is it? How can we know?* Princeton University Press, 2005. (Cited on page 142.)

Thompson, D.W. *On growth and form*. University press, Cambridge, 1917. (Cited on pages 83 and 85.)

Trupin, A. and Wahr, J. Spectroscopic analysis of global tide gauge sea level data. *Geophysical Journal International*, 100(3):441–453, 1990. ISSN 1365-246X. URL http://dx.doi.org/10.1111/j.1365-246X.1990.tb00697.x. (Cited on pages 67, 68, 74, and 79.)

Uunk, L., Wijnberg, K., and Morelissen, R. Automated mapping of the intertidal beach bathymetry from video images. *Coastal Engineering*, 57(4):461 – 469, 2010. ISSN 0378-3839. URL http://dx.doi.org/10.1016/j.coastaleng.2009.12.002. (Cited on pages 120 and 121.)

Vautard, R., Cattiaux, J., Yiou, P., Thépaut, J., and Ciais, P. Northern hemisphere atmospheric stilling partly attributed to an increase in surface roughness. *Nature Geoscience*, 3(11):756–761, 2010. ISSN 1752-0894. URL http://dx.doi.org/10.1038/ngeo979. (Cited on pages 50 and 82.)

Vellinga, P. *Beach and dune erosion during storm surges*. Waterloopkundig Laboratorium, Delft, 1986. URL http://repository.tudelft.nl/file/773510/375532. (Cited on page 34.)

Verlaan, M., Zijderveld, A., De Vries, H., and Kroos, J. Operational storm surge forecasting in the Netherlands: developments in the last decade. *Philosophical Transactions of the Royal Society A-Mathematical Physical and Engineering Sciences*, 363(1831):1441–1453, 2005. ISSN 1364-503X. URL http://dx.doi.org/{10.1098/rsta.2005.1578}. (Cited on pages 102 and 128.)

Voinov, A. and Shugart, H.H. "Integronsters", integral and integrated modeling. *Environmental Modelling and Software*, 2012. ISSN 1364-8152. URL http://dx.doi.org/10.1016/j.envsoft.2012.05.014. (Cited on page 142.)

Vousdoukas, M., Almeida, L., and Ferreira, O. Modelling storm-induced beach morphological change in a meso-tidal, reflective beach using xbeach. *Journal of Coastal Research*, (SI 64):1916–1920, 2011. (Cited on page 113.)

de Vriend, H.J. Mathematical modelling and large-scale coastal behaviour. *Journal of Hydraulic Research*, 29(6):727–740, 1991. URL http://dx.doi.org/10.1080/00221689109498955. (Cited on page 33.)

de Vries, H. Probability forecasts for water levels at the coast of the netherlands. *Marine Geodesy*, 32(2):100–107, 2009. URL http://dx.doi.org/10.1080/01490410902869185. (Cited on pages 114, 115, and 117.)

van Thiel de Vries, J.S.M. *Dune erosion during storm surges*. Ph.D. thesis, Delft University of Technology, 2009. (Cited on pages 34 and 120.)

Vrijling, J. Probabilistic design of water defense systems in The Netherlands. *Reliability Engineering & System Safety*, 74(3):337–344, 2001. URL http://dx.doi.org/10.1016/S0951-8320(01)00082-5. (Cited on page 33.)

Walstra, D. and Bos, C. Noodmaatregelen voor de bescherming van de Delflandse kust. Report 1200465, Deltares, 2009. In Dutch. (Cited on page 95.)

Weenink, M. *A Theory and method of calculation of wind effects on sea levels in a partly-enclosed sea, with special application to the Southern coast of the North Sea.* Ph.D. thesis, Utrecht University, 1958. (Cited on page 57.)

Werner, M., Cranston, M., Harrison, T., Whitfield, D., and Schellekens, J. Recent developments in operational flood forecasting in england, wales and scotland. *Meteorological Applications*, 16(1):13–22, 2009. ISSN 1469-8080. URL http://dx.doi.org/10.1002/met.124. (Cited on page 102.)

Wheeler, D., Garcia-Herrera, R., Wilkinson, C.W., and Ward, C. Atmospheric circulation and storminess derived from royal navy logbooks: 1685 to 1750. *Climatic Change*, 101(1-2):257–280, 2010. URL http://dx.doi.org/DOI10.1007/s10584-009-9732-x. (Cited on page 49.)

Whitaker, J. and Loughe, A. The relationship between ensemble spread and ensemble mean skill. *Monthly Weather Review*, 126(12):3292–3302, 1998. ISSN 1520-0493. URL http://dx.doi.org/10.1175/1520-0493(1998)126$<$3292:TRBESA$>$2.0.CO;2. (Cited on page 23.)

Wickham, H. *ggplot2: elegant graphics for data analysis*. Springer New York, 2009. ISBN 978-0-387-98140-6. URL http://had.co.nz/ggplot2/book. (Cited on page 181.)

Wilkinson, L. *The grammar of graphics*. Springer Verlag, 2005. ISBN 978-0387245447. (Cited on pages 135 and 141.)

Wilks, D. *Statistical Methods in the Atmospheric Sciences*, volume 100 of *International Geophysics*. Academic Press, 2011. URL http://dx.doi.org/10.1016/B978-0-12-385022-5.00001-4. (Cited on pages 114 and 135.)

Winter, R., Sterl, A., Vries, J., Weber, S., and Ruessink, G. The effect of climate change on extreme waves in front of the dutch coast. *Ocean Dynamics*, 62:1139–1152, 2012. ISSN 1616-7341. URL http://dx.doi.org/10.1007/s10236-012-0551-7. (Cited on page 81.)

WL | Delft Hydraulics. Dune erosion; Product 3: Probabilistic dune erosion prediction method. Technical Report H4357 / A1414, WL | Delft Hydraulics / Alkyon, 2007. (Cited on pages 55 and 59.)

Woodworth, P. and Player, R. The permanent service for mean sea level: An update to the 21st century. *Journal of Coastal Research*, 19(2):287–295, 2003. (Cited on pages 66 and 74.)

Woodworth, P.L. A search for accelerations in records of European mean sea level. *International Journal of Climatology*, 10(2):129–143,

1990. URL http://dx.doi.org/10.1002/joc.3370100203. (Cited on page 66.)

Woodworth, P.L. High waters at Liverpool since 1768: the UK's longest sea level record. *Geophysical Research Letters*, 26(11):1589–1592, 1999. URL http://dx.doi.org/10.1029/1999GL900323. (Cited on page 67.)

Wuertz, D. *fExtremes: Rmetrics - Extreme Financial Market Data*, 2009. URL http://CRAN.R-project.org/package=fExtremes. R package version 2100.77. (Cited on page 46.)

CURRICULUM VITÆ

PERSONALIA

Fedor Baart

♓ 23-02-1976, Portsmouth, United Kingdom

EDUCATION

Alfrink College, Zoetermeer, VWO (1988–1994)

Leiden University, Psychology: Research methods and statistics (1994–2000, met genoegen)

EMPLOYMENT

Foundation of Pharmaceutical Statistics (SFK) 2000–2006

Waterloopkundig Laboratorium, 2006–2007

Deltares, 2008–

TU Delft, 2008–

PUBLICATIONS AND TALKS

REVIEWED

1. Real-time forecasting of morphological storm impacts: a case study in the Netherlands, Baart et al. [2009b]

2. Confidence in real-time forecasting of morphological storm impacts, Baart et al. [2011c]

3. Using 18th century storm-surge data from the Dutch Coast to improve the confidence in flood-risk estimates, Baart et al. [2011a]

4. A comparison between WCS and OPeNDAP for making model results and data products available through the internet, Baart et al. [2012b]

5. The Effect of the 18.6-Year Lunar Nodal Cycle on Regional Sea-Level Rise Estimates, Baart et al. [2012c]

6. Trends in Sea-Level Trend Analysis, Baart et al. [2012d]

7. Functional Coverages, Donchyts et al. [2012b]

8. Assessment of dune failure along the Dutch coast using a fully probabilistic approach, den Heijer et al. [2012]

NON REVIEWED

1. DelftShell-integrated modeling environment with elements of GIS, Data Management and OpenMI support, AGU Fall Meeting, Donchyts et al. [2008]

2. OpenEarth: an open source system for sharing data, models and tools by marine and coastal scientists and engineers, NCK International Symposium *best presentation award, presented by Gerben de Boer*, Baart et al. [2009a]

3. Visualization of coastal data through KML, AGU Fall Meeting, Damsma et al. [2009]

4. A stereoscopic view on the coast, NCK International Symposium, Baart and de Haan [2010]

5. Reducing the invasiveness of modeling frameworks, AGU Fall Meeting, Baart and Donchyts [2010]

6. Development of the Delta Shell as an integrated modeling environment, Donchyts et al. [2010]

7. The effect of the 18.6 year lunar nodal cycle on regional sea-level rise estimates, Deltas in Times of Climate Change, Baart et al. [2010]

8. Delta Shell: Integrated Modeling by Example, AGU Fall Meeting, Donchyts et al. [2011]

9. OPeNDAP vs. WCS, Free and Open Source Software for Geospatial, Baart et al. [2011b]

10. An integrated coastal model for aeolian and hydrodynamic sediment transport, EGU, Baart et al. [2012a]

11. Open source integrated modeling environment Delta Shell, EGU, Donchyts et al. [2012a]

12. OpenEarth: using Google Earth as outreach for NCK's data, NCK International Symposium, de Boer et al. [2012]

13. Is er al versnelde zeespiegelstijging?, Dillingh et al. [2012b]

14. Do we have to take an acceleration of sea-level rise into account?, Dillingh et al. [2012a]

15. OpenEarth - Inter-Company Management of: Data, Models, Tools & Knowledge, van Koningsveld et al. [2010]

SOFTWARE

The following software packages where extended or developed as part of this thesis. All software is available as open source.

1. OpenEarth
2. R sealevel package
3. KustViewer (lizard-kml)
4. Delft3D
5. XBeach

ACKNOWLEDGEMENTS

The European Union (Seventh Framework Programme under grant agreement 202798) and the Dr Cornelis Lely Foundation are acknowledged for their financial support.

I am grateful to Mark van Koningsveld for his supervision, the fruitful cooperation and his thorough reviews. We had many interesting discussions and we wrote many papers and proceedings together. This resulted in an increased quality and reduced the time it takes me to write new publications.

I want thank Marcel Stive for giving me the opportunity and freedom to conduct this study at the hydraulic engineering department.

Much of the work in this thesis was created in cooperation with others. The cooperation within the Morphological Impacts and COastal Risks induced by Extreme storm (MICORE) project was great. I thank the Dutch team for their effort. Together with Dano Roelvink, Ap van Dongeren, Jaap van Thiel de Vries, Robert McCall, Pieter van Geer and Bas Hoonhout we worked on improving the XBeach model. Marije Smit and I worked to gather the information on historic storms. Maarten van Ormondt did the most work in setting up the operational forecast system. From the other countries I thank the Uniwersytet Szczeciński (Kazimierz, Joanna, Pawel and Natalia) and the Proudman Oceanographic Laboratory (Jenny, Alejandro) for inviting me over. I thank Paolo, Oscar and Piet for their effort in making it a succesful project.

I spent part of the time at the Delft University, where I was able to discuss several statistical topics with Pieter van Gelder. Kees den Heijer and I started at about the same time and shared an office for four years. We had great fun working together. I also enjoyed the company of my other roommates Jaap, Dongju and Poonam. I also thank my other colleagues for the enjoyable time. I explicitly want to thank Ad, Sierd, Martijn, Howard, Han, Dirk Jan, Wim, Mark, Hua, Gerwin, Chantal, Inge, Judith and Judith for their help. I also thank the master students Arend, Dirk, Marco, Bas and Joost for their effort.

The other half of my time I spent at Deltares. Together with Gerben de Boer I worked on setting up the OpenEarth system, which turned out to be quite succesful. Gennadii Donchyts and I worked together on the next generation of integrated models. I worked together with John de Ronde and Douwe Dillingh on the sea-level rise research. At Deltares I shared my office with Katherine Cronin and Marcel Taal, both are thanked for their interesting discussions on methodological and coastal topics. Katherine also helped with correcting the text of this thesis. I also would like to thank from the coastal departement

Ankie, Giorgio, Bert, Theo, Krista and Johan and from the software department Bert, Arthur, Frank and my cousin Arthur.

I received help from people from several other institutes. From the Royal Netherlands Meteorological Institute (KNMI) I thank Maarten Plieger, Bert Wouters for working together on publications and Caroline Katsman and Bart van der Hurk for their comments. I would like to thank Ernst Schrama, Herman Gerritsen, Phil Woodworth for their comments on the discussions on the nodal tide analysis. From the Dutch government I would like to thank Wim de Haas, Quirijn Lodder and Marc Philippart. From Nederlandse Organisatie voor Toegepast-Natuurwetenschappelijk Onderzoek (TNO) I thank Marcel Bakker and Sytze van Heteren for their contributions to our publication. From van Oord I thank Thijs Damsma. From the Universiteit van Amsterdam I thank Adriaan de Kraker and Tamara van Batenburg-Eddes for their comments. I visited Florida several times, where I had interesting discussion at the United States Geological Survey (USGS) with Nathaniel Plant, Abby Sallenger, Peter Howd and at the University of Miami with Ad Reniers.

Finally I want to thank my family and friends for their support. Especially my parents and sister and Tabitha who helped out by supporting me and also by commenting on and correcting several parts of this thesis.

COLOPHON

This document was typeset using the typographical look-and-feel *classicthesis* developed by André Miede using the typesetting software LaTeX. Figures were created using R Project for Statistical Computing (R), the R package *ggplot2* [Wickham, 2009], the python packages *matplotlib* [Hunter, 2007], *basemap*, *mayavi2* [Ramachandran and Varoquaux, 2011] and *blender*, some figures have been enhanced, combined and reordered with *Adobe Illustrator* ®. The cover is a combination of a photo from the present church of Katwijk (source: http://www.panoramio.com) and a sketch of the church of Egmond by H. Spilman just after the storm in 1741.

Final Version as of Thursday 23rd May, 2013 (classicthesis Revision : 5014).